Stony Brook University

Modulation of Monocytic Activation following Spinal Cord Injury Reduces Secondary Injury and Neurodegeneration

A Dissertation Presented

by

Jaime Emmetsberger

to

The Graduate School

in Partial Fulfillment of the

Requirements

for the Degree of

Doctor of Philosophy

in

Molecular and Cellular Pharmacology Program

Stony Brook University

December 2010

Stony Brook University
The Graduate School

Jaime Emmetsberger

We, the dissertation committee for the above candidate for the
Doctor of Philosophy degree, hereby recommend
acceptance of this dissertation.

Styliani-Anna E. Tsirka, Ph.D. – Dissertation Advisor
Professor, Department of Pharmacological Sciences

Joel Levine, Ph.D. – Chairperson of Defense
Professor, Department of Neurobiology and Behavior

Holly Colognato, Ph.D.
Assistant Professor, Department of Pharmacological Sciences

Sanford R. Simon, Ph.D.
Professor, Departments of Biochemistry and Cell Biology and Pathology

This dissertation is accepted by the Graduate School.

Lawrence Martin
Dean of the Graduate School

Abstract of Dissertation

Modulation of Monocytic Activation following Spinal Cord Injury Reduces Secondary Injury and Neurodegeneration

By

Jaime Emmetsberger

Doctor of Philosophy

in

Molecular and Cellular Pharmacology

Stony Brook University

2010

Spinal cord injury (SCI) sets off a cascade of biochemical and cellular events that destroy neurons, cause demyelination, and trigger an inflammatory immune response. Microglia, the immune-competent cells of the central nervous system, migrate to the site of injury, become activated and are thought to contribute to secondary damage and neurodegeneration following SCI. Conversely, growth factors and cytokines released by activated microglia may promote regeneration. Controversy exists over the neurodegenerative verses the neuroregenerative roles of activated microglia, and which role predominates following SCI. The activation state of microglia determines their neurotoxic and neurotrophic properties that influence the surrounding environment to have restorative or detrimental effects.

To address the question of whether the spatio-temporal distribution of activated microglia determines their neurotoxic or neuroprotective behavior the

dorsal hemisection of SCI was performed on wild type or CD11b-HSVTK$^{+/-}$ (herpes simplex virus thymidine kinase) mice. Microglia were either ablated or activation was inhibited via the administration of ganciclovir (GCV) or macrophage/microglial inhibitory factor (MIF), respectively. Ablation of or suppressing activation of microglia at early time points post SCI reduced secondary injury around the lesion epicenter, decreased the hypertrophic change of astrocytes and caused a increase in the number of axons present within the lesion epicenter. Moreover, inhibition of microglial activation with MIF reduced oligodendrocyte apoptosis and demyelination. In addition, microglia located within or proximal to the lesion produced more toxic factors, such as tumor necrosis factor alpha (TNF-α), while microglial distal to the lesion produce more trophic factors, such as interleukin-10 (IL-10). This suggests that microglia within the epicenter at early time points post injury are neurotoxic, contributing to demyelination and axonal degeneration.

Table of Contents

List of Tables

Chapter I

List of Figures

Chapter II

Chapter III

Chapter IV

Chapter V

Chapter VI

Chapter VII

List of Abbreviations

BBB	blood brain barrier
BSB	blood spinal cord barrier
BDNF	brain-derived neurotrophic factor
BrdU	5-bromo-2'-deoxyuridine
CNS	central nervous system
CTB	cholera toxin beta subunit
DNA	deoxyribonucleic acid
dpi	days post injury
e.g.	for example, exempla gratia
ELISA	Enzyme Linked Immunosorbent Assay
FBS	Fetal Bovine Serum
GFAP	Glial fibrillary acidic protein
HMW	high molecular weight
HRP	Horseredish peroxidase
IL	interleukin
iNOS	nitric oxide synthase
i.p.	Intra-peritoneal
LPS	lipopolysaccharide
MBP	myelin basic protein
MCP-1	monocyte chemoattractant protein-1
M-CSF	macrophage colony stimulating factor

MHC II	class II major histocompatibility
MIF	macrophage/microglial inhibitory factor
MIP	macrophage inflammatory protein
mRNA	messenger ribonucleic acid
NFκB	Nuclear Factor kappa B
NGF	nerve growth factor
NO	nitric oxide
OPC	oligodendrocyte precursor cell
RT-PCR	reverse transcriptase polymerase chain reaction
SCI	spinal cord injury
SDS	Sodium dodecyl sulfate
SDS-PAGE	SDS polyacrylamide gel electrophoresis
TNF-α	tumor necrosis factor alpha
TUNEL	Terminal deoxynucleotidyl Transferase Biotin-dUTP Nick End Labeling

Acknowledgements

Throughout graduate school many people have been supportive of me and my work and have helped me through the years. First and foremost I would like to thank my thesis advisor, Dr. Stella Tsirka, for molding me into scientist and helping me to think analytically and skeptically, and thank you for being a wonderful friend. I loved working with you.

I would also like to thank my thesis committee members, Joel Levine, Holly Colognato, and Sanford Simon, for your time, thoughts and guidance throughout my thesis work.

Of particular note I would like to give special thanks to my lab members, Kyungmin Ji, Hayian Zhai, Jill Cypser, Noreen Bukhari, Ariel Abraham, Yao Yao and Zhen Giao, who have worked with me through the years and helped in critiquing my data. I would also like to thank past lab members, Wesley Nolin, Iordanis Gravanis, Martine Mirrione and Muzho Wu, that took time out of their busy schedules to teach me all the methods and procedures that I now use daily.

Lastly, but most important I would like to thank my family. I would like to thank my mother and father for their unconditional love and support throughout graduate school and my whole life. You have always driven me to excel in anything that I did and if I failed you were always there to cushion my fall. I would have not made it this far in life without you being my backbone especially at times when I felt I would not succeed. I love you both dearly. I would like to also thank my Aunt Fran, who understood me and what I was going throughout graduate school when no one else did. And finally I would like to thank my fiancé, James. It was a difficult road and hard for someone not scientifically inclined to understand the passion and drive that

motivated me but you stood by me in the good times and the bad, trying to be understanding and supportive throughout obtaining my Ph.D., I thank and love you for that.

Dedicated in Loving Memory of My Grandmother, Antoinette DiRusso

Chapter I

General Introduction

Spinal Cord Injury

The mammalian CNS is a complex organ comprised of highly specialized cells that are divided into four major groups; neurons, astrocytes, oligodendrocytes and microglia. Injury to the CNS causes reactive cellular changes that physically and chemically alter the neural environment. Depending on the degree of pathology, the cellular response can be reparative or degenerative (Schwab and Bartholdi, 1996; Hagg and Oudega, 2006), although the latter appears to be predominant.

Of the many CNS pathologies, spinal cord injury (SCI) can be one of the most devastating, afflicting approximately 2.5 million people worldwide (Schwab et al., 2006). The location and severity of the impact determines the degree of loss of sensory, motor and autonomic functions. There are three phases of SCI: acute (seconds to hours after the injury), secondary (hours to weeks after the injury), and chronic (months to years after the injury). In each phase a variety of cells are affected and themselves become involved in the injury outcome: these include cells from the nervous, immune, and vascular systems. The cellular response and molecular events that occur in each phase can be involved both in the healing process as well as in further damage.

SCI occurs when a sudden impact crushes or tears the spinal tissue causing immediate cell death within the site of impact (the lesion epicenter). The impact leads largely to necrosis that results in the instantaneous death of neurons and glia at the site of injury. Following the initial injury, ischemia and membrane depolarization occur leading to the release of the excitatory neurotransmitter glutamate, which reaches toxic levels by 15 minutes following insult (Wrathall et al., 1996). The cellular necrotic debris triggers an inflammatory response within minutes. Chemokines, such as CCL2, CCL3, CXCL2/3 and CXCL10 (Rice et al., 2007), produced by parenchymal immunocompetent cells, the microglia, are upregulated in minutes, and recruit and activate peripheral polymorphonuclear leukocytes and monocytes (Wolpe et al., 1988; Wolpe and Cerami, 1989; Carr et al., 1994; Xu et al., 1996). Within hours the gene expression of several pro-inflammatory cytokines and their receptors is upregulated (Ahn et al., 2006). Studies of the acute phase of SCI in animals have revealed that a plethora of inflammatory genes are upregulated such as IL-β, IL-6, macrophage inflammatory protein-1α (MIP-1α), and MIP-2. Microarray analysis has also shown that the expression of genes linked to neuronal function is decreased at 6h following insult, which is ascribed to neuronal loss. The early release of pro-inflammatory cytokines and chemokines following injury mediates the recruitment of inflammatory cells to the injury site and leads to the development of secondary damage. Over time the injury expands and cells that survived the initial impact may become damaged or undergo apoptotic cell death, which is referred to as secondary injury (Crowe et al., 1997; Liu et al., 1997).

Secondary Injury and the glial scar

Biochemical and cellular events are triggered by the initial injury and mediate secondary apoptotic cell death that destroy neurons, cause demyelination, and trigger an inflammatory immune response (Liu et al., 1997; Beattie et al., 2000). A contributing factor to secondary injury is reactive gliosis, a term used to describe a milieu characterized by the accumulation of myelin debris and remnants of damaged axons which attract various types of glial cells to the site of injury and lead to glial cell activation. Glial cells that contribute to reactive gliosis following trauma include astrocytes, oligodendrocyte precursor cells (OPCs), and microglia (Fawcett and Asher, 1999). Over time these cells form a dense matrix that acts as a physical and biochemical barrier around the lesion epicenter, and is called the gliotic or glial scar (Liuzzi and Lasek, 1987; Rudge and Silver, 1990; Fitch and Silver, 1997; Tan et al., 2006).

Astrocytes are the main cellular component of the glial scar. They become hypertrophic and form a dense barrier of cells in response to nervous system trauma. Reactive astrocytes secrete and express growth promoting molecules as well as growth inhibitory molecules, such as laminins and proteoglycans, respectively. Proteoglycans are extracellular matrix (ECM) molecules that consist of a protein core linked by four sugar moieties to sulfated glycosaminoglycan (GAG) chains. Astrocytes can express four types of proteoglycans: heparan sulfate proteoglycan (HSPG), dermatan

sulfate proteoglycan (DSPG), keratin sulfate proteoglycan (KSPG) and chondroitin sulfate proteoglycan (CSPG). The family of CSPG includes aggrecan, brevican, neurocan, NG2, phosphacan and versican, and following injury the expression of these CSPG molecules increases in and around the lesioned area (Levine, 1994; McKeon et al., 1999; Asher et al., 2000; Jones et al., 2002; Jones et al., 2003; Tang et al., 2003). Reactive astrocytes are not the only cell types that express proteoglycans found within the glial scar; OPCs (Levine and Stallcup, 1987; Stallcup and Beasley, 1987; McTigue et al., 2001) and peripheral macrophages express the CSPG, NG2 (Smirkin et al.; Bu et al., 2001; Jones et al., 2002). *In vitro* and *in vivo* work from various groups has demonstrated the inhibitory properties of CSPGs on axon outgrowth (Levine and Stallcup, 1987; Levine, 1994; Asher et al., 2000; Tan et al., 2006). When axons, in an attempt to regenerate, encounter the environment of the glial scar, dystrophic endbulbs form. Activated glial cells express proteoglycans and this expression is concentrated around the lesion epicenter. Accumulated CSPGs alter the regenerative capacity of axons, which is determined by the interactions with the neuronal growth cones and molecular environment, thus limiting axonal regeneration within the lesion.

Inflammation is another factor that is associated with secondary degeneration or damage and results in the apoptosis of neurons and myelinating oligodendrocytes and in the reduction of neuronal function (Blight et al., 1995; Popovich et al., 1997; Gonzalez et al., 2003; Glaser et al., 2004). In fact, the inflammatory response in the spinal cord is substantially greater than the

inflammatory response in the brain following injury (Schnell et al., 1999). The initial contributors to the immune response in the CNS are the resident immunocompetent cells, microglia. These cells migrate to the site of damage and rapidly become activated, releasing pro-inflammatory cytokines, reactive oxygen species and proteases that are thought to contribute to the bystander damage (Popovich et al., 2002). Conversely, microglia can promote neuronal regeneration by phagocytosing (and thus removing) myelin debris and by releasing trophic and anti-inflammatory factors (Rabchevsky and Streit, 1997). Other inflammatory cells that invade the lesioned area, through a compromised blood brain barrier (BBB) or blood spinal cord barrier (BSB), at later time points are peripheral immune cells such as neutrophils, macrophages, and T-lymphocytes, which express a cocktail of cytokines. The cytokines released by parenchymal cells and peripheral immune cells are thought to promote detrimental effects through the generation of free radicals, that may lead to apoptotic death (Hu et al., 1997). One of the most well studied cytokines is TNF–α, which accumulates quickly at the site of SCI (Bethea et al., 1999) and attributes to cell death of oligodendrocytes and the consequent demyelination of spared axons. TNF–α can be produced by various cells types such as neutrophils, macrophages, microglia, astrocytes and T cells (Yan et al., 2001), stimulating the production of other cytokines and promoting migration of cells to the injury. Another cytokine that has an opposing effect is IL-10, which is produced by many of the same cells as TNF-α. IL-10 administration has been shown to be neuroprotective after

experimental spinal cord injury, possibly by inducing antiapoptotic genes and suppressing the inflammatory response, as it inhibits the synthesis and release of pro-inflammatory mediators such as TNF-α, IL-1β, IL-6, IL-8, and IL-12 (Howard et al., 1992; Brewer et al., 1999; Moore et al., 2001)

Microglia

The CNS is considered an immune-privileged organ, a term that infers that only a few immune cells are found present in the tissue under normal physiological conditions. This sparsity of immune cells is due to the presence of the blood brain barrier (BBB) and blood-spine-barrier (BSB), which are physical and metabolic barriers between the CNS and the systemic circulation and prevent the CNS entry of pathogens and peripheral immune cells. Microglia, the resident innate immune cells of the CNS, are not of neuroectodermal, but rather of mesodermal and monocytic origin. These macrophage-like cells, originate in the bone morrow, migrate to the CNS during embryogenesis and differentiate into resident microglia that contribute to normal neural development and CNS function (Perry et al., 1985; Morris et al., 1991; Takahashi, 1994; Rezaie and Male, 2002; Chan et al., 2007). During neurogenesis microglia assume an ameboid morphology consisting of round somata with short lamellopodial extensions, analogous to peripheral phagocytes, where they function in the removal of apoptotic neurons. In development, the ameboid forms of microglia are precursors of

ramified or “resting” cells that possess many processes necessary for neural tissue surveillance (Kaur et al., 2001).

Microglia present the first line of defense against pathogens and injury through antigen presentation, cytokine secretion, and phagocytosis (Hanisch and Kettenmann, 2007). In response to a variety of CNS insults such as SCI, microglia reactivate, migrate to and accumulate at the site of injury, retract their processes, and assume an ameboid shape, an event known as microglial activation or microgliosis (Rock et al., 2004). Microglia have the capacity not only to dramatically change their morphology, but also to rapidly up-regulate a large number of receptors, as well as, produce and release a plethora of secretory products that are thought to contribute to the defense of, or promote secondary injury to the spinal cord.

Reactive microglia and macrophages are present several months following injury (Hausmann, 2003) releasing various factors in the CNS parenchyma including cytokines, chemokines, and growth factors that can be both beneficial or harmful. Rabchevsky and colleagues demonstrated that microglia have regenerative properties, as grafting cultured microglia into an injured spinal cord promoted axonal regrowth into the lesioned area (Rabchevsky and Streit, 1997). These restorative effects could be due to the release of trophic factors, such as nerve growth factor (NGF), neurotrophin-3 (NT-3), interleukin (IL)-1α, IL-10, and brain derived growth factor (BNDF), which influence axon regeneration. Reactive microglia are also active phagocytes and following SCI are involved in the removal of

degenerating axons and inhibitory myelin debris, where the removal of tissue debris enhances the regeneration of axons. Conversely, microglia can generate toxic molecules that potentially damage neurons and surviving glial cells when released into the extracellular milieu. These toxic molecules include reactive oxygen intermediates (ROIs), reactive nitrogen intermediates (RNIs), tumor necrosis factor-α (TNF-α), IL-6, and IL-1β (Lee et al., 1993; Hanisch, 2002). Pro-inflammatory cytokines produced acutely after spinal cord injury, primarily by activated microglia, lead to a secondary response (Bartholdi and Schwab, 1997; Pineau and Lacroix, 2007). Suppressing the local inflammatory response following SCI has been demonstrated in some reports to reduce secondary injury around the lesion epicenter and improve functional outcome (Gris et al., 2004).

Controversy however exists over the neurodegenerative versus neuroregenerative roles of activated microglia, and which role predominates in SCI. There are increasing data supporting the idea that the early phases of inflammation are deleterious, whereas the later phases of inflammation are protective. Hence, the goal of this work was to address the function of microglia activation following severe spinal cord trauma by ablation of microglia in transgenic mice or, administration of natural inhibitors of microglial activation to wild-type mice.

Table I-1. Phases and events following spinal cord injury

Primary damage (0-2hours)	Acute Phase (1-2 days)	Secondary Phase (3-14days)	Chronic Phase (days-months)
Primary mechanical injury Severing or crushing of axons Necrotic cell death Microglial activation Release of pro-inflammatory cytokines (IL-β, TNF-α, and IL-6)	ROS production Glutamate – mediated toxicity Neutrophil invasion Early demyelination (oligodendrocytes cell death) Neuronal death Release of anti-inflammatory cytokines	Macrophage infiltration Formation of Astrogliotic scar Lesion stabilization Continued demyelination	Wallerian degeneration Potential structural and functional plasticity of spared tissue

Chapter II

Methods and Materials

Animals and genotyping *(All chapters)*

For microglial ablation experiments, transgenic mice expressing herpes simplex thymidine kinase (TK) under the CD11b promoter (CD11b-HSVTK$^{+/-}$) in cells of monocytic origin were generated (generous gifts from Drs Frank Heppner and Adriano Aguzzi) (Heppner et al., 2005). Mice were backcrossed to C57Bl/6 mice for 9 generations. Since a phenotype of HSVTK transgene expression is male sterility, wild-type males were bred with heterozygous females (CD11b-HSVTK$^{+/-}$) and offspring were genotyped via RT-PCR with the following sense and anti-sense primers: 5'-GACTTCCGTGGCTTCTTGCTGC-3' and 5'-GTGCTGGCATTACAGGCGTGAG-3'. Male mice were used for spinal cord injury and wild-type (wt) littermates were used as controls whenever possible along with additional C57Bl/6 wt animals. For experiments inhibiting microglial activation, wt mice were used for all conditions.

Dorsal Hemisection Spinal Cord Injury Model *(All Chapters)*

Mice were anesthetized using isoflurane and a dorsal hemisection was performed by generating an incision at the T8 thoracic vertebra. An incision was made in the skin rostrocaudally, which exposed the spinal column. To gain access to the spinal column, muscles and ligaments

surrounding the spinal column were torn and cut. Once exposed, the vertebra at the T8 area was filed away with a dental drill to decrease the bone thickness, such that it was possible to break it away from the cord without causing any damage to the cord. The remaining bone was removed with forceps and a micro-scissor. The exposed spinal cord was initially cut in a dextro-sinister direction using a fine (271/2) gauge needle followed by cut with a micro-knife. Following the hemisection, micro osmotic pumps (Alzet) were placed under the skin and sutured under the muscle, so that the contents were distributed over the lesioned area. The muscles and skin above the injury site were sutured and the animals were administered buprenorphine and placed on the heating pad until fully recovered from the anesthesia. Bladder expression was performed on the mice daily and behavioral symptoms (paralysis of the hind legs) were monitored until specific time points post injury when the mice were euthanized and analyzed. All animal procedures were approved by the Institute for Animal Care and Use Committee (IACUC) at Stony Brook.

Drug administration *(All Chapters)*

GCV (100μg/g of body weight/day) was either injected intraperitoneally from 0 days post injury (dpi) to 3dpi or from 3dpi to 7dpi or delivered via micro-osmotic pump for 7 continuous days following injury. MIF (100μg/g of body weight/day) was administered via micro-osmotic pump directly on the lesioned area for 0dpi to 7dpi or for 0dpi to 14dpi.

Immunofluorescence *(All Chapters)*

Terminally anesthetized mice were perfused trans-cardially with PBS, followed by 4% paraformaldehyde in PBS (pH 7.4). Spinal cords were isolated, post fixed for 1 h and cryoprotected in 30% sucrose overnight. Frozen sections (18μm) were prepared, blocked for 1 h with blocking solution (5% serum and 0.1% triton-X100 in PBS) and then incubated with primary antibodies in diluted blocking solution overnight at 4^{o}C. Sections were washed and incubated with conjugated secondary antibodies for 1 hr. Slides were then washed and coverslips were mounted with fluoromount G.

Immunoperoxidase Staining *(Chapters III & IV)*

Sections were incubated for 2 minutes in 3% hydrogen peroxide to block peroxidase activity. Sections were then washed blocked for 1h in blocking solution, followed by an overnight incubation of diluted primary antibody at 4^{o}C. After a second wash series, diluted secondary antibody conjugated to biotin was added to the sections for 1h. Sections were then incubated for 30 min with horseradish peroxidase-streptavidin ABC reagent (Vector Laboratories) Following wash the sections were incubated with DAB for 5 minutes or until the chromogenic reaction fully developed. Slides were dehydrated in an ethanol series followed by two 2 min incubations in xylenes, and were mounted with Permount (Fisher).

***In vivo* quantification** *(All Chapters)*

For the quantification of microglia/macrophages, astrocytes, oligodendrocytes, OPCs and CSPGs, six 40X field were imaged from various areas surrounding the lesion (Figure II-1) and cell number or fluorescent intensity was quantified.

Immunocytochemistry *(Chapters IV & VI)*

Cells were washed of media and generally fixed with 4%PFA (unless otherwise denoted). Following 3 gentle washes cells were blocked for 1 h with blocking solution (same as immunohistochemistry), diluted primary antibodies were added and incubated for 2h at RT. Cells were washed and incubated with conjugated secondary antibodies for 1 hr. Chamber slides or coverslips were then washed and mounted with Fluoromount G.

Primary Antibodies *(All Chapters)*

Primary antibodies used include: activated caspase-3 (Sigma), rat anti-F4/80 (Serotec), rabbit-anti BrdU, sheep anti-BrdU, rabbit anti-iba-1 (Wako), goat anti-CTB (List Biologicals), rabbit anti- GFAP (DAKO), mouse anti-CS56 (Sigma), rabbit anti-NG2 (a generous gift from Joel M. Levine), anti-neurocan (DSHB) and rabbit anti-ki67 (AbCam) mouse anti-CC1, rat anti-MBP (AbD Serotec), and mouse anti-CNPase (Sigma).

Tissue collection for Immunoblotting and ELISA *(All Chapters*)

To quantify protein and cytokine expression a separate group of mice were used and perfused with PBS. The spinal cords from these mice was isolated and immediately frozen at –80^{o}C.

Immunoblotting *(All Chapters)*

Immunoblots were performed on spinal cord homogenates and total cell lysates. The protein content was quantified by Bradford assay (Bio-Rad). Aliquots of samples were denatured and reduced with sodium dodecyl sulfate (SDS) and β-mercaptoethanol and equivalent concentrations of total protein were separated by SDS-PAGE. The proteins were electrotransfered onto polyvinylidene difluoride (PVDF) membranes. Non-specific protein binding was blocked by preincubation with 5% FBS in PBS for 1 hr at room temperature (RT), The membranes were incubated with primary antibodies overnight at 4°C, washed and then probed with peroxidase conjugated secondary antibodies. Densitometry was performed on images of immunoblots for quantification with image J software. For quantitative analysis, membranes were preincubated with Odyssey blocking buffer (LI-COR Biosciences) in PBS (1:1), and probed with primary antibodies in Odyssey blocking buffer in PBS + 0.2% Tween-20. Membranes were probed with anti-rabbit IR dye 800 (Rockland), anti-rat Alexa Fluor 680 and anti-mouse Alexa Fluor 680 (Molecular Probes Inc.) diluted in PBS-T. The Odyssey Infrared Imaging System (LI-COR Biosciences) was

used to detect the proteins of interest and quantify their levels. Quantification was performed with the Odyssey application software 2.1.

Enzyme Linked Immuno-Absorbent Assay (ELISA) (*Chapters III & IV)*

Spinal cord tissue from various time points issue was homogenized and sonicated. Total protein concentrations were determined using the Bradford Assay. Protein concentrations of IL-10 and TNF-α were determined utilizing the BD OptEIA quantitative sandwich enzyme immunoassay per manufacturer's protocol. Briefly, 96 well plates were coated with diluted Capture antibody (100 µl per well) and incubate overnight at 4°C. The plates were then blocked for 1 hr at RT with Assay Diluent (200 µl per well) followed by a 2h incubation of standard or sample (100 µl per well). Working detector solution (100 µl per well) was then added and incubated for 1 hr RT, followed by substrate solution (100 µl per well) was then added and incubated for 30 min at RT in the dark followed by 50 µl of Stop Solution. Absorbancies of each well were read at a 450 nm light wavelength with a microplate reader.

Primary microglial cell cultures *(Chapters IV & VI)*

Cerebral cortices from postnatal day 1 C57BL/6J mice were dissected, digested with trypsin (0.25% in HBSS) for 10 mins at 37^{o}C, and mechanically dissociated by trituration. Mixed cortical cells were plated in DMEM medium, 10% FBS, 1% sodium pyruvate and gentamycin on poly-D-

lysine coated dishes. After 10 days microglial cells were dislodged by the addition of 12mM lidocaine and shaking, and the isolated microglia were seeded on poly-D-lysine coated coverslips.

Biotinylation of MIF and diffusion within the spinal cord *(Chapter IV)*

MIF was conjugated to biotin label using EZ-Link NHS-Biotin (Thermo Scientific) by incubating MIF with the EZ-Link biotin on ice for 2h. MIF conjugated to biotin was then administered *in vivo* via a 7-day micro-osmotic pump. At 7dpi mice were euthanized and biotin label was analyzed by incubating the spinal cord slices with strepavidin conjugated Alexa Fluor 555. (n=3)

Quantification of lesion volume *(Chapter V)*

To analyze lesion volume alternating sagittal spinal cord sections were stained with the astrocytic marker GFAP since astrocytes form the border of the lesioned area. Lesion size was analyzed from digital images of 5 alternate sections (2 sections right of the center of the lesion, 1 section of the approximate center of the lesion and 2 section left of the center of the lesion) that had been immunofluorescently stained as described above. The lesion was defined as the area devoid of stain bordered by GFAP+ staining. Data from each time point and treatment group where compared using the one-way ANOVA statistical method.

Primary oligodendrocyte cultures *(Chapter VI)*

Cerebral cortices from postnatal day 1 C57BL/6J mice were dissected, digested in HEPES/MEM, 30units/ml papain, 0.24mg/ml l-cysteine, and 40μg/mlDNase for 60 mins at 37°C, and mechanically dissociated. Cells were plated on PDL coated flasks in DMEM 10% FBS, penicillin, streptomycin and gentamicin. Every 3 days media was changed, at day 10 microglia were shaken off for 1 hr at 200rpm and fresh media was added to culture. To isolate OPCs the flasks were then shaken for 24 hrs at 350rpm. To remove any remaining microglia, media from the flask was transferred to a 10cm bacteriologic plastic dish for 30 minutes. Media was then pipetted several times to remove any loosely attached OPCs. OPCs were then resuspended in SATO (DMEM, 5000 U/ml penicillin/streptomycin, 4 mM L-Glutamine (Sigma), 16 μg/ml putrescin (Sigma), 400 μg/ml L-thyroxine (Sigma), 400 μg/ml Tri-iodothyroxine (Sigma), 6.2 ng/ml progesterone (Sigma), 5ng/ml sodium selenite (Sigma), 100 μg/ml BSA fraction V (Sigma), 5 μg/ml insulin (Sigma), 50 μg/ml holo-transferrin (Sigma)).

Microglia and Oligodendrocyte Coculture *(Chapter VI)*

Eight well chamber slides were coated with PDL overnight at 37°C. Chambers were washed and OPCs were plated (20,000 cells/chamber) either in SATO with 0.5% FBS or in SATO with 10ng/ml PDGF (PeproTech) and 10ng/ml FGF (PeproTech) to facilitate differentiation or maintain the

progenitor population, respectively. After 2 d, microglial cells were added to the chamber slides and allowed to adhere for 24 hrs. The cells were then either treated with 20ng/ml LPS, 5mM MIF, or then combination of both at 5 days cells were fixed with 4% PFA.

TUNEL assay *(Chapter VI)*

TUNEL assays were performed by using the ApopTag Fluorescein *In Situ* Apoptosis Detection Kit (Chemicon) per manufacturer's protocol. Briefly, sections were fixed in 4% PFA in PBS, pH 7.4 for 10 minutes at RT. Following washing in PBS, sections were post-fixed cold ethanol:acetic acid 2:1 for 5 minutes at -20°C and then washed again. Equilibration buffer was then added directly on samples and incubated for 10 seconds at RT. The liquid was then drained and working strength TdT enzyme was applied to each specimen and incubated at 37°C for 1h. Samples were then immersed in stop/wash buffer for 10 min at RT followed by 3 PBS washes. Anti-Digoxigenin conjugate was then added directly to samples and incubated for 30 minutes at RT in the dark. After, sample were washed, counter stained and mounted with Fluoromount-G with DAPI according to the immunohistochemistry protocol above.

BrdU proliferation assay *(Chapter III & VI)*

Cellular proliferation was examined by using the 5-Bromo-2´-deoxy-uridine Labeling and Detection Kit II (Roche) according to manufacturer's protocol. Briefly, mice were injected intravenously via tail vein injections with

10mM BrdU (2 ml/100 g body weight) or cells were incubated with 10μM BrdU. Mice were treated for up to a 7 day time period via tail vein injection and cells were treated with BrdU for 24 h. Cells and section were fixed or post-fixed and incubated in 2 N HCl for 90 min to hydrolyze the DNA followed by immersion in 0.1 M sodium borate for 5 min. Sections or cells were probed for BrdU via the mouse anti-BrdU antibody provided and stained with a fluorescently conjugated secondary antibody.

Eriochrome Cyanine stain *(Chapter III)*

Spinal cord sections were air-dried for 1h at RT followed by 1h incubation at 37°C. Sections were incubated with acetone for 5 mins, air-dried for 30 mins and placed in eriochrome cyanine solution (0.2% eriochrome cyanine (Sigma), 0.5% H_2SO_4 (Sigma), 10% iron alum (Sigma) in distilled water) for 30 min. Then sections were differentiated for 10 mins in 5% iron alum (Sigma) diluted in distilled water, incubated in borax-ferricyanide solution (1% borax (Sigma), 1.25% potassium ferricyanide (Sigma), in distilled water) for 5 mins, dehydrated via graded ethanol solutions and coverslipped using Permount (Fisher Scientific).

Electron Microscopy *(Chapter VI)*

Mice were deeply anesthetized and transcardial perfused for 1 hr with Karlsson-Schultz fixative (4% formaldehyde, 2.5% glutaraldehyde, 0.5% NaCl, 0.1 M phosphate buffer pH 7.4). Spinal cords were isolated and post fixed

over night with perfusate. Areas of interest were blocked and then vibratomed at approximately 50um in ice cold PBS. Samples were then placed in 2% osmium tetroxide in 0.1M PBS, pH 7.4, dehydrated in a graded series of ethyl alcohol and embedded with Durcupan resin in between two pieces of ACLAR sheets (EMS, Hatfield,Pa.). Ultrathin sections of 80nm were cut with a Reichert-Jung UltracutE ultramicrotome and placed on formvar coated slot copper grids. Sections were then counterstained with uranyl acetate and lead citrate and viewed with a FEI Tecnai12 BioTwinG^2 electron microscope. Digital images were acquired with an AMT XR-60 CCD Digital Camera system.

Retrograde Axonal Tracing *(Chapters III & VI)*

Retrograde neuronal tracing was performed via injection the cholera toxin Beta-subunit (CTB) following injury. Four days prior to euthanization, the mice were re-anesthetized, with a constant delivery of isoflurane, and the right sciatic nerve was exposed. Two microliters of a 1.5% solution of CTB (List Biological Laboratories) was injected into the nerve using a Hamilton syringe. The solution was slowly injected over an 1 min period and the syringe was withdrawn over an additional 2 mins to prevent reflux. The muscle and skin were then sutured. Spinal cords were isolated, and cryosectioned at a18μm thickness. Alternating sections were stained against CTB via goat anti CTB genotoxiod (List Biologicals) and detected with a fluorescently conjugated secondary. The ImageJ software (NIH) was used to measure the pixel density of axons stained against CTB with in the lesioned area.

Figure II-1

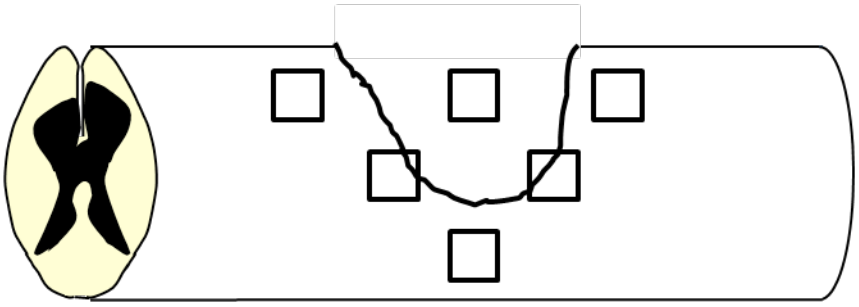

Figure II-1. Diagram of imaged areas for *in vivo* quantification.
Quantification of cells and CSPGs was performed by imaging six 40x fields surrounding the lesioned area including the epicenter and the penumbra, where boxes denote fields taken.

Chapter III

Selective ablation of microglia promotes axonal regeneration following spinal cord injury.

Introduction

Microglia are the first immune cells that respond to CNS injury. The ultimate goal of microglial activation following injury is to restore neural tissue homeostasis by removal of inhibitory cellular debris and facilitating tissue repair and axon regeneration. Unfortunately, considerable evidence points towards microglial activation as deleterious. Activated microglia can induce degeneration of neurons and damage oligodendrocytes, either directly through the release of neurotoxic mediators or indirectly by recruiting peripheral immune cells into the CNS. Preliminary data suggest that pharmacologically altering microglial activation with minocycline (Tikka et al., 2001; Ekdahl et al., 2003; Tan et al., 2009), naloxone (Chang et al., 2000; Liu et al., 2000) and dextromethorphan (Liu et al., 2003) has neuroprotective affects in various disease models, although these drugs are not microglial cell specific and can affect other immune cells. Determining the contribution of microglia to disease progression will be invaluable. Since microglia produce reparative and degenerative factors following injury, it is hypothesized that the

spatiotemporal distribution of microglia determines their neuroprotective and neurotoxic properties.

In this chapter, we sought to determine the properties of microglia in a spatiotemporal manner by conditionally ablating microglia in CD11b-HSVTK$^{+/-}$ transgenic mice. CD11b-HSVTK$^{+/-}$ transgenic mice have been used in various models of neurodegeneration, such as pilocarpine induced seizures and experimental autoimmune encephalomyelitis (EAE) where ablation of microglia reduced seizure severity and significantly reduced clinical EAE symptoms, respectively (Mirrione et al.; Heppner et al., 2005). Organotypic hippocampal slice cultures of CD11b-HSVTK$^{+/-}$ brains have shown that with GCV treatment, the release of nitrite, TNF-α and macrophage inflammatory protein (MIP)-1 was abrogated (Heppner et al., 2005). CD11b-HSVTK$^{+/-}$ animals express the herpes simplex thymidine kinase (HSVTK) in cells of monocytic origin under the control of the CD11b promoter. Cells that express the *HSVTK* suicide gene are sensitive to the drug ganciclovir (GCV), a synthetic analogue of 2'-deoxy-guanosine. When administered to CD11b-HSVTK$^{+/-}$ mice, the drug ganciclovir (GCV) is first converted to its monophosphorylated form by HSVT-K, and then into a toxic triphosphate by endogenous cellular kinases (Fyfe et al., 1978). These toxic triphosphates competitively inhibit the incorporation of dGTP by DNA polymerase, resulting in the termination of DNA elongation and apoptosis of proliferating cells (Elion, 1980) of monocytic origin that are CD11b positive. The GCV-triphosphate is incorporated into replicating DNA by cellular

DNA polymerase, thereby arresting DNA replication and causing cell death (Elion, 1980).

Results

GCV effectively ablates microglia following SCI

Dorsal hemisections were performed on male CD11b-HSVTK$^{+/-}$ transgenic mice or wt litter mates, and GCV was administered intraperitonally or via a micro-osmotic pump (Heppner et al., 2005). First to determine if GCV effectively ablated microglia in the dorsal hemisection spinal cord injury model, GCV was administered for 7 full days via osmotic pump. Immunohistochemical analysis showed that GCV was non-toxic when injected in wild-type mice that did not express HSVTK, but when administered to mice expressing the transgene, microglia were significantly ablated (Figure III-1). Endogenous thymidine kinases can monophosphorylate GCV but HSVTK is 1000 times more efficient thereby inducing cell death in cells that express the transgene (Elion et al., 1977). The administration of GCV in transgenic mice did not significantly affect the number of Iba-1 positive cells 24 h after injury, but did so at 3, 7, and 14 dpi (Figure III-1A). Since GCV affects proliferating monocytic cells, the observed delay in reduction of microglia numbers with GCV treatment was due to microglial proliferation which is maximal between 48–72 h after SCI which was confirmed via BrdU (Figure III-2).

To confirm that microglia were being ablated, spinal cord homogenates from mice that were injured and treated with GCV or PBS for

7 days were subjected to SDS-PAGE electrophoresis and the levels of the microglial marker F4/80 was analyzed. In all time points examined, the post injury F4/80 levels were substantially less in the GCV groups in comparison to PBS groups (Figure III-3). Caspase-3 activation in F4/80 expressing microglia was also assessed following injury. Low numbers of microglia expressing the activated form of caspase-3 were detected in the WT spinal cords, while microglia in spinal cords isolated from HSVTK mice treated with GCV expressed higher numbers of activated caspase-3 indicating that the number of microglia undergoing apoptotic cell death increased with GCV treatment in the CD11b-HSVTK$^{+/-}$ mice most notably at 3dpi (Figure III-1B,C). Thus, proliferating microglia and macrophages were efficiently being ablated following GCV treatment in the CD11b-HSVTK$^{+/-}$ mice thereby reducing the number of activated microglia.

Ablation of microglia alters cytokine expression

Since microglia were ablated following GCV in CD11b-HSVTK$^{+/-}$ mice, microglial activation was presumably prevented thereby altering the release of pro-inflammatory or anti-inflammatory cytokines and chemokines. To determine the microglial contribution to cytokine expression at specific time points post injury, GCV was administered for particular time intervals post injury (0-3dpi, 3-7dpi, 0-7dpi). To verify whether the spatial location of microglia influenced cytokine production, the isolated cords were cut into three 3mm segments separating the epicenter and areas rostral and caudal

to the lesion. An ELISA assay was performed to determine cytokine expression for the pro-inflammatory cytokine TNF-α and the anti-inflammatory cytokine IL-10 and their potential association with different areas of the spinal cords at different time points post injury were examined. To ascertain microglial contribution to cytokine expression in the injured spinal cord, cytokine levels measured in wild-type spinal cords were compared with those of the spinal cords from the CD11b-HSVTK$^{+/-}$ mice treated with GCV. An early elevation in TNF-α expression was observed within the epicenter of wild-type mice and CD11b-HSVTK$^{+/-}$ mice that were treated for 3-7dpi. When microglia were ablated for 0-3dpi or 0-7dpi in CD11b-HSVTK$^{+/-}$ mice TNF-α levels were dramatically reduced within the epicenter (Figure III-4A). Analysis of regions rostral and caudal of the lesion epicenter showed a minor increase in TNF-α levels in wild-type mice and CD11b-HSVTK$^{+/-}$ mice where microglia were ablated for 3-7dpi in comparision to wild-type CD11b-HSVTK$^{+/-}$ mice that were treated with GCV for 0-3dpi or 0-7dpi. This data indicates that microglia are necessary for the acute expression of TNF-α particularly within the epicenter post injury. Interestingly, ablation of microglia early after injury (0-3dpi) had a beneficial effect, since the IL-10 levels were elevated in CD11b-HSVTK$^{+/-}$ at an earlier time point in comparison to wild-type. In contrast, ablation of microglial at the later time points (3-7dpi) reversed the effect on IL-10 production, indicating that microglia are critical in de novo production of IL-10 or are

indirectly stimulating other cells to secrete IL-10, at later time points post injury (Figure III-4B).

At early time points post injury, microglia located distal to the lesion seemed to express more IL-10 or induce expression of IL-10 in other cell types, as determined by the reduction in IL-10 expression observed when microglia are ablated. whereas at later time points post injury an increase of IL-10 within the epicenter was observed. It is possible that protective microglia migrate to the lesion epicenter to create a more trophic environment. Such possibility would justify the fact that when examining cytokine expression in various areas, TNF-α is localized around the lesion core and IL-10 is expressed within the lesion core and distal to the lesion.

The reduction in microglial population reduces demyelination, astrocyte cell reactivity and increases axon regeneration

Loss of myelin was evaluated at various time points post injury. Histologic evaluation of spinal cord coronal sections by eriochrome cyanine stain revealed reduced myelin stain intensity in the wild-type mice in comparison to the CD11b-HSVTK$^{+/-}$ mice (FigureIII-5A). Spinal cords were also examined for the presence of myelin basic protein (MBP) via immunofluorescence. At 1dpi the lesion epicenter displayed many fragments of what appeared to be myelin debris, although ablation of microglia showed a slight presence of myelin tubes present. A more notable difference was observed at 3dpi where the GCV treatment resulted in an

increase in MBP staining and myelin tubes bordering the lesioned area (Figure III-5B).

To trace axonal regeneration, the cholera toxin B (CTB) subunit was injected into the sciatic nerve four days before sacrificing the mice, as described by Tan et al (Tan et al., 2006). At 14dpi spinal cords were removed and immunohistochemistry was performed to visualize both the regenerated neurons and the astrocytes which would determine the lesion border. Compared to wild-type, in all GCV treatment groups there was an increase in CTB positive axons present within the lesioned area. Ablation of microglia for 7 full days resulted in increased axon entry into the lesion area (Figure III-6A,B,C). Microglia ablated at the later time points in the HSVTK mice resulted in more axonal growth than in wild-type litter mates, whereas the numbers of axons crossing the lesion border was less than that of the early GCV treatment (Figure III-6 B, C). Early microglial ablation (0-3dpi), yielded a significant increase in axon regeneration (Figure III-6B,C). Thus, it is possible that microglia that are present at later time points secrete neurotrophic cytokines and factors and the expression of these cytokines facilitate axonal regeneration while microglia that are present acutely after injury are associated with the secretion of deleterious factors.

Figure III-1

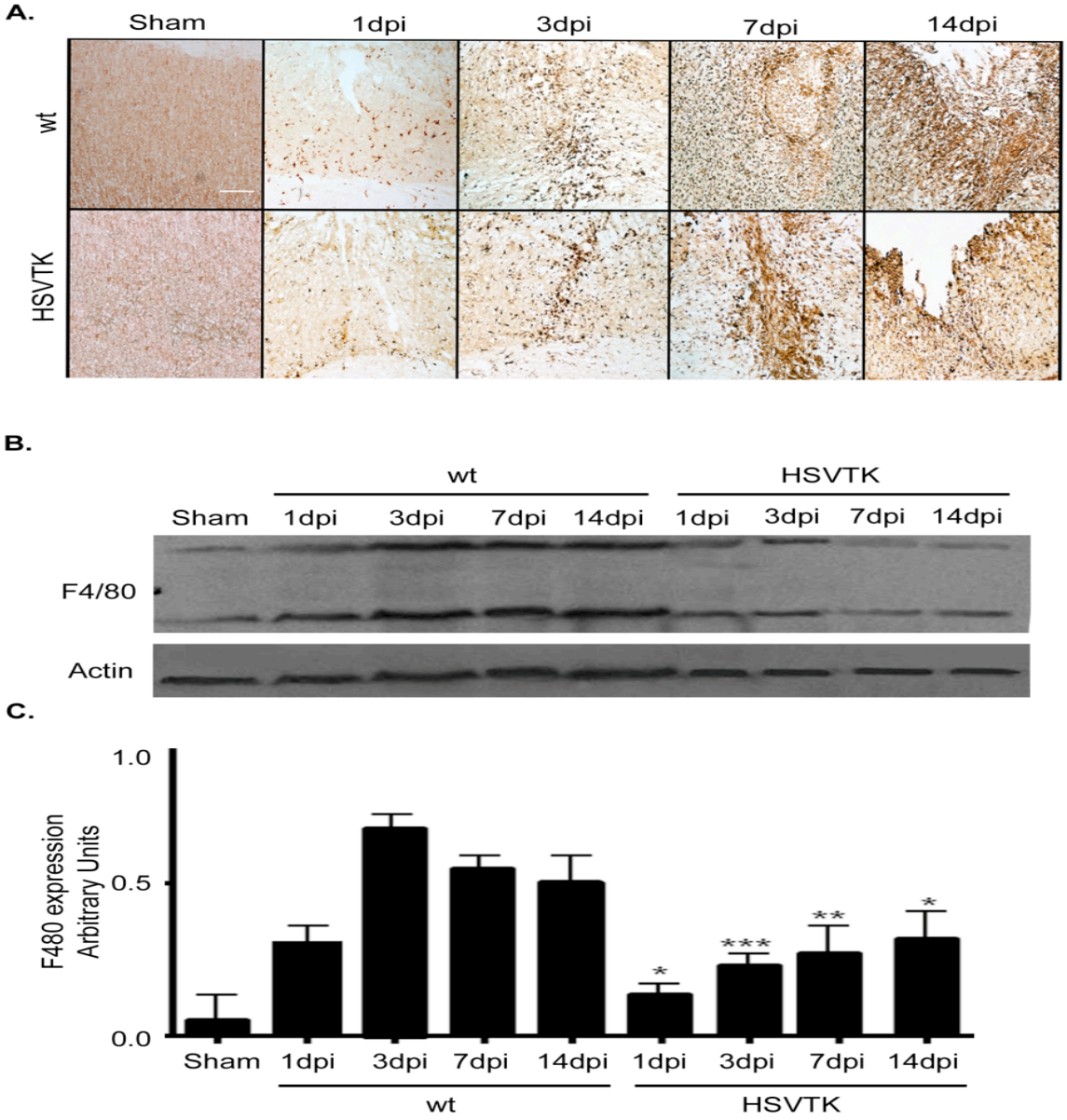

Figure III-1. Ganciclovir treatment causes ablation of microglia and macrophages in HSVTK mice.

HSVTK and wt spinal cords were treated with GCV for 7 consecutive days and spinal cord were isolated at various time points. **A**, Bright field images of 3, 3' diaminobenzidine (DAB) detection of Iba-1(brown) in sagittal sections of the lesioned area. **B,** Immunoblot analysis of F4/80 expression (double bands indicate glycosylation state) from wt and HSVTK spinal cord homogenates isolated at various time points post injury. **C**, F4/80 expression was quantified by densitometric analysis and wt and HSVTK expression of F4/80 at specific time points post injury was compared. Error bars represent SEM, where *p<0.05, **p<0.01, ***p<0.001 by ANOVA followed by Bonferroni's post hoc test. Scale bar: 200 μm

Figure III-2

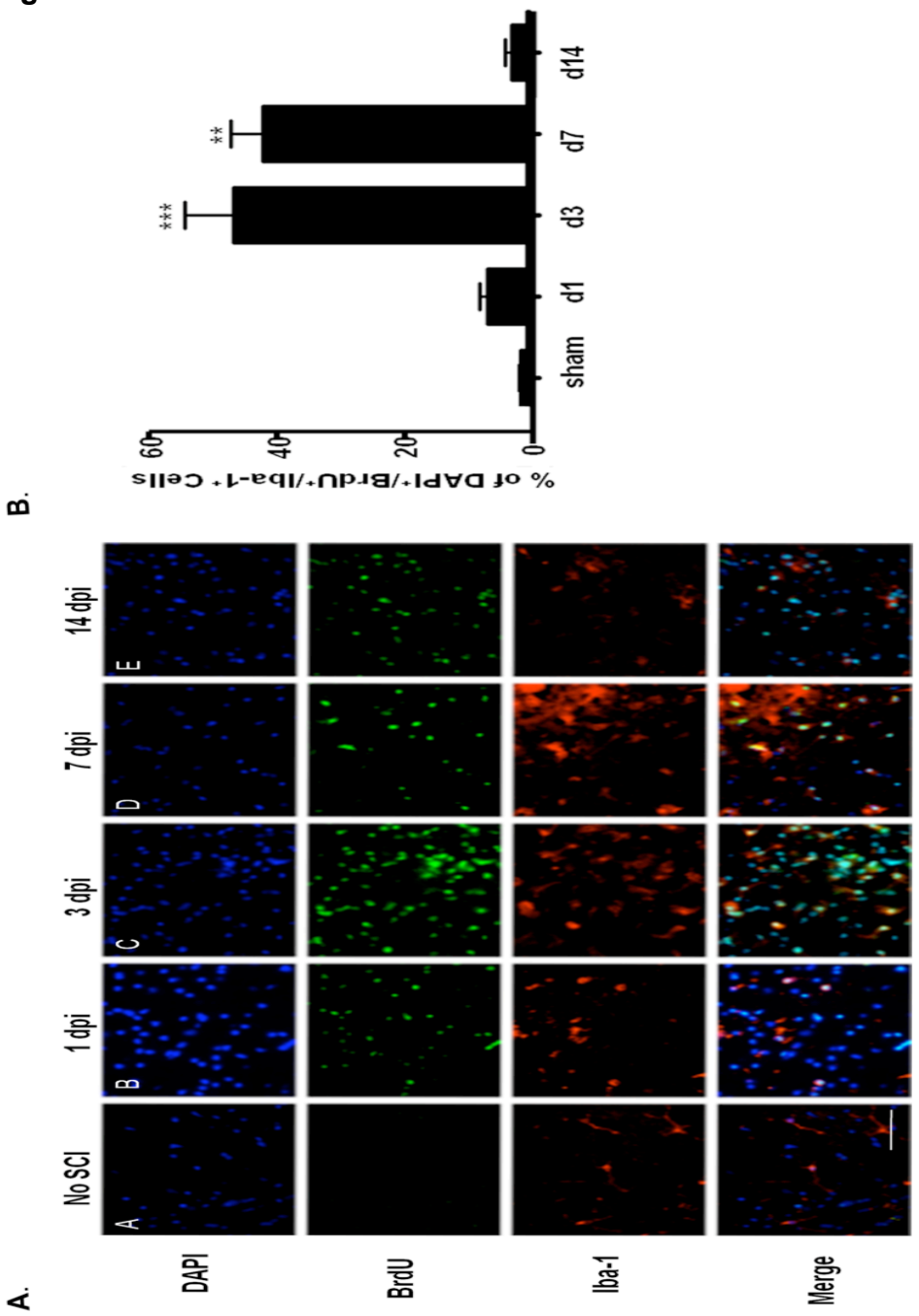

Figure III-2. Microglial proliferation peaks at 3 days injury.
Microglial proliferation was analyzed in wt injured spinal cords at various time point post injury via administration of BrdU via tail vein injections for 7 days. **A,** Fluorescent images of iba-1 expressing microglia (red), BrdU (green), and DAPI stained nuclei (blue). **B,** Quantification of proliferating microglia determined by the number of $BrdU^+$ iba-1 $^+DAPI^+$ divided by total iba-1^+cells. Error bars represent SEM, where $*p<0.05$, $**p<0.01$, $***p<0.001$ by ANOVA followed by Bonferroni's post hoc test Scale bar: 100μm.

Figure III-3

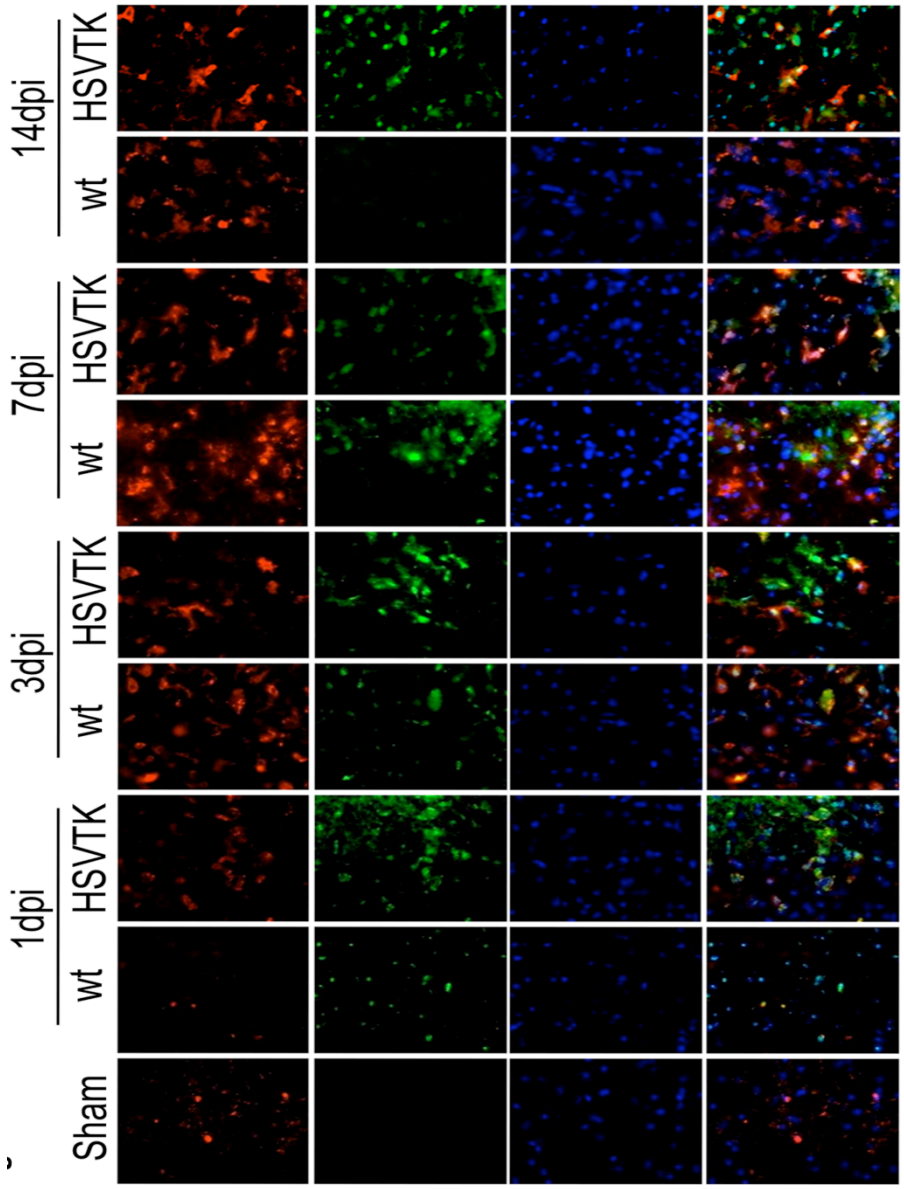

Figure III-3 Ganciclovir induces apoptotic cell death of microglia and macrophages in HSVTK mice.
Fluorescent images of sagittal sections stained against the pro-apoptotic marker activated caspase-3 (green) and the microglial marker, F4/80 (red), from wt and HSVTK spinal cords treated for 7 days with GCV. Scale bar: 100 μm.

Figure III-4

A.

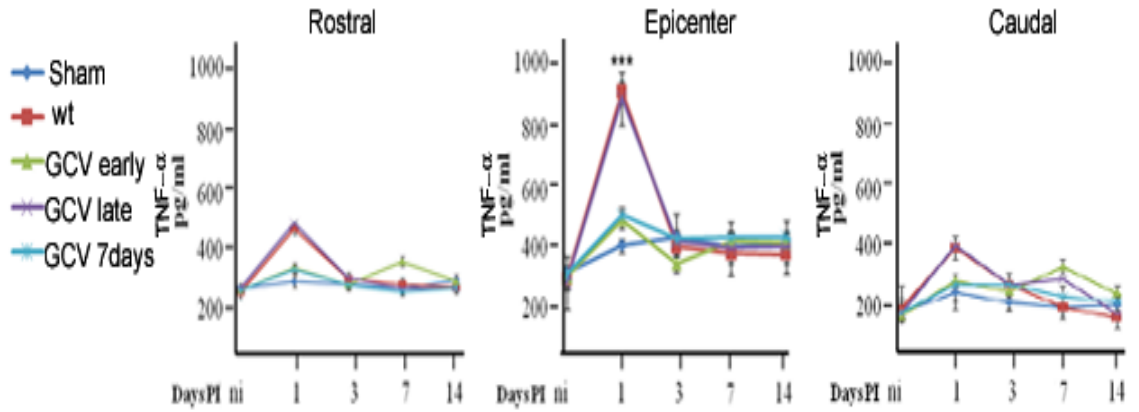

B.

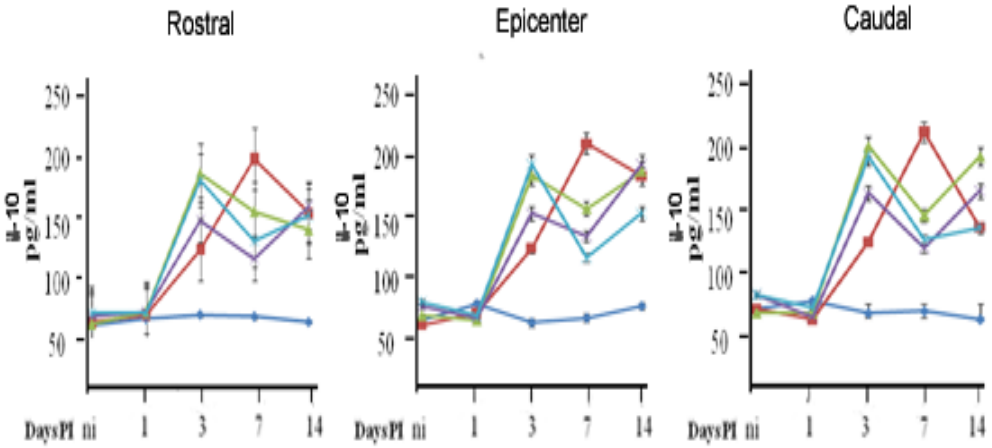

Figure III-4. Ablation of Microglia Alters Cytokine Production following Spinal Cord Injury.

An Enzyme linked Immunosorbent Assay (ELISA) was performed on spinal cords that were treated with GCV for different time periods to detect TNF-α and IL-10 levels. The spinal cords were cut into three 3 mm segments (rostral to the lesion, lesion epicenter, and caudal to the lesion) and the spatiotemporal expression of **(A)** TNF-α and **(B)** IL-10 were assessed. Error bars represent SEM, where **p*<0.05, ***p*<0.01, ****p*<0.001 by ANOVA followed by Bonferroni's post hoc test (n=6 individual experiments/group)

Figure III-5

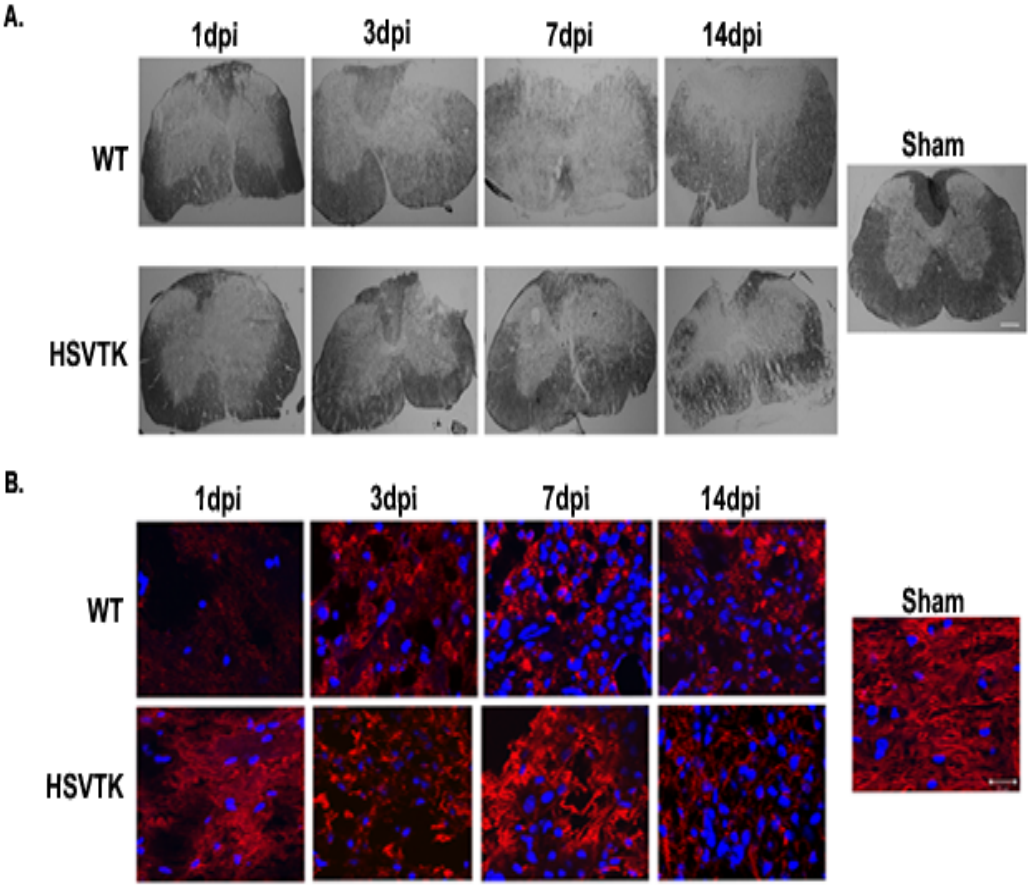

Figure III-5. Depleting the microglial population causes a reduction in demyelination.
A, Bright field images of coronal sections of spinal cords (approximately 100μm rostral from the lesion core). Spinal cords were stained with eriochrome cyanine for myelin detection. **B,** fluorescent images of Myelin basic protein bordering the lesion epicenter. Scale bar: **(A)**300 μm **(B)** 50μm

Figure III-6

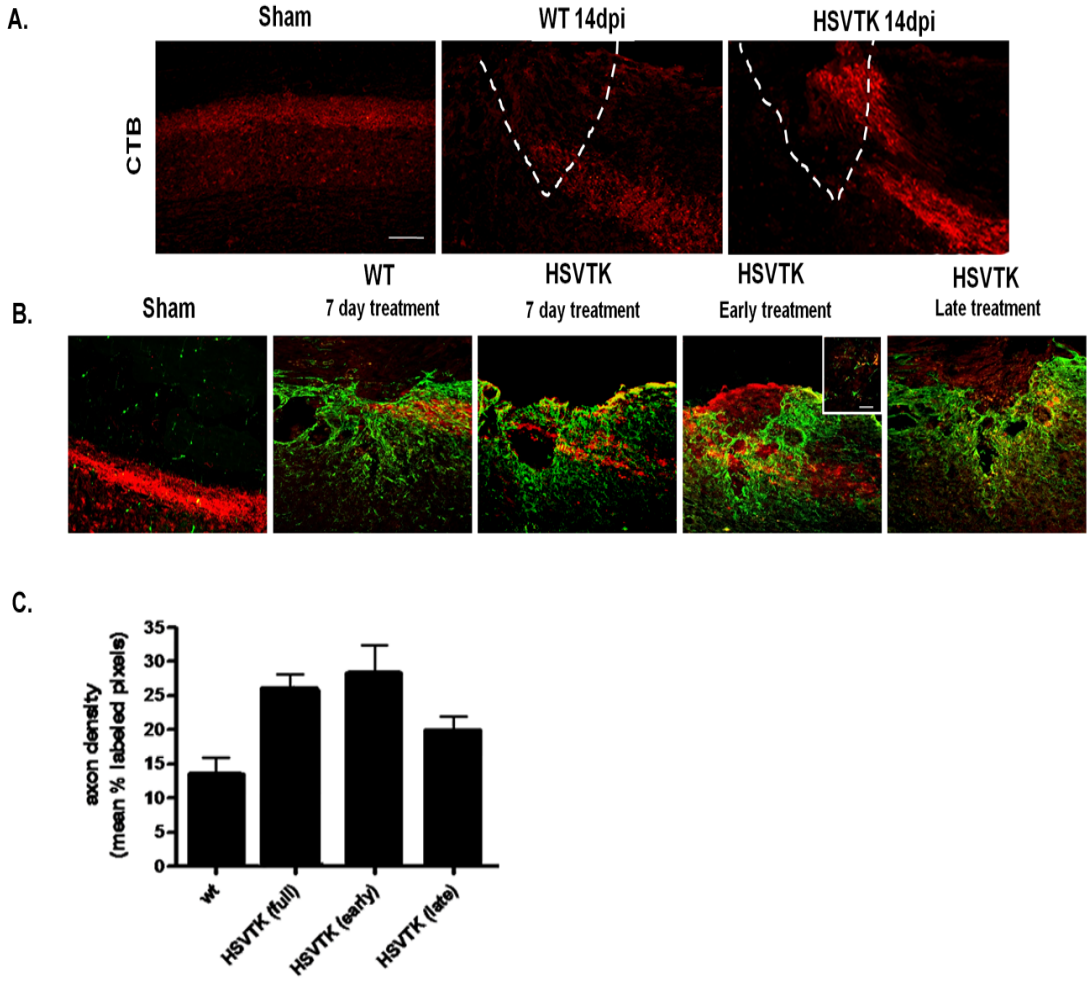

Figure III-6. Ablation of microglia at early time points enhances axon regeneration or prevents axonal die back.
Retrograde axon tracing was performed by injecting cholera toxin b subunits into the sciatic nerve four days prior to isolating the spinal cords. Sagittal sections are shown with the orientation of rostral to the left and caudal to the right. **A,** Spinal cords were isolated from mice treated for 7 days with GCV and stained against CTB (red). Dashed lines denotes the lesion core. **B,** Images of spinal cords treated at various time points with GCV, where the spinal cord were stained against CTB labeled axons (red) and GFAP (green) which defines the astrocytic lesion boarder. A confocal image of a regenerating axon growing into the lesion core in the early treated HSVTK spinal cord (inset). **C,** Alternating sections were stained and the density of CTB-labeled axons within the lesion area was quantified with NIH Image J software. Scale bar: **A-B,** 200μm.

Discussion

Conditional ablation of proliferating microglia significantly reduced the proliferating microglial population following severe spinal cord injury. This study was designed to determine the role that microglia play at specific time points in different regions of the spinal cord relative to the lesion post injury. Ablation of microglia for 7 days improved axon growth or prevented dieback within the lesioned area, reduced the expression the pro-inflammatory cytokine TNF-α, and reduced demyelination. When proliferating microglia were ablated at early time points, the expression of the pro-inflammatory cytokine TNF-α was reduced and the density of neurites that were found crossing the lesion boarder increased, indicating the at early time points post injury microglia have a deleterious role. Ablation of microglia at later time points did not alter TNF-α levels, although IL-10 levels diminished in comparison to wild-type, demonstrating that microglial response at later time points may beneficial. Although more neurites were observed in the lesion core in comparison to wild-type mice it was not as significant as during the early microglial ablation. It is conceivable that ablating microglia at early time points has a protective effect, while that the microglia that are activated with in the first three days are deleterious to the molecular environment.

Since astrocytes are a major component of the glial scar, it is plausible that the prevention of microglia activation at early time points delayed the astrocytic response to injury, since astrocytic activation follows in time and is promoted by the microglial response (Kreutzberg, 1996; Popovich et al., 1997).

The ablation of microglia may inhibit the hypertrophic changes and proliferation of astrocytes following injury. This may also delay secondary damage, since microglia and astrocytes both release pro-inflammatory cytokines (Aloisi, 2001; Dong and Benveniste, 2001).

Early cytokine release from microglia and astrocytes recruit neutrophils, peripheral macrophages and T cells that are known to contribute to secondary injury. The absence of microglia at early time points reduced cytokine release and potentially reduced the infiltration of peripheral immune cells thereby having a neuroprotective effect. Neutrophils infiltrate the spinal cord within 1 day and macrophages infiltrate around 3dpi, therefore it is conceivable that microglia/macrophage ablation at later time point PI may allow for the recruitment of these cells to the lesion which would lead to further cytokine production from the peripheral cells. This could possibly be the reason for less axon regeneration when ablating microglia in a later time point treatment in comparison to the early ablation. Unfortunately, this hypothesis cannot be supported at the early time point. The reason for this is that the promoter that drives the HSVTK expression in the CD11b-HSVTK$^{+/-}$ mice, CD11b, is also expressed by granulocytes, so the ablation of cells is not specific to cells of monocytic origin (Heppner et al., 2005). This implies that neutrophil infiltration and activity would be affected, and neutrophils, like macrophages and microglia, could also contribute to detrimental effects via the production of free radicals that cause oxidative damage on cells.

The long-term use of GCV in the CD11b-HSVTK$^{+/-}$ mice can cause aplastic anemia, where the bone marrow does not produce new blood cells since the drug GCV is abolishing proliferating CD11b positive cells. Such an adverse effect results in reduction in the survival time of these mice; usually mice did not survive past 7 days and rarely lived up to the 14 days time point. This adverse effect only allowed us to evaluate the effect of ablation in acute and secondary injury, but not in chronic stages of SCI.

Chapter IV

MIF reduces microglial/macrophage activation in the dorsal hemisection spinal cord injury model

Introduction

Since GCV had peripheral effects and caused aplastic anemia in CD11b-HSVTK$^{+/-}$ we could not further our experiments to study the chronic phases of SCI. To analyze the affect of microglial inhibition and examine the chronic phase of SCI we used the tripeptide MIF (Thr-Lys-Pro) that derives from the naturally occurring degradation product of the second constant domain of immunoglobulin G (IgG). MIF, macrophage/microglial inhibitory factor, is also known as the tuftsin1-3 fragment (Auriault et al., 1983). The tetrapeptide tuftsin (Thr-Lys-Pro-Arg) is a monocytic activator (Wagle et al., 1989) and the lack of the single amino acid shifts tuftsin activation properties to inhibitory.

Auriault demonstrated that MIF decreases cell migration, phagocytosis, chemotaxis and super oxide anion generation in peripheral macrophages, which are of monocytic origin similar to microglia (Auriault et al., 1983). MIF has also been shown to inhibit microglial function in the CNS as well. Administration of MIF during trans-section of the optic nerve reduced axotomy induced ganglion cell degeneration in the retina by

suppressing microglial activation (Thanos et al., 1993). EAE models of multiple sclerosis demonstrated that MIF reduced demyelination and t-cell infiltration into the spinal cord thereby abrogating EAE symptoms (Bhasin et al., 2007) and reduced lesion volume, edema and the number of degenerative neurons in intra cerebral hemorrhage models (Wang and Tsirka, 2005; Bhasin et al., 2007). The possible beneficial effect of MIF has not yet been examined in models of spinal cord injury. In the experiments described in the following chapters, C57BL6 mice were treated with MIF and various time points post injury were analyzed. Here we wanted to examine whether MIF is capable of overcoming microglia activation in a severe model of SCI.

Results

MIF inhibits microgliosis following dorsal hemisection

To confirm that MIF effectively inhibits microglial activation *in vivo* following spinal cord injury, a dorsal hemisection was performed on mice and a 7 day or 14 day micro-osmotic contain MIF or PBS was placed over the lesioned area. Microglial activation following SCI was examined at various time points post injury (7, 14, and 30dpi) via immunohistochemistry to detect the microglial marker iba-1 and post stained with DAB to visualize microglial morphology (Figure IV-1A). Microglia of mice that received laminectomey only, sham, had a ramified morphology indicative of a resting or inactive state. Microglia of injured mice treated with PBS exhibited

activated ameboid morphology, predominantly around the lesion epicenter at all time points analyzed, although it appeared that by 30dpi a number of microglia reverted back to resting state. The administration of MIF for 14 days abrogated microglial activation at all time points analyzed in comparison to PBS treatment. Although the administration of MIF for 7days reduced morphological changes associated with activation in comparison to PBS treatment, examination of 14dpi showed that more microglia exhibited an activated morphology in relationship to spinal cords treated for MIF for 14 days at the 14 day time point. This increase in microglial activation observed at 14dpi for the 7 day MIF treatment is possibly due the due to the cessation of MIF administration after 7 days, therefore the absence of the inhibitor after 7dpi allowed for some microglial activation.

To corroborate these results quantitative immunoblotting was performed and Iba-1 protein levels were examined from homogenates of the lesion epicenter, since microglia and macrophages filled the lesioned area subsequent to injury (Figure IV-1B). At 7dpi the PBS treatment group displayed a dramatic increase in Iba-1 expression, consistent with microglial activation, which gradually declined over the 30 day time period, corresponding to the deactivation of microglia. Inhibition of microglial activation for 7 days with MIF significantly reduced the protein levels of Iba-1 were when compared to PBS treated groups at 7dpi, however at 14dpi the microglial activation response was delayed given that there was no significant difference in the levels of Iba-1 protein expression observed at

the 14 day time point. Alternatively, treatment of MIF for 14 days significantly reduced Iba-1 at 14dpi and 30dpi, indicating that administration of MIF for 14 days was sufficient to inhibit activation up to 30dpi (Figure IV-1B,C).

A reduction in microglial proliferation contributed to the observed reduction in iba-1 expression for MIF treated animals, as determined by the proliferation marker Ki67 (Figure IV-2A,B). PBS treatment revealed that microglia proliferation peaked around 3dpi and declined slowly thereafter. MIF administration significantly reduced microglial proliferation at 1, 3, and 7 dpi. Analysis of 14 and 30dpi showed no significant differences in proliferation for both treatment courses.

MIF inhibitory activity is sustained after 14 days.

Since MIF was administered *in vivo* for 7 or 14 days via an osmotic pump, MIF inhibitory properties were tested *in vitro* to determine whether MIF retained inhibitory capabilities and was stable after 14 days. Primary microglial cultures were treated with freshly prepared MIF or MIF that had been incubating at physiological temperature of 37^{o}C for 14 days (14day MIF). Microglial cells were treated with 50 mg/ml MIF and/or 20 ng/ml lipopolysaccharide (LPS), a known activator of microglia, for 24 hrs and microglial morphology and TNF$-\alpha$ levels were assessed. Non-treated and fresh MIF-treated microglia exhibited a resting rod-shaped morphology, while LPS treatment caused approximately 82% of microglia to undergo

morphological changes and assume a fully active ameboid morphology (Figure IV-3A,B). Microglia treated with LPS and fresh or 14 day MIF showed a significant reduction in morphological changes ($p=0.001$) indicating that MIF still retained some inhibitory activity after 14 days at physiological temperatures.

Given that microglia secrete TNF-α as they become activated, the levels of the pro-inflammatory cytokine TNF-α was determined via ELISA to confirm the morphological changes that were observed in the above experiment. Primary microglia were treated with fresh MIF, 14 day MIF, and/or LPS as stated above and the supernatant was collected after 24h (Figure IV-3C). TNF-α production was virtually absent in the untreated and the MIF only treatments, and although there was slight increase in TNF-α in the fresh MIF and LPS treatment group, it was not statistically significant when compared to untreated cultures. LPS treatment caused a significant increase in TNF-α ($p=0.001$), and although the 14 day MIF and LPS treatment resulted in a significant increase in TNF-α in comparison to untreated ($p=0.001$), it was significantly less that LPS treatment alone ($p=0.001$). These results suggest that the functional activity of MIF is reduced over 14 days, but its inhibitory properties still remain significant. IL-10 was also detected by ELISA at 24 hrs but the amount of IL-10 production at this time point was negligible.

MIF alters cytokine production following spinal cord injury

Since TNF-α production was affected by MIF treatment in microglial cultures, we wanted to further investigate cytokine production *in vivo* subsequent to SCI. To assess cytokine production *in vivo* in a spatiotemporal manner spinal cords from different time points post injury were cut into 3mm segments corresponding to the lesion epicenter, rostral and caudal to the lesion, and the concentrations of the pro-inflammatory cytokine TNF-α and the anti-inflammatory cytokine, IL-10, were analyzed via ELISA (Figure IV-4). TNF-α expression was elevated rostral and caudal to the lesion but most dramatically in the lesion epicenter 1dpi, and declined thereafter in PBS-treated groups. MIF treatment significantly decreased TNF-α production although not to the levels of uninjured sham groups. Interestingly, when animals were treated for 7 days with MIF, there seemed to be a slight increase in TNF-α expression after the treatment stopped, which was not observed when the animals were treated for 14 days (Figure IV-4A). This could be due to a possible delayed response of microglia/macrophages when treatment ceased. Analysis of IL-10 was quite surprising; since IL-10 levels were significantly higher in groups treated with MIF at all time points during MIF administration. IL-10 levels peaked between 3-7dpi in comparison to PBS treated groups. A modest elevation of IL-10 was observed over time in all segments of the spinal cord, but was more pronounced rostrally and caudally (Figure IV-4B). The observed elevation of IL-10 levels could be a direct effect of microglial inhibition,

where activated microglia could be secreting factors that regulate the expression of anti-anti-inflammatory cytokines and the absence of these factors allows for an increase in IL-10 expression.

MIF diffusion within the spinal cord

To determine how far MIF diffuses within the spinal cord, MIF was conjugated to biotin label using EZ-Link NHS-Biotin (Thermo Scientific) and then administered *in vivo* via a 7-day micro-osmotic pump. At 7dpi mice were euthanized and biotinylated MIF was analyzed by incubating the spinal cord slices with strepavidin conjugated Alexa Fluor 555. MIF treatment diffused approximately 0.8 mm rostrally and 0.6 mm caudally to the lesion epicenter but the concentration of MIF was highest at the lesion core (Figure IV-5 A, B). Higher magnification images show MIF either clustering on the surface of macrophages or in a subcellular compartment possibly binding to cell surface receptors or altering intracellular signaling pathways (Figure IV-5B).

Figure IV-1

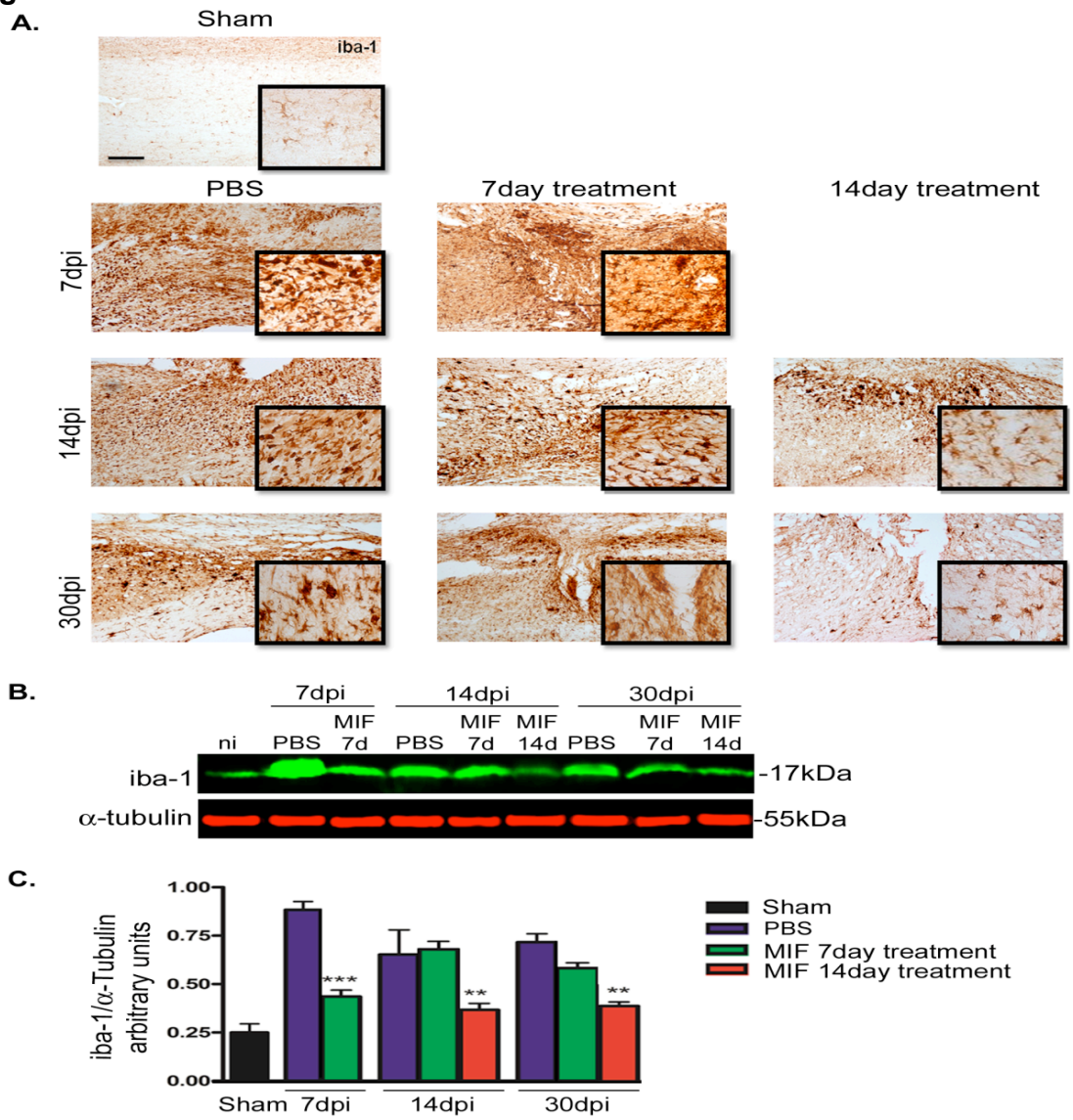

Figure IV-1. MIF inhibits microglial activation following the dorsal hemisection model of spinal cord injury. A, Bright field images of spinal cord sections (7, 14, 30dpi) stained against the microglial marker iba-1 (brown) and detected with a DAB. **B,** Representative image of iba-1 expression of spinal cords collected at various time points post injury analyzed by quantitative immunoblotting. **C,** Quantitative measurements of iba-1 were performed using the Odyssey 2.1 software and the data were plotted as a ratio of the pixel volume of iba-1 over the pixel volume of actin. For statistical analysis, MIF treated groups were compared to PBS controls for each time point evaluated. Error bars

represent SEM, where *p<0.05, **p<0.01, ***p<0.001 by ANOVA followed by Bonferroni's post hoc test (n=6 individual experiments).

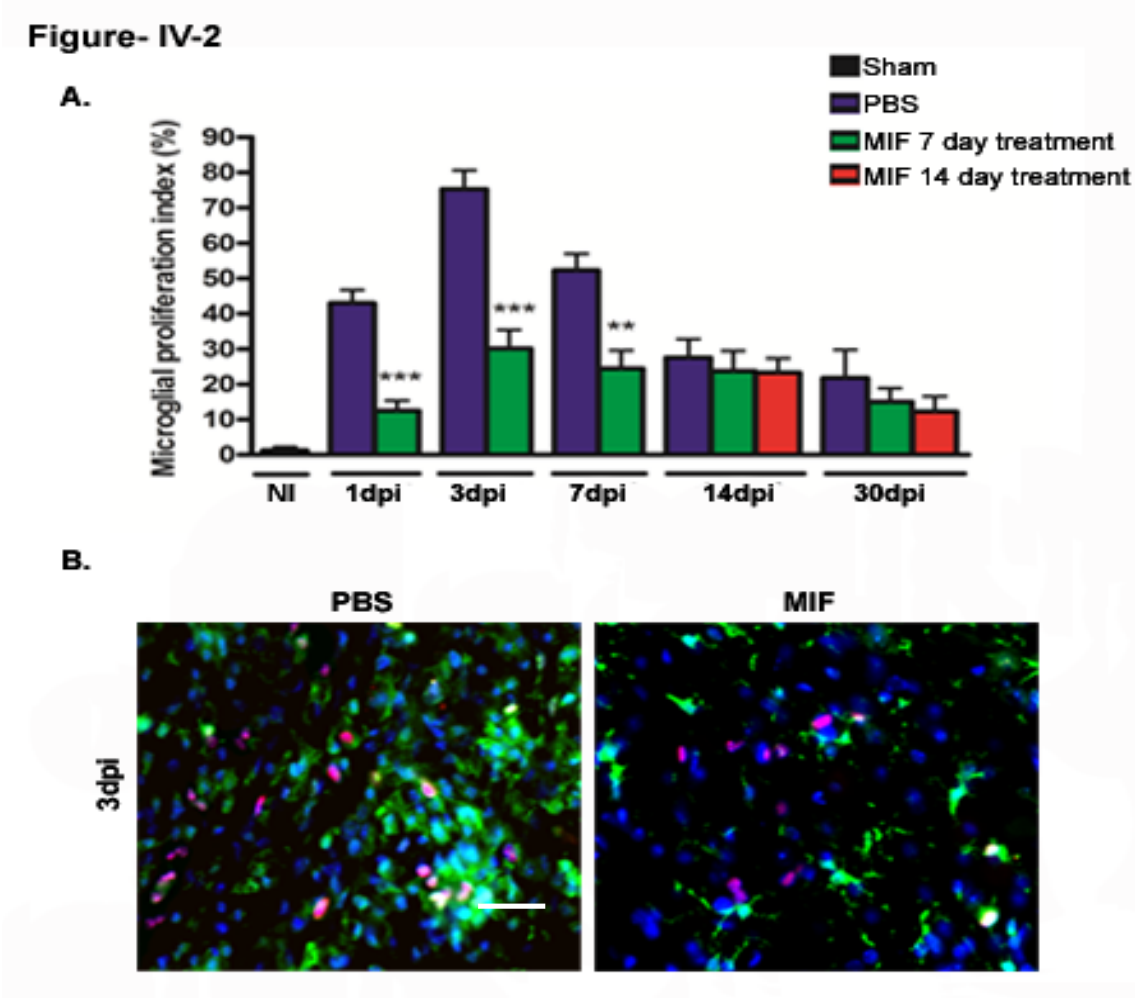

Figure IV-2. MIF reduces microglial proliferation.
A, Quantification of microglial proliferation of various time points post injury. For statistical analysis, PBS treatment was compared with MIF treatments from the same time points. **B,** Representative images of 3dpi of iba-1 (green) and the proliferation marker Ki-67 (red). Error bars represent SEM, where *p<0.05, **p<0.01, ***p<0.001 by ANOVA followed by Bonferroni's post hoc test (n=6 individual experiments).

Figure IV-3

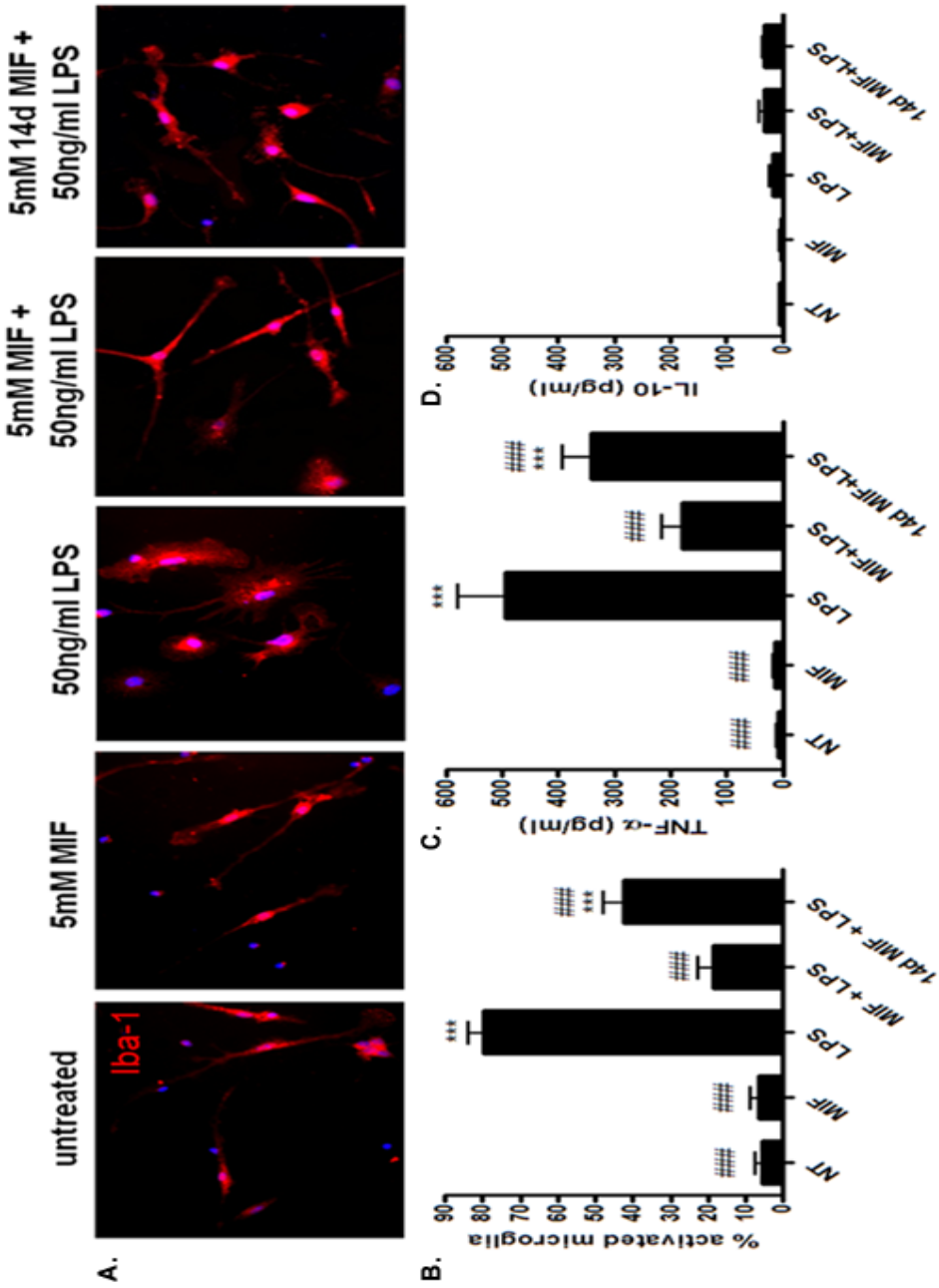

Figure IV-3. The inhibitory properties of MIF are still effective after 14 days. **A,** Fluorescent images of primary microglia incubated with fresh 5mM MIF, 14 day MIF and /or LPS. **B,** The activation state of Iba-1^{+} microglia (red) was determined morphologically (less than 2 processes were considered activated, 2 or more microglia were considered resting) and via (**C)** TNF-α production**.** **C,D,** ELISA assays were performed on the microglial culture supernatant and **(C)**TNF-α and **(D)** IL-10 levels were measured. Error bars represent SEM, where *p<0.05, ***p<0.001, and $^{\#\#\#}p$<0.001 by ANOVA followed by Bonferroni's *post hoc* test (* comparison to sham; $^{\#}$ comparison to LPS). Scale bar, 50μm. (n= 3 individual experiments)

Figure IV-4

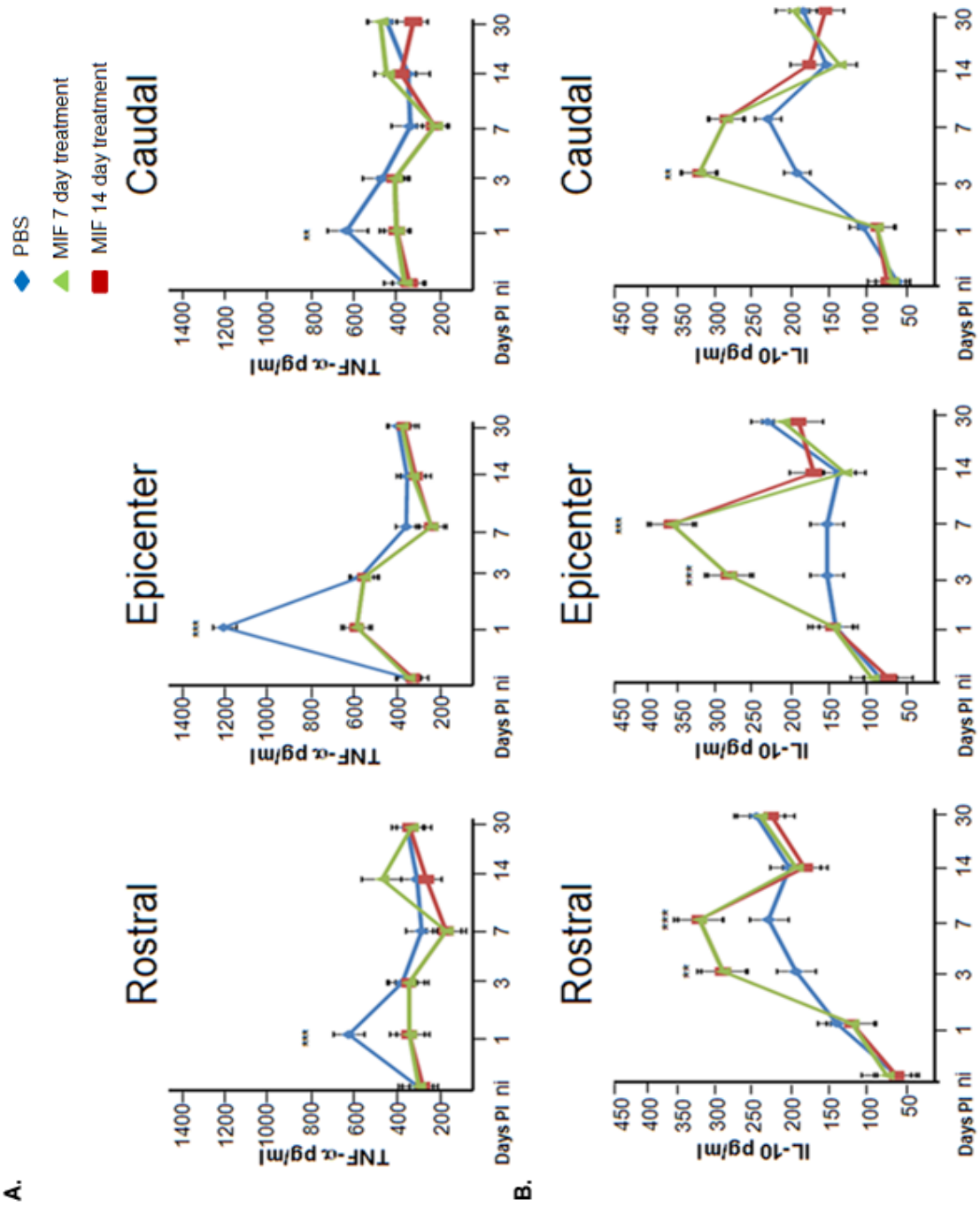

Figure IV-4. Inhibition of microglia with MIF alters cytokine production following spinal cord injury.
Spinal cords from PBS and MIF treated mice were cut into three 3 mm segments (rostral to the lesion, lesion epicenter, and caudal to the lesion) and homogenates were made for different time points post injury. Spinal cord homogenates were then subjected to ELISA to detect **A,** TNF-α and **B,** IL-10 levels. Error bars represent SEM, where *p<0.05, ***p<0.001, and $^{###}p$<0.001 by ANOVA followed by Bonferroni's *post hoc* test (n=3 individual experiments).

Figure IV-5

A.

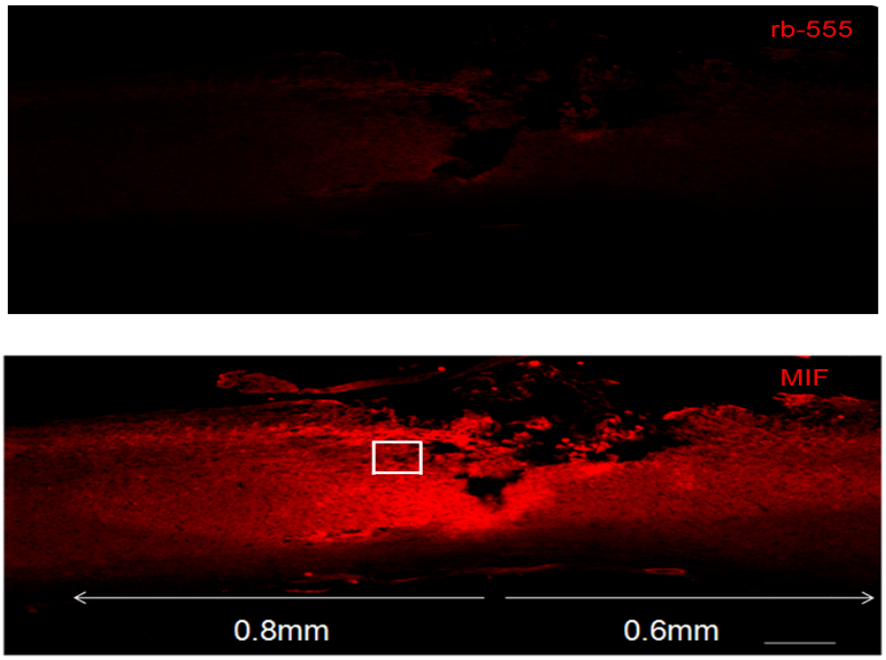

B.

Rostral	Caudal
0.72 mm	0.55 mm
1.00 mm	0.76 mm
0.83 mm	0.66 mm

C.

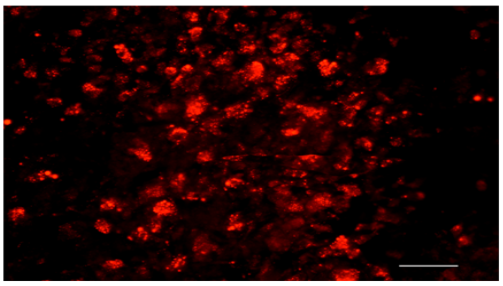

Figure IV-5. MIF distribution in the spinal cord.
PBS or biotinylated MIF was administered to mice via a micro-osmotic pump over the lesioned area of the spinal cord for 7 days and spinal cords were isolated at 7dpi. **A,** Representative images of secondary antibody control of PBS treated spinal cord (upper panel) and MIF (bottom panel) distribution in biotinylated-MIF treated spinal cord. **B,** MIF distribution was measured using ImageJ software (n=3). **C,** Higher magnification image of MIF (inset denoted by white box in **A**). Scale bar, 100μm; 50μm

Discussion

MIF effectively inhibited microglial activation *in vitro* and *in vivo* following spinal cord dorsal hemisections and was relatively stable after a 14 day incubation period at physiological temperatures. Administration of MIF via osmotic pump localized MIF distribution to the lesion area where it diffused rostrally and caudally to the lesion, but the highest concentration of MIF was found within the lesion area. The MIF diffusion pattern could explain the alterations observed in cytokine secretion in different areas of the spinal cord. Inhibition of microglia with MIF resulted in significant reduction of TNF-α production following injury, but increased IL-10 expression at later time points.

TNF-α and IL-10 are mainly produced by cells of monocytic origin. Following CNS injury TNF–α is involved in mediating inflammation, neutrophil recruitment and apoptosis of glia thereby contributing to secondary damage. Alternatively, IL-10 has been shown to have beneficial effects in various CNS pathologies, shown by decreasing astrogliosis, and pro-inflammatory cytokine production (Woiciechowsky et al., 2004). Evidence suggests that IL-10 can suppress the cell death response, decrease tissue damage, reduce pain, increase neuronal survival and induce functional recovery (Bethea et al., 1999; Brewer et al., 1999; Bachis et al., 2001; Boyd et al., 2003; Jackson et al., 2005). Injury was exacerbated in mice deficient in IL-10 injury, suggesting that IL-10 is

neuroprotective in models of stroke and excitotoxic spinal cord injury (Grilli et al., 2000; Abraham et al., 2004).

Interestingly, in this study, MIF treatment enhanced IL-10 production similar to various pharmacological inhibitors of microglia. Minocycline, a tetracycline that has been shown to inhibit microglia and macrophages, increased IL-10 mRNA levels and concomitantly decreased the proinflammatory cytokine, TNF-α (Lee et al., 2003). Methylprednisolone, a steroid inhibitor of monocytic activation, increased the biosynthesis of IL-10 while inhibiting TNF-α production in models of endotoxaemia (Marchant et al., 1996). Moreover, a recent study of microglial inhibition with the drug dimethylfumarate reduced expression of NO, TNF-α, IL-6 and IL-1β with contemporaneous increase of expression of IL-10 in EAE (Wilms et al.). The concomitant increase of IL-10 along with the decrease in TNF-α in these various models was of interest since IL-10 plays a role as a feedback inhibitor of TNF-α, where TNF-α can trigger the IL-10 response. However, IL-10 has been shown to stimulate macrophages by several endogenous and exogenous factors such as endotoxin (via Toll-like receptor 4 and NF-κB dependent pathways), TNF-α (via TNF receptor p55 and NF-κB-dependent pathways), catecholamines, and drugs that elevate cyclic adenosine monophosphate (both via protein kinase A and CREB-1/ATF-1 dependent pathways) (Platzer et al., 1995; Meisel et al., 1996; Woiciechowsky et al., 1998; Platzer et al., 1999; Platzer et al., 2000; Riese et al., 2000; Woiciechowsky and Volk, 2005). It is feasible, that MIF inhibits monocytic activation causing alterations in the signaling pathways, thereby causing an

increase in IL-10 while reducing TNF-α expression. Another possibility for the observed increase in IL-10 with MIF treatment is that the lack of monocytic activation prevents the release of regulatory molecules that modulate IL-10 expression therefore other cells types may be responsible for the elevation of IL-10 following MIF treatment.

Conceivably, since MIF has been shown to decrease cell migration, phagocytosis, chemotaxis (Auriault et al., 1983), reduce neuronal degeneration and lesion volume (Thanos et al., 1993; Wang and Tsirka, 2005; Bhasin et al., 2007) and reduce demyelination (Bhasin et al., 2007), MIF may have similar effects following spinal cord injury which will be discussed in the following chapters.

Chapter V

Inhibition of microglial activation with MIF alters components of the glial scar

Introduction

Under normal physiological conditions, astrocytes regulate and provide structural support for the CNS by contributing to the formation of the blood brain barrier and by modulating the neuronal environment via neurotransmitter and ionic reuptake (Nedergaard et al., 2003). Under pathological conditions, such as spinal cord injury, astrocytes become reactive and proliferate forming a dense astrocytic scar, which is a major component of the inhibitory glial scar creating a cellular barrier around the lesion epicenter. Astrogliosis has been shown to have both beneficial and deleterious effects following spinal cord injury. The astrocytic scar forms a barrier around the primary insult isolating the injured area in an attempt to reestablish the blood brain barrier (Bignami et al., 1993). Selective ablation of reactive astrocytes following SCI, via the HSVTK transgene driven by the GFAP promoter, increased the inflammatory response, neuronal and oligodendrocyte death, and decreased functional recovery (Faulkner et al., 2004). In contrast, a reduction of inflammation and an increase in functional recovery subsequent to SCI has been demonstrated in mice expressing the dominant negative form of the inhibitor of NF-κB under the control of the GFAP

promoter (Brambilla et al., 2005). Astrogliotic scars are also a major source for the production of extracellular matrix molecules, such as proteoglycans and tenascins, which inhibit neurite outgrowth following trauma (McKeon et al., 1991; Faissner, 1997; Fawcett and Asher, 1999; Garwood et al., 2001; Silver and Miller, 2004).

Of the proteoglycans, CSPGs are quickly upregulated following trauma (Jones et al., 2003; Tang et al., 2003) and deter axon regrowth in the lesioned area. The CSPG neurocan is upregulated by reactive astrocytes following injury and has been shown to inhibit axon regeneration *in vitro* and *in vivo* (McKeon et al., 1999; Asher et al., 2000; Matsui et al., 2002; Deguchi et al., 2005). Although, not expressed by reactive astrocytes, NG2 CSPG, found within the glial scar, has similar inhibitory properties (Levine, 1994; Ughrin et al., 2003; Tan et al., 2005; Tan et al., 2006).

Cytokines released from damaged neurons and microglia stimulate astrogliosis. Real time-PCR indicated that microglial activation precedes astrocytic activation following spinal nerve trans-section and cortical spreading depression models (Gehrmann et al., 1993; Tanga et al., 2004). Chloroquine and colchicine, inhibitors of microglial activation reduced astrogliosis and increased neuronal survival in stroke and trauma models (Giulian et al., 1989; Giulian and Robertson, 1990). We hypothesized that MIF can reduce astrogliosis and thereby blunt CSPG expression. Here, in this chapter, astrogliosis and CSPG expression were analyzed following the inhibition of microglia and macrophages with MIF.

Results

Astrocyte activation and proliferation are reduced around the lesion core

Since microglia regulate astrocytic activation (Kreutzberg, 1996; Popovich et al., 1997) and GFAP is upregulated by astrocytes in the CNS following insult (Eddleston and Mucke, 1993; Ridet et al., 1997) we thus examined GFAP immunoreactivity following inhibition of microglia (Figure V-1A). Low levels of GFAP expression were observed in sham injuries indicating that astrocytes were 'resting'. In PBS treated animals, a significant increase in GFAP expression was observed at 7dpi. This increase was attenuated in the MIF treated groups. The decrease in GFAP immunoreactivity was confirmed by quantitative immunoblots (Figure V-1B,C) where there was an evident downregulation of GFAP expression levels at 7dpi in MIF treatment when compared to those after PBS treatment.

The decrease in GFAP expression could correlate with a decrease in astrocytic reactivity or a decline in astrocytic proliferation. To determine astrocytic proliferation, GFAP and the proliferation marker Ki-67 were analyzed cord for each treatment (n=6/group), where five 40x fields were taken per spinal cord (Figure V-2). The number of proliferative astrocytes declined during MIF administration, with a significant decrease at 7dpi in the MIF treated groups in comparison to groups treated with PBS (Figure V-2). To determine the proliferation index of astrocytes the number of double positive $GFAP^{+}Ki67^{+}$ cells was divided by the total number of astrocytes positive for GFAP ($GFAP^{+}Ki67^{+}$/total $GFAP^{+}$ cells) in each field (Figure V-2B). The amount of proliferating astrocytes was significantly less at 7dpi with MIF treatment in

comparison to PBS although no differences were observed at other time points. An observed difference in astrocytic morphology was noted particularly at 7dpi, where the astrocytes seem more hypertrophic in the PBS groups but retained a 'resting' morphology in the MIF treated groups.

Lesion volume

The inhibitory effect of MIF on microglia/macrophages and the reduction in astrocytic reactivity following SCI led us to evaluate the lesion volume to determine if there was a difference in lesion size when microglia/macrophage activation is inhibited. Sections of the spinal cord were labeled with the astrocytic marker GFAP to determine the lesion border and the lesion volume, which was defined as the area devoid of GFAP signal (Figure V-3A), was analyzed using the NIH ImageJ software. At all time points the lesion volume showed a trend toward reduction with microglial inhibition but was significant at 14dpi with 14 day administration of MIF (Figure V-3B).

Chondroitin sulfate proteoglycan expression following MIF treatment

Given that astrocytic proliferation and reactivity were reduced, we next sought to examine CSPG expression, since CSPGs are expressed by reactive astrocytes and are inhibitory to axonal regeneration following SCI. Using the Pan CSPG antibody (CS-56) the mean fluorescent intensity was determined for each treatment group by taking 5 40x fields and measuring the optical density for each field. Animals that had undergone sham injury exhibited little to no expression of

CSPGs; following injury and PBS treatment a dramatic increase in expression of CSPGs was evident at the lesion epicenter extending out to areas of the penumbra. Pan CSPG expression was significantly reduced at 7dpi and 14dpi with the 14 day MIF treatment (Figure V-3A,B). Two of the CSPGs, NG2 and neurocan, were analyzed individually as they are known to have inhibitory effects on axonal regeneration (Figure V-4,5). In animals that were subjected to SCI and treated with PBS (controls) NG2 expression was elevated at 7dpi, but diminished over time. MIF treatment for 7 days markedly reduced NG2 expression at 7dpi, and 14 day MIF treatment reduced expression both at 14 and 30dpi. Neurocan was differentially expressed: PBS treatments resulted in a rise in neurocan expression peaking at 14dpi and declining thereafter. The reduction in neurocan expression was not statistically significant at any time points except for the 14 day MIF treatment at 14dpi.

Figure V-1

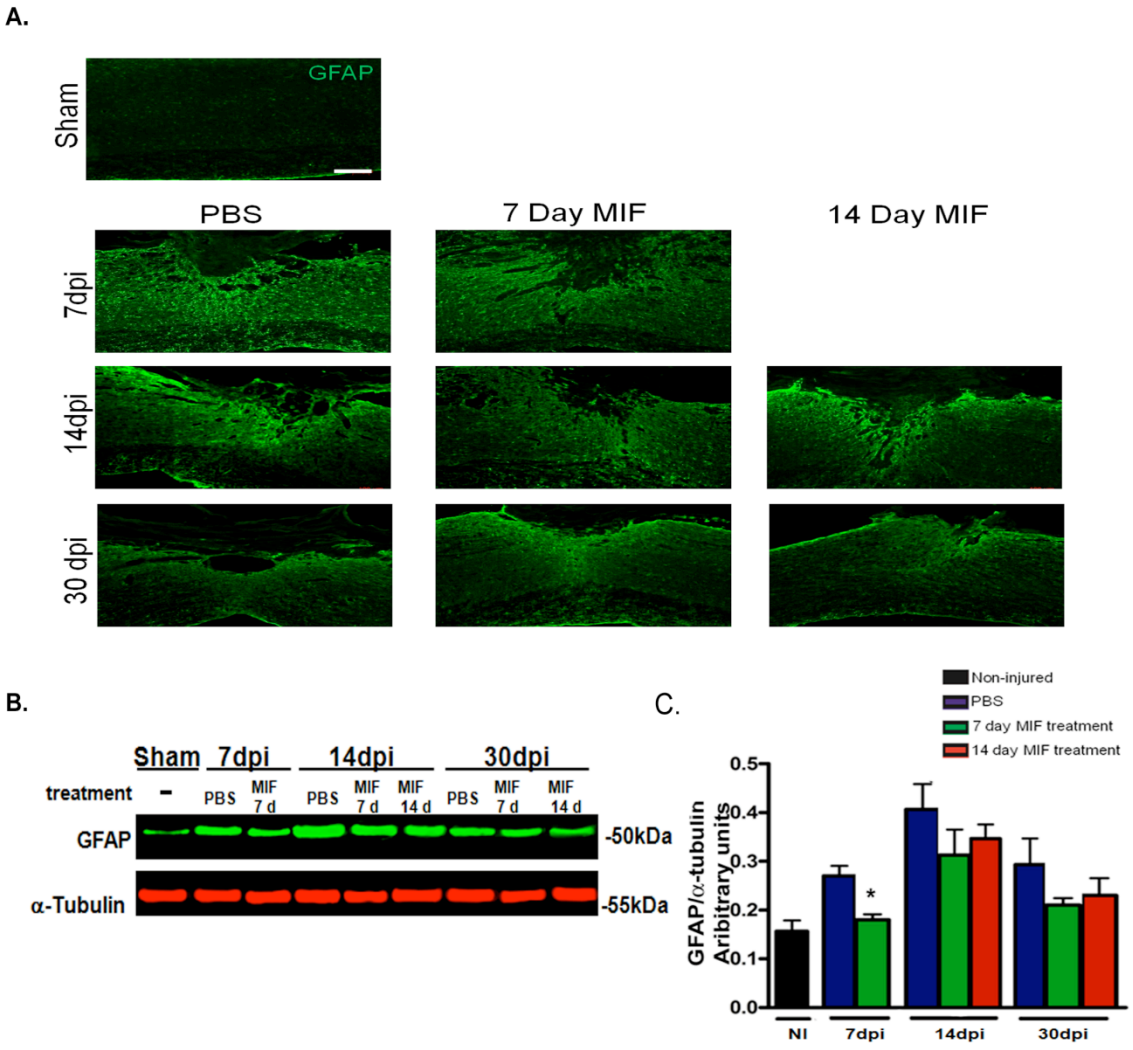

Figure V-1. MIF inhibition of microglia reduces astrocyte reactivity.
A, Fluorescent images of GFAP astrocytes within sagittal sections of spinal cords. **B,** Representative quantitative immunoblot of GFAP levels from PBS and MIF treated spinal cord homogenates taken from various time points post injury. **C,** Quantitative measurements of GFAP were performed using the Odyssey 2.1 software and the data were plotted as a ratio of the pixel volume of GFAP over the pixel volume of actin. For statistical analysis, PBS treatment was compared with MIF treatments from the same time points. Error bars represent SEM, where *p<0.05 by ANOVA followed by Bonferroni's post hoc test. (n=6 individual experiments) Scale bar: 200μm.

Figure V-2

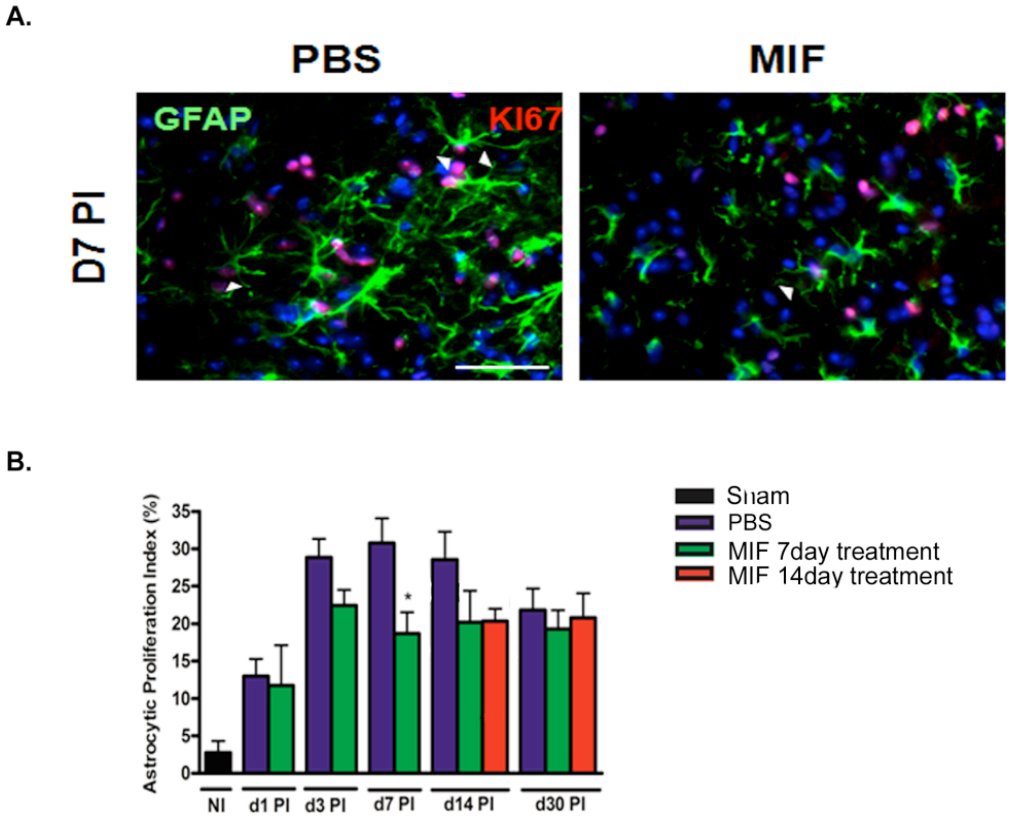

Figure V-2. Microglial inhibition reduces Astrocyte proliferation
A, Representative images of spinal cords, isolated at 7dpi from PBS and MIF treated mice, stained for GFAP (green) and the proliferation marker Ki-67 (red). **B,** Quantitative analysis of proliferative astrocytes at various time points post injury comparing MIF treatment groups to PBS control groups. Error bars represent SEM, where *p<0.05 by ANOVA followed by Bonferroni's post hoc test (n=6 individual experiments). Scale Bar: 20μm.

Figure V-3

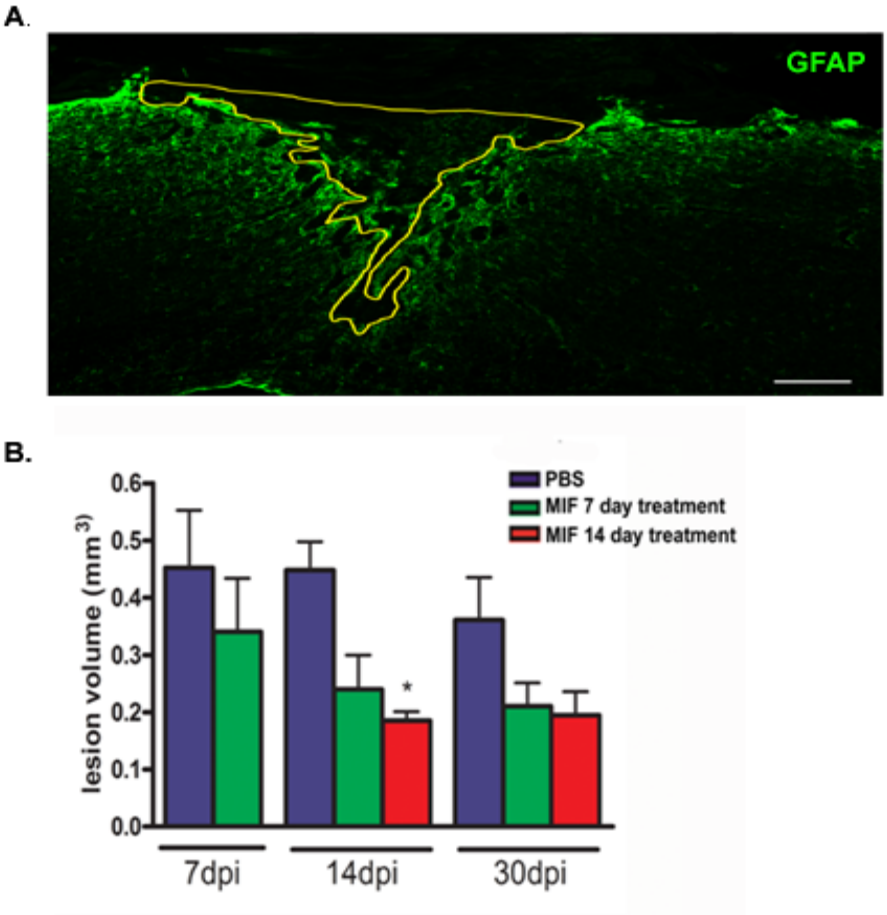

Figure V-3. Lesion volume is reduced during the duration of MIF treatment. **A,** Lesion volume (lesion area) was quantified from six sagittal sections by measuring the area of devoid of stain surrounded by the GFAP+ astrocytic border (demoted by outlined area) and **(B)** average values were obtained from 6 independent samples (n=6/time point/treatment) using the NIH ImageJ software. Error bars represent SEM, where *p<0.05 by ANOVA followed by Bonferroni's post hoc test (n=6 individual experiments). Statistical significance was analyzed between PBS treated and MIF treatments for each time point.

Figure V-4

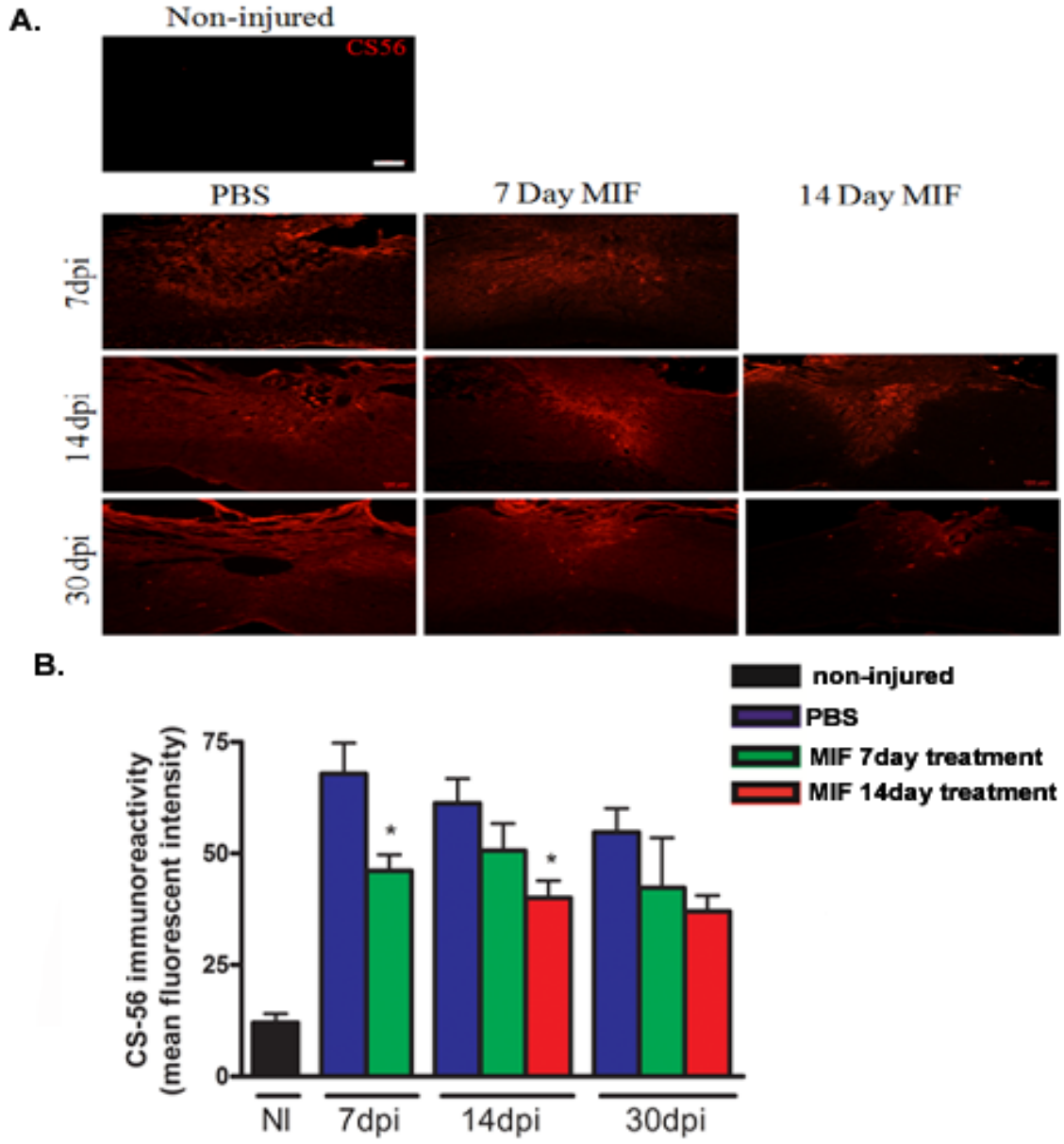

Figure V-4. CSPG expression is reduced with MIF inhibition of microglia. A, Fluorescent images of spinal cords stained against the CSPG marker CS-56 (red), to determine the overall expression of CSPGs. **B,** Quantification of fluorescent intensity of CSPGs using ImageJ. Error bars represent SEM, where **p*<0.05 by ANOVA followed by Bonferroni's post hoc test (n=6 individual experiments). Statistical significance was analyzed between PBS treated and MIF treatments for each time point. Scale Bar: 200μm

Figure V-5

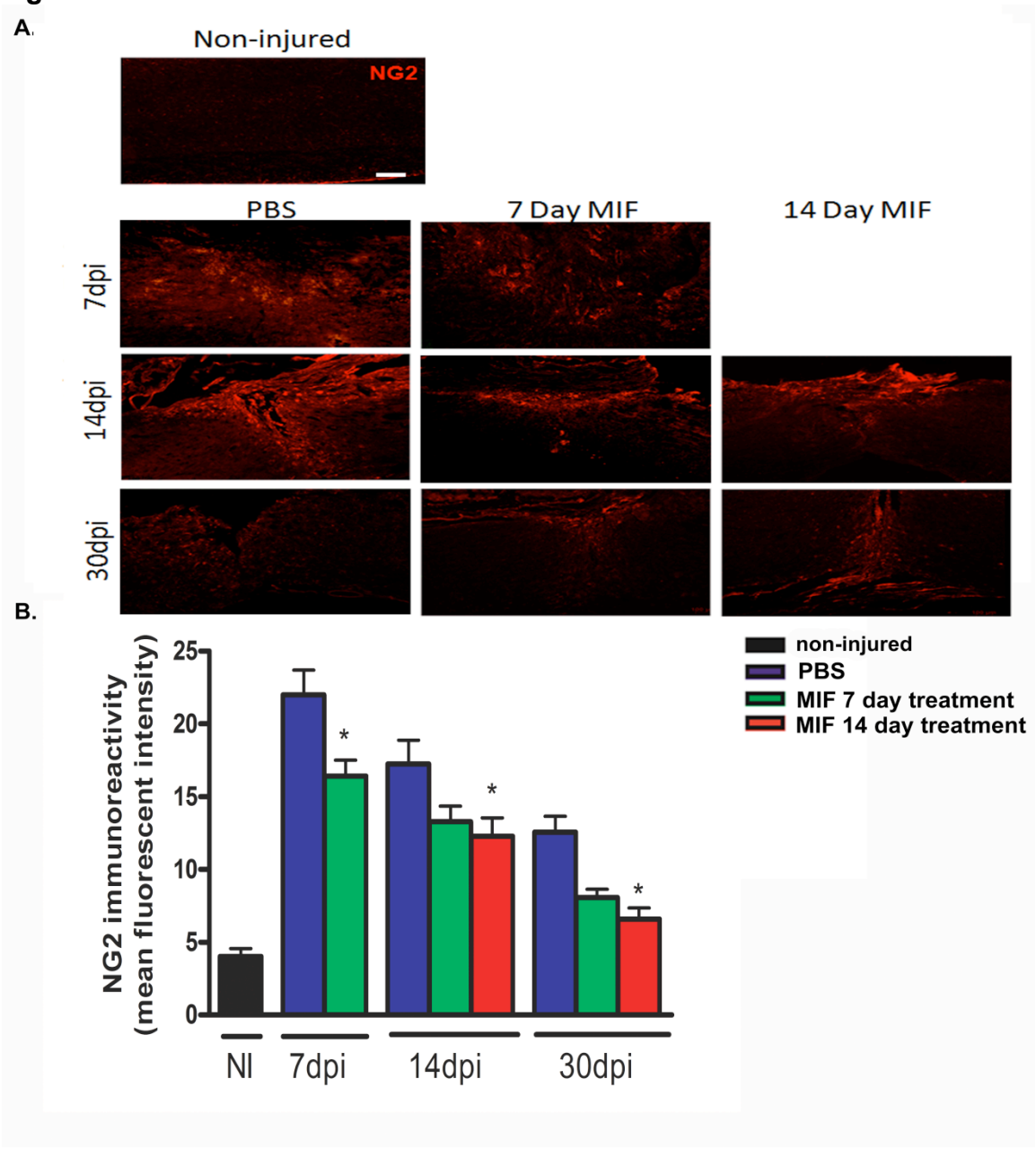

Figure V-5. Suppression of microglial activation causes a reduction in NG2 expression. A, Fluorescent images of spinal cords stained against the NG2 (red). **B,** Quantification of fluorescent intensity of NG2 immunoreactivity using ImageJ. Error bars represent SEM, where *p<0.05 by ANOVA followed by Bonferroni's post hoc test (n=6 individual experiments). Statistical significance was analyzed between PBS treated and MIF treatments for each time point. Scale Bar: 200μm

Figure V-6

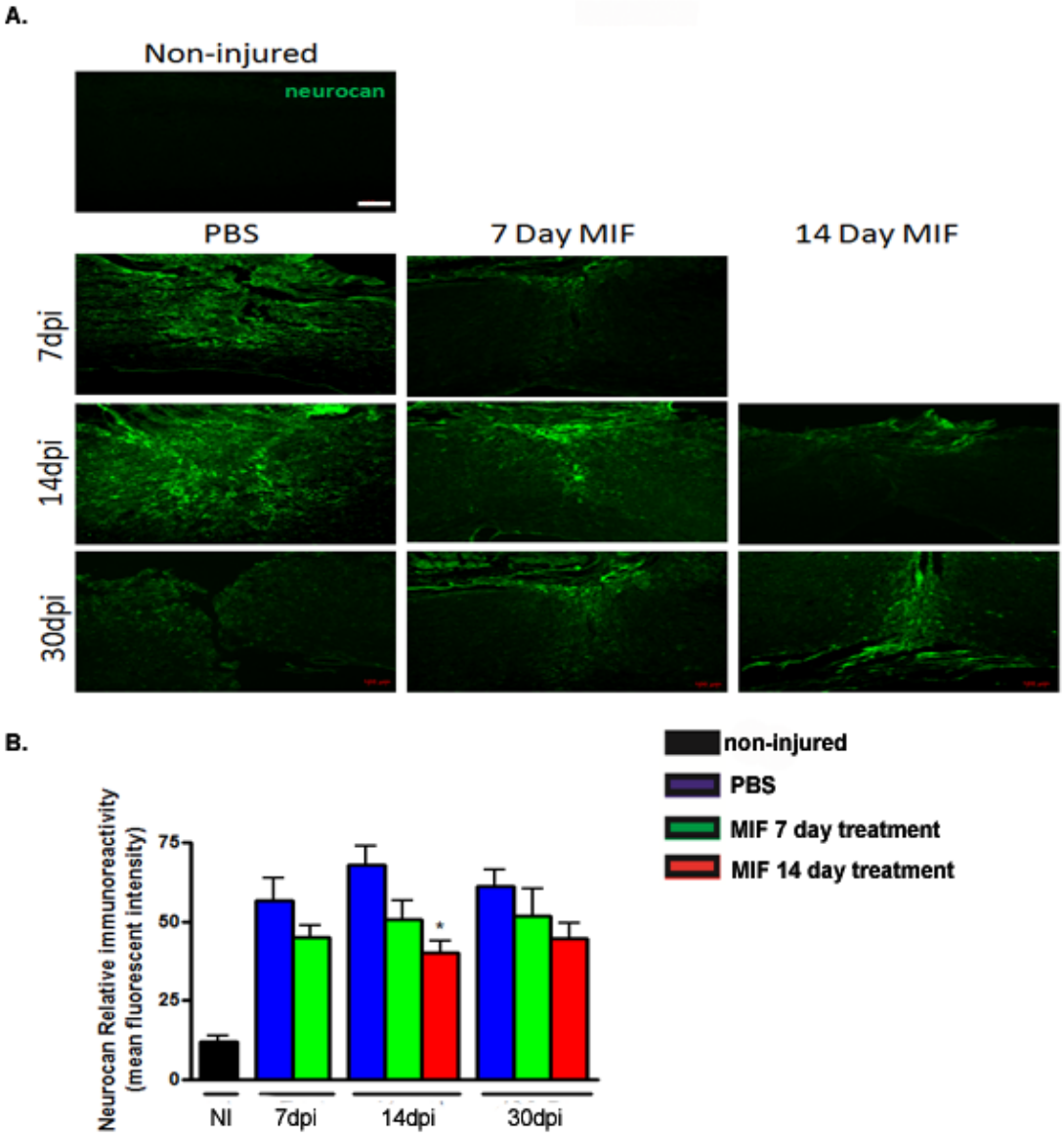

Figure V-6. Inhibition of microglial activation reduces neurocan expression. **A,** Fluorescent images of spinal cords stained against neurocan (red) **B,** Quantification of fluorescent intensity of CSPGs using ImageJ. Error bars represent SEM, where *p<0.05 by ANOVA followed by Bonferroni's post hoc test (n=6 individual experiments). Statistical significance was analyzed between PBS treated and MIF treatments for each time point. Scale Bar: 100μm

Discussion

The lesioned area is devoid of glial cells such as astrocytes or oligodendrocytes, but contains a large number of macrophages and microglia that remain in situ over a period of two months or more after the injury (Wrathall et al., 1998). In this study, we found that MIF treatment significantly reduced lesion volume at 7dpi, but resulted in no significant difference observed at day 30 even though the lesion areas were smaller than the PBS treatment groups. This could be due to the cessation of treatment that allowed microglia to become activated and peripheral macrophages to infiltrate the lesioned area after 14dpi.

Following CNS pathologies, astrogliosis is associated with microgliosis, where microglial activation precedes or complements astrocytic reactivity (Giulian et al., 1989; Tanga et al., 2004). We wanted to investigate if the astrocytic scar was affected following MIF treatment. Although the scar was still present around the lesion, the number, proliferation rate and reactivity of astrocytes were reduced following microglial inhibition with MIF. These findings were similar to results obtained by Balasingam, where treatment with MIF significantly reduced astroglial reactivity following corticectomy (Balasingam and Yong, 1996). This observation could be due to a number of factors since microglia secrete a myriad of cytokines and growth factors, which in turn could act as triggers and modulators of astrogliosis. *In vitro* studies of microglia and astrocytic cocultures have shown that microglial activation with LPS stimulates astrocyte proliferation. Zhang determined by blocking by prostaglandin E_2 with pharmacological inhibitors or by genetic knockout of microglial COX-2 (Zhang et al., 2009) that

microglia secrete prostaglandin E_2 which enhances astrocyte proliferation. It is feasible that the inhibition of microglia with MIF abrogated the expression of factors that are required for astrogliosis thus decreasing astrocytic proliferation and astrocyte hypertrophy.

Astrocytes are also a cellular source of proteoglycan expression, where the CSPGs such as phosphacan (Maeda et al., 1995; McKeon et al., 1999) and brevican (Yamada et al., 1994) are expressed exclusively by astrocytes. Neurocan, although primarily expressed by neurons (Engel et al., 1996), is also expressed by astrocytes in vitro (Oohira et al., 1994; Asher et al., 2000) and in various CNS injury models (McKeon et al., 1999; Matsui et al., 2002; Deguchi et al., 2005). Since astrocyte proliferation and reactivity were decreased following MIF treatment, it is possible that as a consequence the CSPG expression was also reduced. We determined that during the duration of microglial inhibition with MIF pan CSPG expression was significantly reduced using CS-56 immunohistochemistry. Fluorescent staining also revealed that neurocan expression was reduced at 14dpi.

The CSPG NG2 was also analyzed and a decrease in NG2 immunoreactivity was observed with MIF inhibition of microglia. NG2 positive OPCs proliferate rapidly following spinal cord injury (Yoo and Wrathall, 2007) but the decrease may not be due to a decrease in the OPC population, since NG2 expressing macrophages, meningeal, Schwann and endothelial cells infiltrate the spinal cord following injury (Jones et al., 2002; McTigue et al., 2006). The

decline in NG2 expression with MIF treatment could be due to the decrease in macrophage activation since MIF affects all cells of monocytic origin.

Chapter VI

Microglial inhibition with MIF preserves myelin and enhances axon regeneration

Introduction

Oligodendrocytes are particularly vulnerable to apoptotic cell death after CNS trauma (Casha et al., 2001). A single oligodendrocyte is responsible for myelinating multiple axons. The loss of oligodendrocytes causes the demyelination of many spared axons, eventually causing distal axons to lose conduction capacity. Without myelin axons alter the location and efficiency of ion channels necessary for saltatory conduction, which in turn disrupts action potentials (Waxman, 2001; Hains et al., 2003). In addition to affecting axon conductance and signaling, oligodendrocytes also maintain the structural integrity of the axon and contribute to neuronal survival (McTigue and Tripathi, 2008). Following SCI approximately half of the population of oligodendrocytes located in the peri-lesion area are lost within 2 days of the primary injury (Grossman et al., 2001; Lytle and Wrathall, 2007; Rabchevsky et al., 2007). Glutamate excitotoxicity has been associated with early oligodendrocyte loss, since blocking of glutamatergic receptors on oligodendrocytes prevents oligodendrocyte death after experimental spinal cord contusion (Rosenberg et al., 1999). Delayed and

secondary oligodendrocyte death occurs and expands outside the lesion area (Crowe et al., 1997) which can be attributed to the action of activated macrophages and microglia. Resting and activated microglia release glutamate, TNF-α, IL-1β and NOS, all of which have been shown to contribute to oligodendrocyte cell death (Streit et al., 1998; Merrill and Scolding, 1999; Pineau and Lacroix, 2007).

Oligodendrocytes are post-mitotic cells, and new oligodendrocytes must form for remyelination to occur once the mature oligodendrocytes are lost. To compensate for this loss of oligodendrocytes, after trauma oligodendrocyte precursor cells (OPCs) that express NG2 (nerve glia-2) CSPG migrate to the site of injury, proliferate and begin their differentiation. During the differentiation process, OPCs downregulate NG2 expression (Beasley and Stallcup, 1987; Levine and Stallcup, 1987), upregulate expression of myelin associated proteins, increase in process complexity and begin myelinating axons (McTigue and Tripathi, 2008). Under normal physiological conditions OPC numbers are low, but following insult OPCs proliferate rapidly over a time span from 48 hrs to 5 days (Levine, 1994). EAE models demonstrated that during treatment with MIF demyelination is reduced (Bhasin et al., 2007). The loss of oligodendrocytes, insufficient replenishment of new oligodendrocytes, and poor remyelination is predicted to lead to a decrease in neuronal viability since extensive myelin loss is usually followed by axonal degeneration.

The loss of oligodendrocytes following injury is not the sole cause of axonal degeneration, the initial mechanical impact can immediately sever, crush and

destroy axons. Since mature nerve cells are post mitotic, any functional recovery that is occurs after injury is due to the plasticity of the spared neurons. For an axon to regenerate, growth cones must form and be directed towards the target cell and for a functional connection, or synapse. Growth cones are sensitive to environmental factors, and depending on the environment, axon growth can be promoted or inhibited. There are many molecules that are released or upregulated after spinal cord injury that inhibit the intrinsic growth capacity of axons, such as CSPGs (Fitch and Silver, 2008) and myelin inhibitors. Cellular interactions can also prevent regeneration from occurring. Axonal die back, a phenomenon where axons retract long distances from the lesions, is associated with macrophage infiltration. An *in vitro* model of the glial scar provided evidence that macrophages interact with dystrophic axons and directly cause long-distance axonal retraction (Horn et al., 2008; Busch et al., 2009). Minocycline, a tetracycline derivative, inhibits microglia and thus reduces axonal die back of cortical spinal tract (CST) axons, death of oligodendrocytes and improving functional recovery (Stirling et al., 2004; Festoff et al., 2006; Yune et al., 2007). In the previous study, MIF inhibition of microglia/macrophages reduced astogliosis and CSPG upregulation; this in turn could make the environment more permissive for axonal regeneration and reduce axonal die back. Thus, this chapter will analyze the affect of microglial inhibition on oligodendrocyte survival and axonal regeneration in the spinal cord.

Results

More oligodendrocytes are present when microglial activation is inhibited with MIF

Since the number of oligodendrocytes declines following spinal cord injury, we wanted to assess whether inhibition of microglia with MIF had an effect on oligodendrocyte numbers. To examine the presence of mature oligodendrocytes spinal cords were analyzed for $CC1^+$ oligodendrocytes by taking six 40X fields for each time point and treatment group (Figure VI-1A,B). At 14dpi and 30dpi there was a significant difference in oligodendrocyte cell number when microglial activation was inhibited with MIF treatment, where there was a direct correlation with MIF treatment time and the number of oligodendrocytes present. To determine if the increase in oligodendrocyte number was due to oligodendrocyte survival, TUNEL was used to quantify apoptotic cell death of oligodendrocytes (Figure VI-C,D), seeing as secondary cell death associated with macrophage and microglial activation is apoptotic. We found that mice treated with PBS showed a significant increase in oligodendrocyte cell death over sham treated animals in all time points observed. When microglial activation was inhibited the number of TUNEL positive oligodendrocytes decreased significantly at 7dpi ($p<0.01$) and 14dpi ($p<0.05$) in comparison to PBS controls.

To confirm that microglial inhibition with MIF is directly associated with the increase in oligodendrocyte survival *in vivo*, microglia/oligodendrocyte co-cultures were prepared and treated with LPS, MIF alone, or MIF plus LPS (Figure VI-2A). CNPase/TUNEL positive cells were counted in each co-culture condition

(Figure VI-2B). Treatment with MIF alone did not induce cell death in oligodendrocytes as the number of TUNEL positive cells were similar to those observed in non-treated cultures. Oligodendrocytes expressing CNPase seem to be more 'inclined' to undergo cell death, while the MBP positive cells did not show significant cell death in the LPS treated condition, indicating that immature oligodendrocytes are more prone to cell death by LPS activated microglia. When MIF was added along with LPS the number of dying immature oligodendrocytes decreased indicating that microglial inhibition with MIF is sufficient to reduce oligodendrocyte cell death.

OPC proliferation is acutely augmented following microglial suppression

OPCs proliferate dramatically following SCI, so OPC numbers and proliferation were quantified following MIF treatment (Figure VI-3). Microglial inhibition altered the proliferation of OPCs, where significantly higher numbers of proliferative OPCs were observed at 1dpi in comparison PBS treatment (Figure VI-3 A,B). Hence, OPC proliferation is enhanced acutely following MIF treatment possibly differentiating into mature oligodendrocytes by 14dpi and 30dpi. To address if activated microglia decrease OPC proliferation *in vitro,* OPC microglial cocultures were treated with LPS, MIF or MIF plus LPS and incubated with BrdU (Figure VI-3C, D). There was no difference in OPC proliferation in non-treated and MIF treated cocultures. Alternatively, activation of microglia with LPS resulted in a decrease in OPC proliferation in comparison to controls (Figure VI-3C). The addition of MIF and LPS to the cocultures increased the number of

proliferative OPCs in comparison to LPS treatment alone. These results suggest that activated microglia do not induce cell death of OPC but instead decrease their proliferative capacity following insult.

More Myelin is present and more axons are viable when microglia are inhibited with MIF

Due to the increased number of oligodendrocytes present following MIF treatment, myelin basic protein (MBP), a component of myelin and a marker of fully differentiated OLs, was analyzed via immunohistochemistry and quantitative immunoblotting. Analysis of the epicenter region on PBS treated spinal cords showed that after MBP staining there was evidence of representative myelin debris, while MBP immunoreactivity revealed the presence of faint aberrant myelin 'tubes' at 1dpi which increased over time with MIF treatment (Figure VI-4D). Immunoblot analysis showed a decrease in all MBP isoforms following SCI in both PBS and MIF treatments; although MIF treatments resulted in significantly higher levels of MBP compared to those after PBS treatment, the difference never reached significance in comparison to the sham-treated animals (Figure VI-4A). Of particular note the 21kda and the 17kDa isoforms of MBP showed a marked increase in the MIF treatment groups at 7dpi for both isoforms and 30 dpi for the 21.5 kDa isoform when compared PBS treatment groups (Figure VI-4A,B,C). The 21.5 and 17kDa isoforms are upregulated during myelination and remyelination while the 18.5 and 14kDa isoforms of MBP are associated with compact myelin.

To rule out the possibility that what we perceived as results were rather false positives due to myelin debris, another group of mice were treated with MIF for 14 days or PBS and spinal cords were prepared for electron microscopic analysis to determine the fine detail of myelin and axonal survival (Figure VI-5A). Electron microscopic images of myelin and axons determined that demyelination was occurring at 3dpi in both PBS treatment and MIF treatment conditions, although MIF treatment resulted in more myelinated axons (Figure VI-5B). However at 30dpi MIF treatment yielded a dramatic increase in axons possessing myelin. Hence MIF was probably preventing some demyelination earlier on after the injury and was later enhancing remyelination, thus ending with less axonal death which is determined by a dark axonal cytoplasm.

The presence of MIF reduces axonal die back

Since more axons were viable around the approximate lesion epicenter determined by electron microscopy, we sought to analyze axon growth or 'die back' within the lesioned area. Retrograde axon labeling was performed by injecting CTB into the sciatic nerve 4 days prior to sacrificing the mice. When treated for 7 and 14 days with MIF, more neurites were present in the lesioned area in comparison to the PBS treated group alone. The 14 day treatment had more neurites within the lesion than the 7day treatment (Figure VI-6A,B).

Figure VI-1

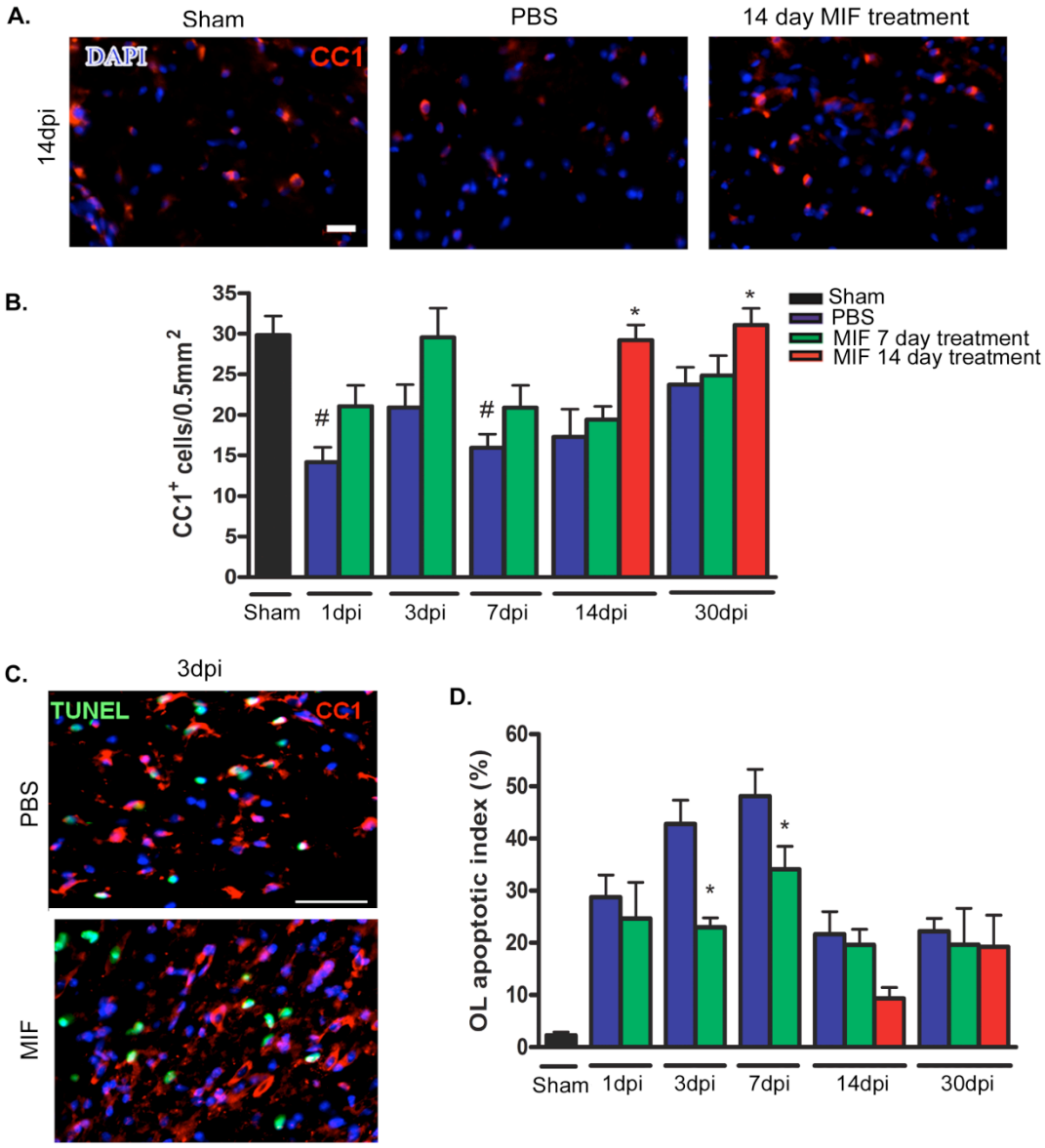

Figure VI-1. Oligodendrocyte numbers are augmented when microglia are inhibited with MIF. Spinal cord sections were stained for the mature oligodendrocyte marker, CC1 (red) and fluorescent images were captured. **A**, Representative images of $CC1^+$ oligodendrocytes in sham, PBS and 14day MIF treatments at 14dpi. **B,** Quantification of the number of $CC1^+$ oligodendrocytes present following spinal cord injury in PBS and MIF treated spinal cords (# comparison to sham; * comparison to PBS treatments). Error bars represent SEM, where *p<0.05, #p<0.05 by ANOVA followed by Bonferroni's post hoc test (n=6 individual experiments). **C,** TUNEL and CC1 stain of spinal cords and **D**, quantification of the percent of oligodendrocyte cell death (* comparison to PBS treated groups). Error bars represent SEM, where *p<0.05 by ANOVA followed by Bonferroni's post hoc test (n=6 individual experiments).

Figure VI-2

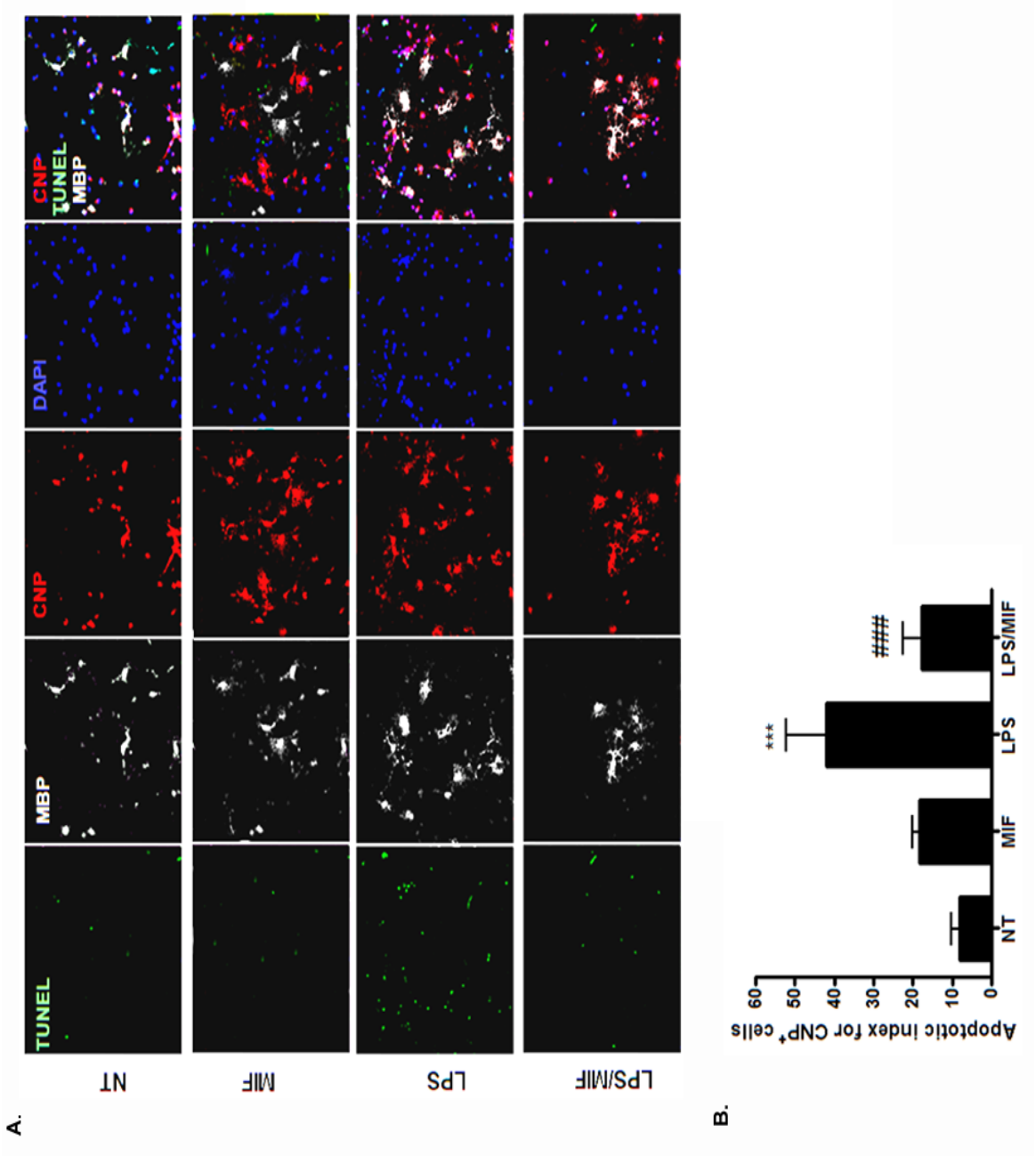

Figure VI-2. Microglia directly affects oligodendrocyte survival.
A, Confocal images of mixed microglial and oligodendrocyte cocultures. Mixed cultures were treated with MIF, LPS, LPS and MIF **B,** and oligodendrocyte cell death was assessed via TUNEL staining. The number of CNPase+/TUNEL+ cells was quantified. (* comparison with nt; # comparison to LPS) Error bars represent SEM, where ***p<0.001 ###p<0.001 by ANOVA followed by Bonferroni's post hoc test (n=6 individual experiments).

Figure VI-3

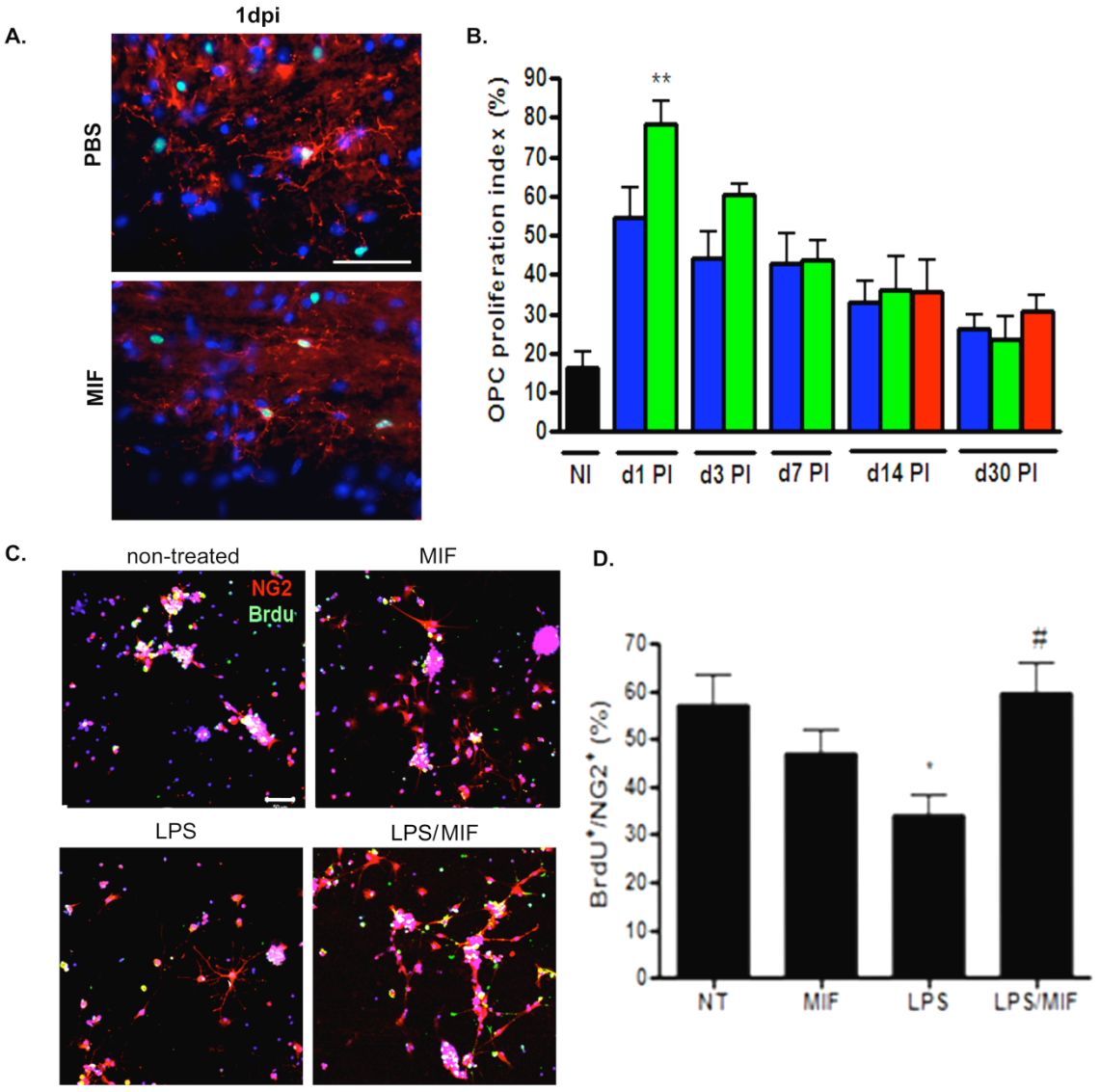

Figure VI-3. Microglial inhibition increased OPC proliferation.
A. NG2 stain for OPC co-stained against ki-67 within the spinal cord and **B,** proliferation was quantified. C**,** Confocal images of OPC and microglia co-cultures. Co-cultures were treated with MIF, LPS, LPS and MIF and BrdU was added to assess **D,** OPC proliferation and **E**, sphere formation. (* comparison with non-treated (NT); # comparison to LPS)Error bars represent SEM, where *p<0.05, **p<0.01, ##p<0.01 by ANOVA followed by Bonferroni's post hoc test (n=6 individual experiments)Scale bar 50μm

Figure VI-4

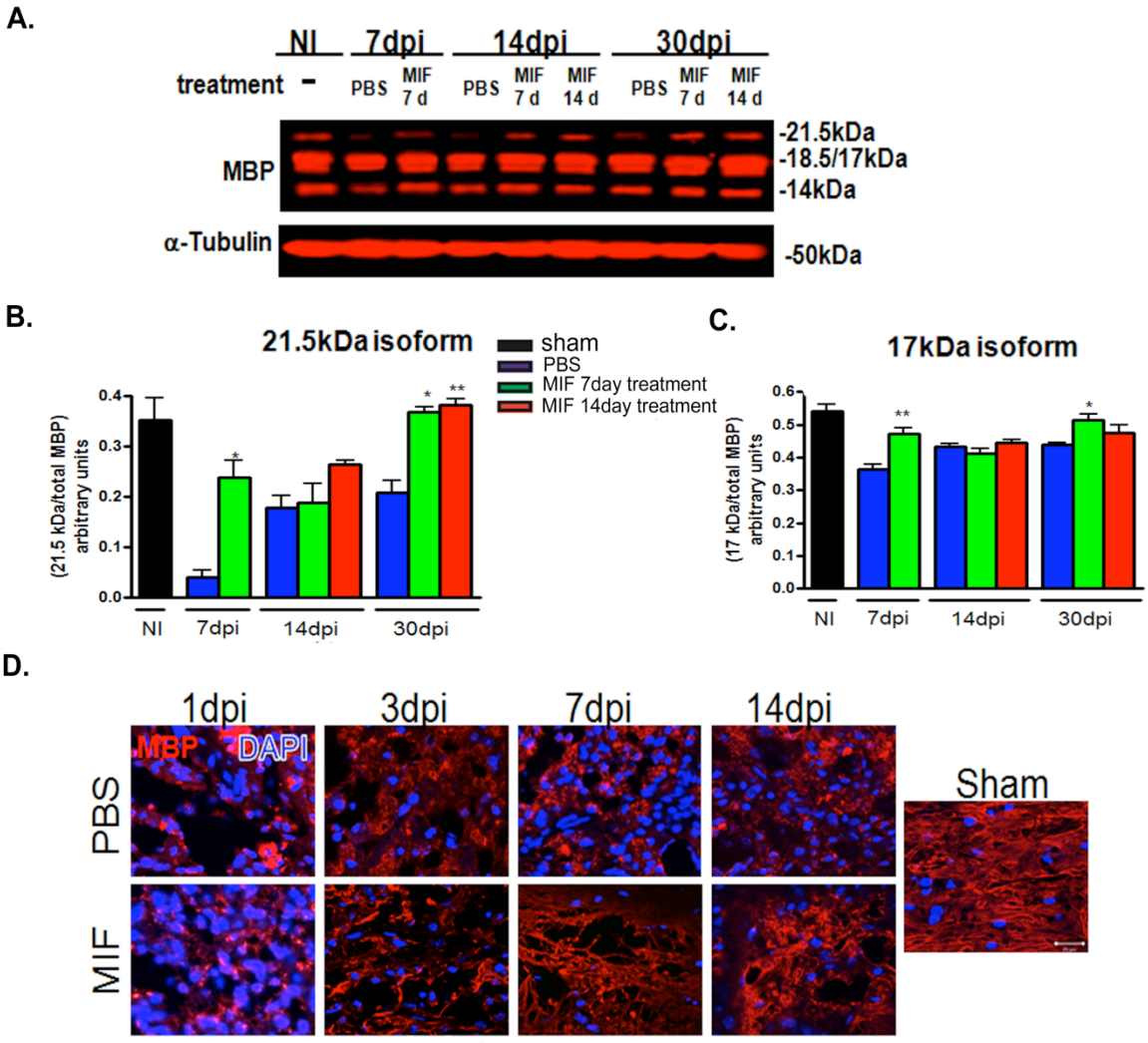

Figure VI-4. More MBP is present with microglial inhibition. A, Quantitative immunoblotting was performed on spinal cord homogenates and MBP expression was assessed and the 21.5 **(B)** and 17kDa **(C)** isoforms expression was quantified. **D,** Fluorescent images of MBP bordering the lesion epicenter. where *p<0.05, **p<0.01, ***p<0.001 by ANOVA followed by Bonferroni's post hoc test (n=6 individual experiments)

Figure VI-5

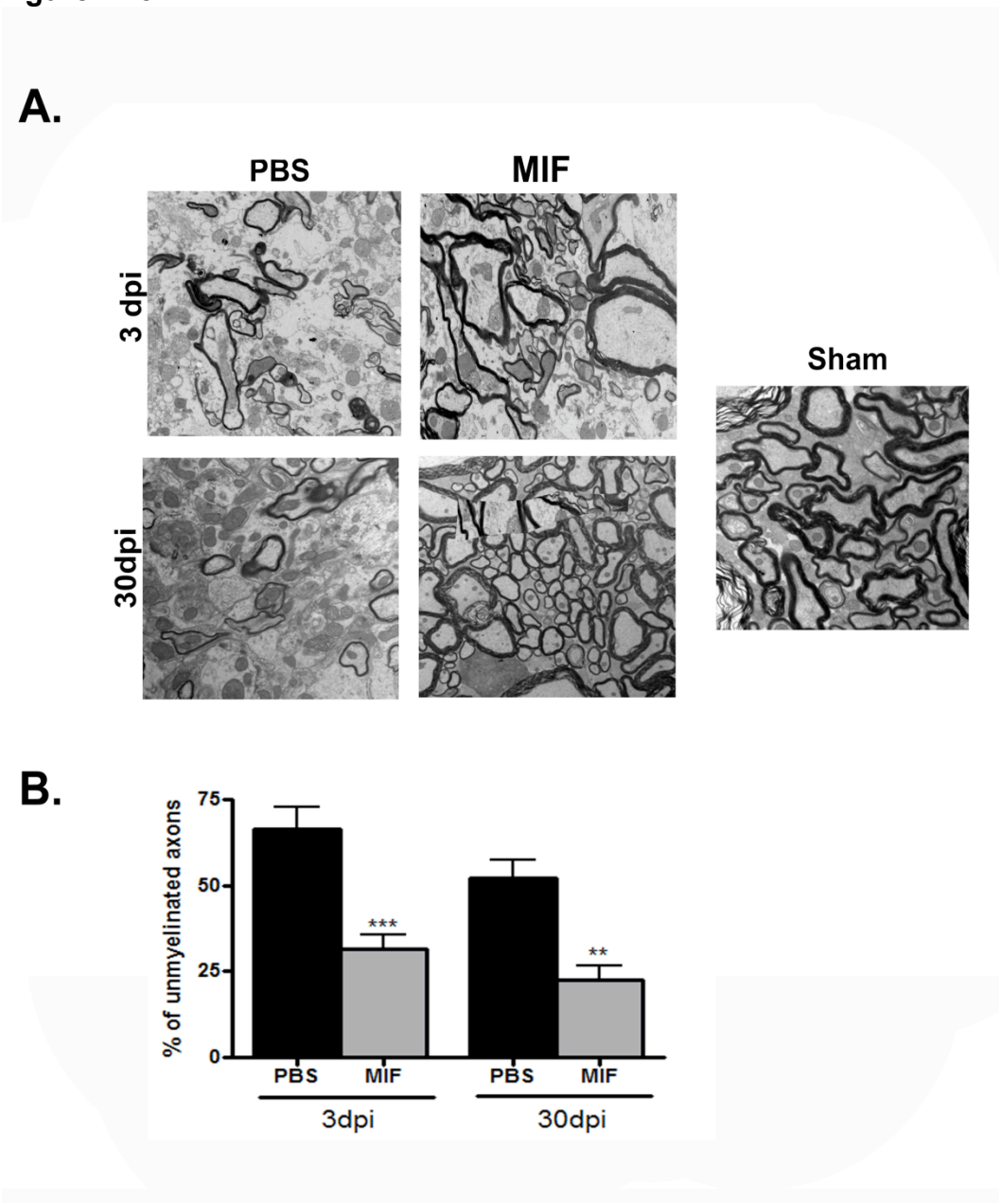

Figure VI-5. Less unmyelinated axons are associated with microglial inhibition.
A, Electron micrographs of spinal cords treated with PBS and MIF for up to 14 dpi. **B,** quantification of number of myelinated/unmyelinated axons from MIF and PBS treated animals, where 100 axons/group were counted. Error bars represent SEM, where *p<0.05, **p<0.01, ***p<0.001 by ANOVA followed by Bonferroni's post hoc test n=3 individual experiments)

Figure VI-6

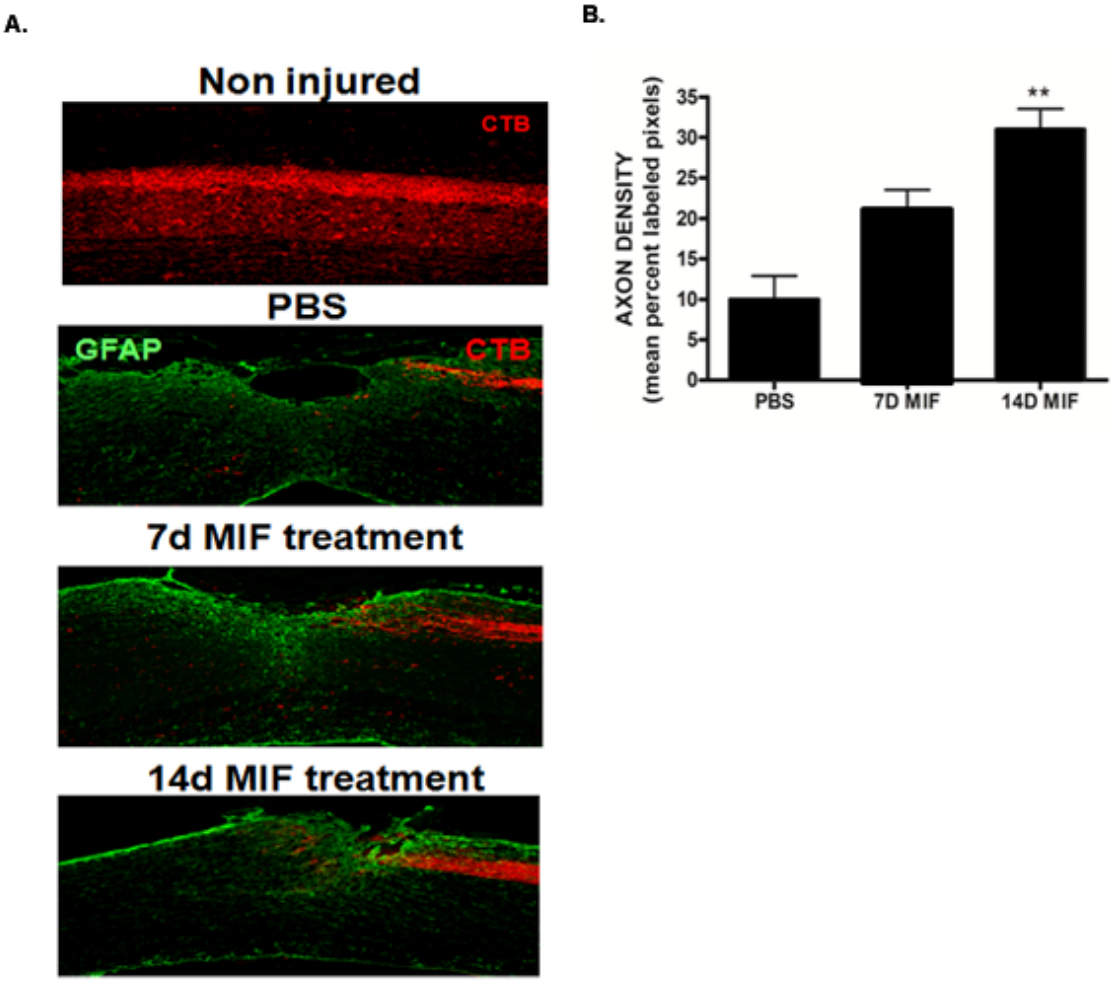

Figure VI-6. Enhancement of neurite outgrowth within the lesion core upon MIF treatment. A, Retrograde axon labeling with CTB via the sciatic nerve was performed on MIF and PBS treated mice and spinal cords were isolated at 30dpi**. B,** Mean axonal density was quantified by imaging serial sections and determining the optical density within the lesioned area. Error bars represent SEM, where **p<0.01by ANOVA followed by Bonferroni's post hoc test (n=6 individual experiments).

Discussion

A large number of oligodendrocytes were lost in PBS control groups with the largest amount of death seen at 7dpi. In contrast, when microglia and macrophages were inhibited with MIF the number of oligodendrocytes was significantly higher throughout MIF treatment in relationship to the PBS control-treated mice. The increase in oligodendrocyte numbers could possibly be due to the observed decrease in cell death of oligodendrocytes. Moreover, macrophages have been shown to influence the proliferation and differentiation of $NG2^+$ progenitors (Schonberg et al., 2007) and we found that inhibition of microglia and macrophages caused an acute enhancement of proliferation of OPCs at 1dpi. This *in vivo* data was supported by *in vitro* co-cultures of oligodendrocytes or OPCs with microglia, where. Activated microglia caused a reduction in OPC proliferation consistent with the report that $NG2^+$ cells proliferation is inhibited by the addition of purified $OX42^+$ microglia/macrophages isolated from injured spinal cords (Wu et al.). MIF treatment increased sphere number to near normal levels. The OPC data presented in this corresponds with the data from Taylor in which TLR4 activated microglia decrease the proliferative properties of OPCs (Taylor et al.).

The 17 and 21.5 kDa isoforms of MBP are upregulated during myelination/remyelination whereas the 18 and 14 kDa isoforms are components of compact myelin. We found that the protein levels of the 17 kDa and 21.5 kDa isoforms were higher in the MIF treatment groups. This result is either indicative of remyelination or, since the levels of 21.5 kDa isoform in the MIF treatment

never exceeded the levels observed in the sham injury, it is plausible that that some demyelination was being prevented. Myelin basic protein staining revealed that demyelination was occurring post injury but not to the extent happening in PBS treated groups. Aberrant myelin formation was observed at later time points post injury suggestive of remyelination. Since the oligodendrocyte numbers were higher and the number of oligodendrocytes undergoing cell death was decreased in the MIF-treatment groups in comparison to the PBS-treatment groups, it is purported that axons were not as dramatically demyelinated. Electron micrographs from 3 and 30dpi support these findings: at 3dpi demyelination was evident, higher numbers of small diameter axons remained myelinated when microglial activation was inhibited, and micrographs of 30dpi showed a significant increase in the number of myelinated axons.

Electron micrograph analysis also showed an increase in axon survival as more axons had bright cytoplasm in comparison to PBS treatment groups. Since more axons were surviving the injury this lead us to investigate if there was a difference in the number of axons entering the lesioned area via retrograde axon labeling with CTB. We found that the density of axons within the lesioned area was significantly greater when microglia were inhibited with the tripeptide MIF.

Chapter VII

Conclusion and Future directions

Thesis Summary

Injury to the spinal cord causes immediate necrosis followed by secondary bystander damage. Secondary damage is attributed to reactive glial cells that attempt to repair the injury but instead cause further destruction. Each glial population responds differently to injury. Mature oligodendrocytes, the myelinating cells of the CNS, do not undergo cellular changes and like neurons are susceptible to deleterious environmental factors that are released or expressed by other glial cells. Astrocytes on the other hand become reactive and are the main cellular component of the glial scar, physically obstructing axonal regrowth in the lesion. Biochemically, astrocytes upregulate surface molecules and secrete a surfeit of factors that can hinder axon growth. Microglia are probably the first cell type to respond to SCI as normal sensors of the environments and part of the immune response. Microglia become reactive within minutes, actively engulfing necrotic and apoptotic debris as well as releasing factors that contribute to inflammation. Due to the dual (neuroprotective and neurotoxic) roles microglia play following SCI, the major contribution of microglia following injury is still debatable. The experiments described in this dissertation investigate the role microglia play in severe SCI and were designed to determine whether lack of microglial activation via ablation or inhibition has deleterious or restorative effects. First, ablation of microglia in CD11b-HSVTK$^{+/-}$ transgenic mice with GCV allowed for the depletion of

proliferating microglia at certain time points post injury and the determination of a microglial temporal pattern and contribution to injury. Isolating different segments of the spinal cord also allowed for the analysis of microglial spatial pattern. The two approaches in combination allowed for the examination of pro- and anti-inflammatory cytokine release following injury in a spatiotemporal pattern. Ablation of microglia at different time points also addressed the question of whether delayed inhibition of microglia could have neuroprotective effects on axonal regeneration. Second, microglia activation was inhibited with the tripeptide, MIF, and reactive gliosis and axonal regeneration were examined, since this could be a potential therapy for SCI.

In this thesis, we have shown that the overall prevailing role of microglia following severe SCI is deleterious, but at later time points microglia can have beneficial properties. Ablation of microglia at various time points post SCI demonstrated that microglia are deleterious the first few days following injury, since early ablation diminished the proinflammatory cytokine TNF-α, enhance IL-10 expression and the number of axons present within the lesion area. Ablating microglia at later time points resulted in TNF-α production and a reduction of IL-10 levels, while the density of axons within the glial scar was not found to be as significant as at early time point ablation, supporting the idea that at later time points microglia tend to be more beneficial post injury. Unfortunately, in this model of ablation, all proliferating $CD11b^+$ cells were affected which included cells of monocytic origin and neutrophils so the effect was not solely specific for cells of monocytic origin. Treatment with GCV also had peripheral affects since

the mice developed aplastic anemia thereby limiting the time the experiment could be performed.

Inhibition of microglia with the tripeptide MIF reduced the activation of astrocytes. The reduction of astrocyte reactivity observed in the MIF treatment concomitantly reduced the expression of CSPGs thereby creating a more permissive environment for axon growth since CSPGS reduce the ability of axons to regenerate in areas of reactive gliosis (Hoke and Silver, 1996; Davies et al., 1997; Davies et al., 1999). Suppression of microglia also had a dramatic effect on the oligodendrocyte population. OPC proliferation was enhanced with inhibition of microglia with MIF *in vitro* and was acutely enhanced *in vivo,* which could differentiate and replenish the oligodendrocyte population that is lost following SCI. MIF treatment also reduced the amount of oligodendrocyte cell death leading to sparing of myelin and prevention of axonal dieback. All of these effects could be attributed to a number of factors that microglia and macrophage secrete. MIF inhibition of microglia and macrophages drastically diminished TNF-α production acutely following the injury, and an increase in IL-10 was observed. TNF-α is associated with oligodendrocyte cell death in models of EAE: high concentrations of TNF-α evident in EAE affect sensitive oligodendrocytes and cause oligodendrocyte cell death (Akassoglou et al., 1998; Jurewicz et al., 2003; Hovelmeyer et al., 2005; Jurewicz et al., 2005). IL-10 down regulates secondary inflammation and reduces cytokine expression following insults (Bethea et al., 1999; Plunkett et al., 2001). The increase in IL-10 expression could be an effector for the observed reduction of astrogliosis since

the cytokine has been shown to attenuate astroglial reactivity (Balasingam and Yong, 1996). Spinal neurons have also been demonstrated to express the IL-10 receptor through which IL-10 induces the growth and survival of neurons (Zhou et al., 2009). Such a scenario could explain the presence of more neurites found crossing through the glial scar in both the microglial ablation and inhibition studies.

In summary, inhibition of macrophages and microglia, reduces TNF-α levels thereby protecting oligodendrocytes and reducing the potential of axonal injury (Figure VII-1). Microglial suppression also cause a concomitant increase in IL-10, which negatively regulates proinflammatory cytokines such as TNF-α, reduces astrogliosis and promotes axonal survival (Figure VII-1). The reduction in astrogliosis would then lead to lower levels of the CSPG, neurocan and NG2 expression will also be reduced since macrophages and microglia express NG2 and inhibition of activation would reduce chemotoxis and recruitment of more NG2+ monocytic cells (Figure VII-1).

Future directions

Current ongoing experiments are being performed to determine the degree of demyelination/remyelination by quantifying G-ratios of electron micrographs. The extent of axon regeneration or dieback is being analyzed by making 3-dimentional composites of the spinal cords. For future experiments, it would be interesting to see if a milder injury causes microglia to be more beneficial, since the predominate role of microglia is deleterious in severe spinal

cord injury. This is a possibility since each injury has a different cellular and molecular outcome, and microglia may not be as reactive in a less severe model. Another question that remains elusive is the mechanism of action of MIF. Does this tripeptide bind to a cell surface receptor inhibiting or enhancing signaling pathways that are, respectively, deleterious or beneficial? Does MIF cause the down-regulation of cell surface receptors or is it internalized, possibly binding to intracellular proteins? This could be first determined by analyzing intracellular signing pathways that are associated with microglial activation. To investigate if MIF binds to a receptor particular receptor antagonist could be used to block the receptor and determine if MIF still has an inhibitory effect.

It is evident that SCI is difficult to treat since so many factors inhibit axonal regeneration. Currently combination therapies are in clinical trials to see if they can enhance axonal regeneration and functional recovery. It is possible that MIF could be used in a combination therapy, such as with chondroitinase ABC which removes inhibitory GAG chains of CSPGs or with transplanted cells, e.g. Schwann or stem cells, thereby enhancing functional recovery.

Figure VII-1

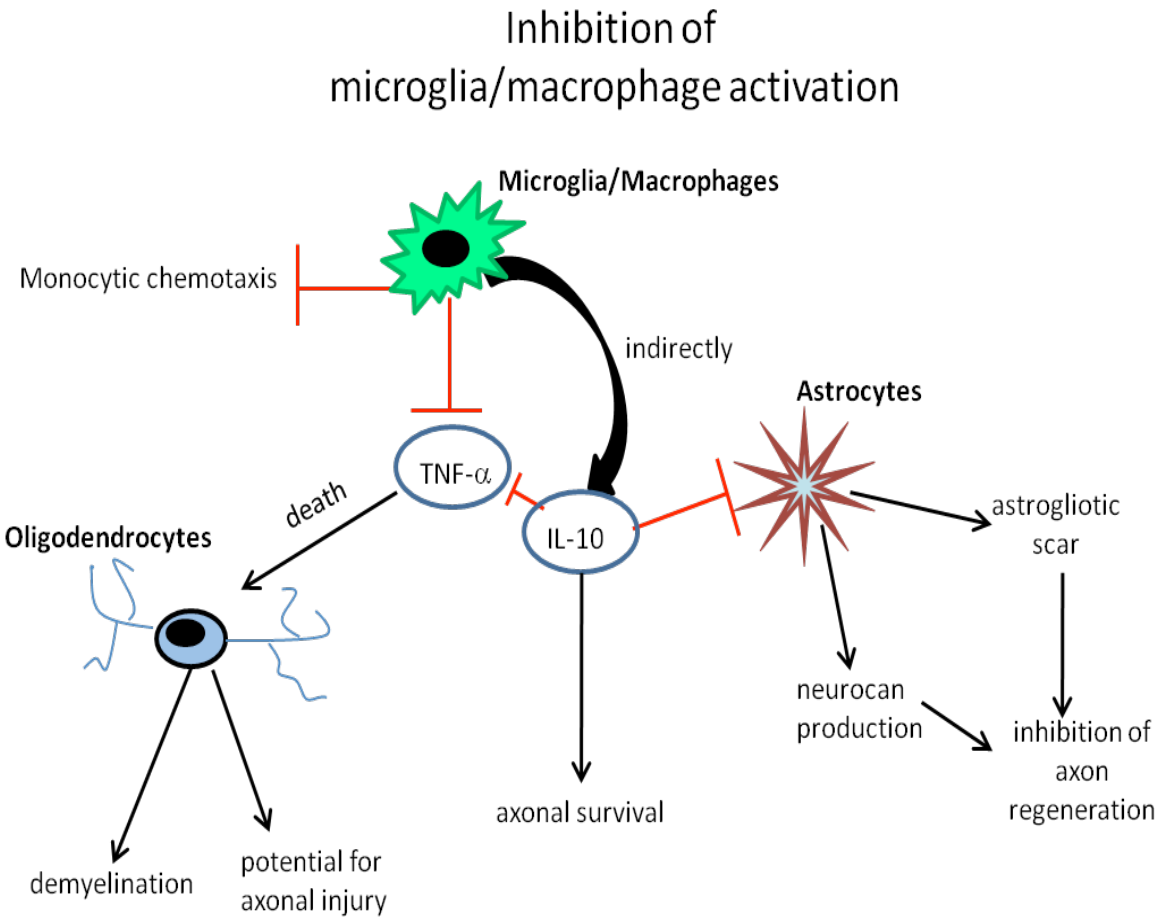

Figure VII-1. Proposed mechanism for microglial inhibition.
Inhibition of microglial activation reduces TNF-α production thereby causing enhanced survival of oligodendrocytes, less demyelination and a reduction in axonal injury. Inhibition of microglia also caused an increase in the anti-inflammatory cytokine IL-10, which in turn directly effects axonal survival and downregulates astrocytic reactivity. The reduction in astrocytic reactivity reduced the expression of inhibitory molecules and decreases the cellular density of the astrogliotic scar.

References

Abraham KE, McMillen D, Brewer KL (2004) The effects of endogenous interleukin-10 on gray matter damage and the development of pain behaviors following excitotoxic spinal cord injury in the mouse. Neuroscience 124:945-952.

Ahn YH, Lee G, Kang SK (2006) Molecular insights of the injured lesions of rat spinal cords: Inflammation, apoptosis, and cell survival. Biochem Biophys Res Commun 348:560-570.

Akassoglou K, Bauer J, Kassiotis G, Pasparakis M, Lassmann H, Kollias G, Probert L (1998) Oligodendrocyte apoptosis and primary demyelination induced by local TNF/p55TNF receptor signaling in the central nervous system of transgenic mice: models for multiple sclerosis with primary oligodendrogliopathy. Am J Pathol 153:801-813.

Aloisi F (2001) Immune function of microglia. Glia 36:165-179.

Asher RA, Morgenstern DA, Fidler PS, Adcock KH, Oohira A, Braistead JE, Levine JM, Margolis RU, Rogers JH, Fawcett JW (2000) Neurocan is upregulated in injured brain and in cytokine-treated astrocytes. J Neurosci 20:2427-2438.

Auriault C, Joseph M, Tartar A, Capron A (1983) Characterization and synthesis of a macrophage inhibitory peptide from the second constant domain of human immunoglobulin G. FEBS Lett 153:11-15.

Bachis A, Colangelo AM, Vicini S, Doe PP, De Bernardi MA, Brooker G, Mocchetti I (2001) Interleukin-10 prevents glutamate-mediated cerebellar granule cell death by blocking caspase-3-like activity. J Neurosci 21:3104-3112.

Balasingam V, Yong VW (1996) Attenuation of astroglial reactivity by interleukin-10. J Neurosci 16:2945-2955.

Bartholdi D, Schwab ME (1997) Expression of pro-inflammatory cytokine and chemokine mRNA upon experimental spinal cord injury in mouse: an in situ hybridization study. Eur J Neurosci 9:1422-1438.

Beasley L, Stallcup WB (1987) The nerve growth factor-inducible large external (NILE) glycoprotein and neural cell adhesion molecule (N-CAM) have distinct patterns of expression in the developing rat central nervous system. J Neurosci 7:708-715.

Beattie MS, Li Q, Bresnahan JC (2000) Cell death and plasticity after experimental spinal cord injury. Prog Brain Res 128:9-21.

Bethea JR, Nagashima H, Acosta MC, Briceno C, Gomez F, Marcillo AE, Loor K, Green J, Dietrich WD (1999) Systemically administered interleukin-10 reduces tumor necrosis factor-alpha production and significantly improves functional recovery following traumatic spinal cord injury in rats. J Neurotrauma 16:851-863.

Bhasin M, Wu M, Tsirka SE (2007) Modulation of microglial/macrophage activation by macrophage inhibitory factor (TKP) or tuftsin (TKPR) attenuates the disease course of experimental autoimmune encephalomyelitis. BMC Immunol 8:10.

Bignami A, Hosley M, Dahl D (1993) Hyaluronic acid and hyaluronic acid-binding proteins in brain extracellular matrix. Anatomy and embryology 188:419-433.

Blight AR, Cohen TI, Saito K, Heyes MP (1995) Quinolinic acid accumulation and functional deficits following experimental spinal cord injury. Brain 118 (Pt 3):735-752.

Boyd ZS, Kriatchko A, Yang J, Agarwal N, Wax MB, Patil RV (2003) Interleukin-10 receptor signaling through STAT-3 regulates the apoptosis of retinal ganglion cells in response to stress. Invest Ophthalmol Vis Sci 44:5206-5211.

Brambilla R, Bracchi-Ricard V, Hu WH, Frydel B, Bramwell A, Karmally S, Green EJ, Bethea JR (2005) Inhibition of astroglial nuclear factor kappaB reduces inflammation and improves functional recovery after spinal cord injury. J Exp Med 202:145-156.

Brewer KL, Bethea JR, Yezierski RP (1999) Neuroprotective effects of interleukin-10 following excitotoxic spinal cord injury. Exp Neurol 159:484-493.

Bu J, Akhtar N, Nishiyama A (2001) Transient expression of the NG2 proteoglycan by a subpopulation of activated macrophages in an excitotoxic hippocampal lesion. Glia 34:296-310.

Busch SA, Horn KP, Silver DJ, Silver J (2009) Overcoming macrophage-mediated axonal dieback following CNS injury. J Neurosci 29:9967-9976.

Carr MW, Roth SJ, Luther E, Rose SS, Springer TA (1994) Monocyte chemoattractant protein 1 acts as a T-lymphocyte chemoattractant. Proc Natl Acad Sci U S A 91:3652-3656.

Casha S, Yu WR, Fehlings MG (2001) Oligodendroglial apoptosis occurs along degenerating axons and is associated with FAS and p75 expression following spinal cord injury in the rat. Neuroscience 103:203-218.

Chan WY, Kohsaka S, Rezaie P (2007) The origin and cell lineage of microglia: new concepts. Brain Res Rev 53:344-354.

Chang RC, Rota C, Glover RE, Mason RP, Hong JS (2000) A novel effect of an opioid receptor antagonist, naloxone, on the production of reactive oxygen species by microglia: a study by electron paramagnetic resonance spectroscopy. Brain Res 854:224-229.

Crowe MJ, Bresnahan JC, Shuman SL, Masters JN, Beattie MS (1997) Apoptosis and delayed degeneration after spinal cord injury in rats and monkeys. Nat Med 3:73-76.

Davies SJ, Goucher DR, Doller C, Silver J (1999) Robust regeneration of adult sensory axons in degenerating white matter of the adult rat spinal cord. J Neurosci 19:5810-5822.

Davies SJ, Fitch MT, Memberg SP, Hall AK, Raisman G, Silver J (1997) Regeneration of adult axons in white matter tracts of the central nervous system. Nature 390:680-683.

Deguchi K, Takaishi M, Hayashi T, Oohira A, Nagotani S, Li F, Jin G, Nagano I, Shoji M, Miyazaki M, Abe K, Huh NH (2005) Expression of neurocan after transient middle cerebral artery occlusion in adult rat brain. Brain Res 1037:194-199.

Dong Y, Benveniste EN (2001) Immune function of astrocytes. Glia 36:180-190.

Eddleston M, Mucke L (1993) Molecular profile of reactive astrocytes--implications for their role in neurologic disease. Neuroscience 54:15-36.

Ekdahl CT, Claasen JH, Bonde S, Kokaia Z, Lindvall O (2003) Inflammation is detrimental for neurogenesis in adult brain. Proc Natl Acad Sci U S A 100:13632-13637.

Elion GB (1980) The chemotherapeutic exploitation of virus-specified enzymes. Adv Enzyme Regul 18:53-66.

Elion GB, Furman PA, Fyfe JA, de Miranda P, Beauchamp L, Schaeffer HJ (1977) Selectivity of action of an antiherpetic agent, 9-(2-hydroxyethoxymethyl) guanine. Proc Natl Acad Sci U S A 74:5716-5720.
Engel M, Maurel P, Margolis RU, Margolis RK (1996) Chondroitin sulfate proteoglycans in the developing central nervous system. I. cellular sites of synthesis of neurocan and phosphacan. J Comp Neurol 366:34-43.
Faissner A (1997) The tenascin gene family in axon growth and guidance. Cell Tissue Res 290:331-341.
Faulkner JR, Herrmann JE, Woo MJ, Tansey KE, Doan NB, Sofroniew MV (2004) Reactive astrocytes protect tissue and preserve function after spinal cord injury. J Neurosci 24:2143-2155.
Fawcett JW, Asher RA (1999) The glial scar and central nervous system repair. Brain research bulletin 49:377-391.
Festoff BW, Ameenuddin S, Arnold PM, Wong A, Santacruz KS, Citron BA (2006) Minocycline neuroprotects, reduces microgliosis, and inhibits caspase protease expression early after spinal cord injury. J Neurochem 97:1314-1326.
Fitch MT, Silver J (1997) Glial cell extracellular matrix: boundaries for axon growth in development and regeneration. Cell Tissue Res 290:379-384.
Fitch MT, Silver J (2008) CNS injury, glial scars, and inflammation: Inhibitory extracellular matrices and regeneration failure. Exp Neurol 209:294-301.
Fyfe JA, Keller PM, Furman PA, Miller RL, Elion GB (1978) Thymidine kinase from herpes simplex virus phosphorylates the new antiviral compound, 9-(2-hydroxyethoxymethyl)guanine. J Biol Chem 253:8721-8727.
Garwood J, Rigato F, Heck N, Faissner A (2001) Tenascin glycoproteins and the complementary ligand DSD-1-PG/ phosphacan--structuring the neural extracellular matrix during development and repair. Restor Neurol Neurosci 19:51-64.
Gehrmann J, Mies G, Bonnekoh P, Banati R, Iijima T, Kreutzberg GW, Hossmann KA (1993) Microglial reaction in the rat cerebral cortex induced by cortical spreading depression. Brain Pathol 3:11-17.
Giulian D, Robertson C (1990) Inhibition of mononuclear phagocytes reduces ischemic injury in the spinal cord. Ann Neurol 27:33-42.
Giulian D, Chen J, Ingeman JE, George JK, Noponen M (1989) The role of mononuclear phagocytes in wound healing after traumatic injury to adult mammalian brain. J Neurosci 9:4416-4429.
Glaser J, Gonzalez R, Perreau VM, Cotman CW, Keirstead HS (2004) Neutralization of the chemokine CXCL10 enhances tissue sparing and angiogenesis following spinal cord injury. J Neurosci Res 77:701-708.
Gonzalez R, Glaser J, Liu MT, Lane TE, Keirstead HS (2003) Reducing inflammation decreases secondary degeneration and functional deficit after spinal cord injury. Exp Neurol 184:456-463.
Grilli M, Barbieri I, Basudev H, Brusa R, Casati C, Lozza G, Ongini E (2000) Interleukin-10 modulates neuronal threshold of vulnerability to ischaemic damage. Eur J Neurosci 12:2265-2272.
Gris D, Marsh DR, Oatway MA, Chen Y, Hamilton EF, Dekaban GA, Weaver LC (2004) Transient blockade of the CD11d/CD18 integrin reduces secondary damage after

spinal cord injury, improving sensory, autonomic, and motor function. J Neurosci 24:4043-4051.
Grossman SD, Rosenberg LJ, Wrathall JR (2001) Temporal-spatial pattern of acute neuronal and glial loss after spinal cord contusion. Exp Neurol 168:273-282.
Hagg T, Oudega M (2006) Degenerative and spontaneous regenerative processes after spinal cord injury. J Neurotrauma 23:264-280.
Hains BC, Klein JP, Saab CY, Craner MJ, Black JA, Waxman SG (2003) Upregulation of sodium channel Nav1.3 and functional involvement in neuronal hyperexcitability associated with central neuropathic pain after spinal cord injury. J Neurosci 23:8881-8892.
Hanisch UK (2002) Microglia as a source and target of cytokines. Glia 40:140-155.
Hanisch UK, Kettenmann H (2007) Microglia: active sensor and versatile effector cells in the normal and pathologic brain. Nat Neurosci 10:1387-1394.
Hausmann ON (2003) Post-traumatic inflammation following spinal cord injury. Spinal Cord 41:369-378.
Heppner FL, Greter M, Marino D, Falsig J, Raivich G, Hovelmeyer N, Waisman A, Rulicke T, Prinz M, Priller J, Becher B, Aguzzi A (2005) Experimental autoimmune encephalomyelitis repressed by microglial paralysis. Nat Med 11:146-152.
Hoke A, Silver J (1996) Proteoglycans and other repulsive molecules in glial boundaries during development and regeneration of the nervous system. Prog Brain Res 108:149-163.
Horn KP, Busch SA, Hawthorne AL, van Rooijen N, Silver J (2008) Another barrier to regeneration in the CNS: activated macrophages induce extensive retraction of dystrophic axons through direct physical interactions. J Neurosci 28:9330-9341.
Hovelmeyer N, Hao Z, Kranidioti K, Kassiotis G, Buch T, Frommer F, von Hoch L, Kramer D, Minichiello L, Kollias G, Lassmann H, Waisman A (2005) Apoptosis of oligodendrocytes via Fas and TNF-R1 is a key event in the induction of experimental autoimmune encephalomyelitis. J Immunol 175:5875-5884.
Howard M, O'Garra A, Ishida H, de Waal Malefyt R, de Vries J (1992) Biological properties of interleukin 10. J Clin Immunol 12:239-247.
Hu S, Peterson PK, Chao CC (1997) Cytokine-mediated neuronal apoptosis. Neurochemistry international 30:427-431.
Jackson CA, Messinger J, Peduzzi JD, Ansardi DC, Morrow CD (2005) Enhanced functional recovery from spinal cord injury following intrathecal or intramuscular administration of poliovirus replicons encoding IL-10. Virology 336:173-183.
Jones LL, Margolis RU, Tuszynski MH (2003) The chondroitin sulfate proteoglycans neurocan, brevican, phosphacan, and versican are differentially regulated following spinal cord injury. Exp Neurol 182:399-411.
Jones LL, Yamaguchi Y, Stallcup WB, Tuszynski MH (2002) NG2 is a major chondroitin sulfate proteoglycan produced after spinal cord injury and is expressed by macrophages and oligodendrocyte progenitors. J Neurosci 22:2792-2803.
Jurewicz A, Matysiak M, Tybor K, Selmaj K (2003) TNF-induced death of adult human oligodendrocytes is mediated by c-jun NH2-terminal kinase-3. Brain 126:1358-1370.

Jurewicz A, Matysiak M, Tybor K, Kilianek L, Raine CS, Selmaj K (2005) Tumour necrosis factor-induced death of adult human oligodendrocytes is mediated by apoptosis inducing factor. Brain 128:2675-2688.
Kaur C, Hao AJ, Wu CH, Ling EA (2001) Origin of microglia. Microsc Res Tech 54:2-9.
Kreutzberg GW (1996) Microglia: a sensor for pathological events in the CNS. Trends Neurosci 19:312-318.
Lee SC, Liu W, Dickson DW, Brosnan CF, Berman JW (1993) Cytokine production by human fetal microglia and astrocytes. Differential induction by lipopolysaccharide and IL-1 beta. J Immunol 150:2659-2667.
Lee SM, Yune TY, Kim SJ, Park DW, Lee YK, Kim YC, Oh YJ, Markelonis GJ, Oh TH (2003) Minocycline reduces cell death and improves functional recovery after traumatic spinal cord injury in the rat. J Neurotrauma 20:1017-1027.
Levine JM (1994) Increased expression of the NG2 chondroitin-sulfate proteoglycan after brain injury. J Neurosci 14:4716-4730.
Levine JM, Stallcup WB (1987) Plasticity of developing cerebellar cells in vitro studied with antibodies against the NG2 antigen. J Neurosci 7:2721-2731.
Liu B, Du L, Hong JS (2000) Naloxone protects rat dopaminergic neurons against inflammatory damage through inhibition of microglia activation and superoxide generation. J Pharmacol Exp Ther 293:607-617.
Liu XZ, Xu XM, Hu R, Du C, Zhang SX, McDonald JW, Dong HX, Wu YJ, Fan GS, Jacquin MF, Hsu CY, Choi DW (1997) Neuronal and glial apoptosis after traumatic spinal cord injury. J Neurosci 17:5395-5406.
Liu Y, Qin L, Li G, Zhang W, An L, Liu B, Hong JS (2003) Dextromethorphan protects dopaminergic neurons against inflammation-mediated degeneration through inhibition of microglial activation. J Pharmacol Exp Ther 305:212-218.
Liuzzi FJ, Lasek RJ (1987) Astrocytes block axonal regeneration in mammals by activating the physiological stop pathway. Science 237:642-645.
Lytle JM, Wrathall JR (2007) Glial cell loss, proliferation and replacement in the contused murine spinal cord. Eur J Neurosci 25:1711-1724.
Maeda N, Hamanaka H, Oohira A, Noda M (1995) Purification, characterization and developmental expression of a brain-specific chondroitin sulfate proteoglycan, 6B4 proteoglycan/phosphacan. Neuroscience 67:23-35.
Marchant A, Amraoui Z, Gueydan C, Bruyns C, Le Moine O, Vandenabeele P, Fiers W, Buurman WA, Goldman M (1996) Methylprednisolone differentially regulates IL-10 and tumour necrosis factor (TNF) production during murine endotoxaemia. Clin Exp Immunol 106:91-96.
Matsui F, Kawashima S, Shuo T, Yamauchi S, Tokita Y, Aono S, Keino H, Oohira A (2002) Transient expression of juvenile-type neurocan by reactive astrocytes in adult rat brains injured by kainate-induced seizures as well as surgical incision. Neuroscience 112:773-781.
McKeon RJ, Jurynec MJ, Buck CR (1999) The chondroitin sulfate proteoglycans neurocan and phosphacan are expressed by reactive astrocytes in the chronic CNS glial scar. J Neurosci 19:10778-10788.
McKeon RJ, Schreiber RC, Rudge JS, Silver J (1991) Reduction of neurite outgrowth in a model of glial scarring following CNS injury is correlated with the expression of inhibitory molecules on reactive astrocytes. J Neurosci 11:3398-3411.

McTigue DM, Tripathi RB (2008) The life, death, and replacement of oligodendrocytes in the adult CNS. J Neurochem 107:1-19.
McTigue DM, Wei P, Stokes BT (2001) Proliferation of NG2-positive cells and altered oligodendrocyte numbers in the contused rat spinal cord. J Neurosci 21:3392-3400.
McTigue DM, Tripathi R, Wei P (2006) NG2 colocalizes with axons and is expressed by a mixed cell population in spinal cord lesions. J Neuropathol Exp Neurol 65:406-420.
Meisel C, Vogt K, Platzer C, Randow F, Liebenthal C, Volk HD (1996) Differential regulation of monocytic tumor necrosis factor-alpha and interleukin-10 expression. Eur J Immunol 26:1580-1586.
Merrill JE, Scolding NJ (1999) Mechanisms of damage to myelin and oligodendrocytes and their relevance to disease. Neuropathol Appl Neurobiol 25:435-458.
Mirrione MM, Konomos DK, Gravanis I, Dewey SL, Aguzzi A, Heppner FL, Tsirka SE Microglial ablation and lipopolysaccharide preconditioning affects pilocarpine-induced seizures in mice. Neurobiol Dis 39:85-97.
Moore KW, de Waal Malefyt R, Coffman RL, O'Garra A (2001) Interleukin-10 and the interleukin-10 receptor. Annu Rev Immunol 19:683-765.
Morris L, Graham CF, Gordon S (1991) Macrophages in haemopoietic and other tissues of the developing mouse detected by the monoclonal antibody F4/80. Development 112:517-526.
Nedergaard M, Ransom B, Goldman SA (2003) New roles for astrocytes: redefining the functional architecture of the brain. Trends in neurosciences 26:523-530.
Oohira A, Matsui F, Watanabe E, Kushima Y, Maeda N (1994) Developmentally regulated expression of a brain specific species of chondroitin sulfate proteoglycan, neurocan, identified with a monoclonal antibody IG2 in the rat cerebrum. Neuroscience 60:145-157.
Perry VH, Hume DA, Gordon S (1985) Immunohistochemical localization of macrophages and microglia in the adult and developing mouse brain. Neuroscience 15:313-326.
Pineau I, Lacroix S (2007) Proinflammatory cytokine synthesis in the injured mouse spinal cord: multiphasic expression pattern and identification of the cell types involved. J Comp Neurol 500:267-285.
Platzer C, Docke W, Volk H, Prosch S (2000) Catecholamines trigger IL-10 release in acute systemic stress reaction by direct stimulation of its promoter/enhancer activity in monocytic cells. J Neuroimmunol 105:31-38.
Platzer C, Meisel C, Vogt K, Platzer M, Volk HD (1995) Up-regulation of monocytic IL-10 by tumor necrosis factor-alpha and cAMP elevating drugs. Int Immunol 7:517-523.
Platzer C, Fritsch E, Elsner T, Lehmann MH, Volk HD, Prosch S (1999) Cyclic adenosine monophosphate-responsive elements are involved in the transcriptional activation of the human IL-10 gene in monocytic cells. Eur J Immunol 29:3098-3104.
Plunkett JA, Yu CG, Easton JM, Bethea JR, Yezierski RP (2001) Effects of interleukin-10 (IL-10) on pain behavior and gene expression following excitotoxic spinal cord injury in the rat. Exp Neurol 168:144-154.

Popovich PG, Wei P, Stokes BT (1997) Cellular inflammatory response after spinal cord injury in Sprague-Dawley and Lewis rats. The Journal of comparative neurology 377:443-464.
Popovich PG, Guan Z, McGaughy V, Fisher L, Hickey WF, Basso DM (2002) The neuropathological and behavioral consequences of intraspinal microglial/macrophage activation. Journal of neuropathology and experimental neurology 61:623-633.
Rabchevsky AG, Streit WJ (1997) Grafting of cultured microglial cells into the lesioned spinal cord of adult rats enhances neurite outgrowth. J Neurosci Res 47:34-48.
Rabchevsky AG, Sullivan PG, Scheff SW (2007) Temporal-spatial dynamics in oligodendrocyte and glial progenitor cell numbers throughout ventrolateral white matter following contusion spinal cord injury. Glia 55:831-843.
Rezaie P, Male D (2002) Mesoglia & microglia--a historical review of the concept of mononuclear phagocytes within the central nervous system. J Hist Neurosci 11:325-374.
Rice T, Larsen J, Rivest S, Yong VW (2007) Characterization of the early neuroinflammation after spinal cord injury in mice. J Neuropathol Exp Neurol 66:184-195.
Ridet JL, Malhotra SK, Privat A, Gage FH (1997) Reactive astrocytes: cellular and molecular cues to biological function. Trends Neurosci 20:570-577.
Riese U, Brenner S, Docke WD, Prosch S, Reinke P, Oppert M, Volk HD, Platzer C (2000) Catecholamines induce IL-10 release in patients suffering from acute myocardial infarction by transactivating its promoter in monocytic but not in T-cells. Mol Cell Biochem 212:45-50.
Rock RB, Gekker G, Hu S, Sheng WS, Cheeran M, Lokensgard JR, Peterson PK (2004) Role of microglia in central nervous system infections. Clin Microbiol Rev 17:942-964, table of contents.
Rosenberg LJ, Teng YD, Wrathall JR (1999) 2,3-Dihydroxy-6-nitro-7-sulfamoyl-benzo(f)quinoxaline reduces glial loss and acute white matter pathology after experimental spinal cord contusion. J Neurosci 19:464-475.
Rudge JS, Silver J (1990) Inhibition of neurite outgrowth on astroglial scars in vitro. J Neurosci 10:3594-3603.
Schnell L, Fearn S, Klassen H, Schwab ME, Perry VH (1999) Acute inflammatory responses to mechanical lesions in the CNS: differences between brain and spinal cord. Eur J Neurosci 11:3648-3658.
Schonberg DL, Popovich PG, McTigue DM (2007) Oligodendrocyte generation is differentially influenced by toll-like receptor (TLR) 2 and TLR4-mediated intraspinal macrophage activation. J Neuropathol Exp Neurol 66:1124-1135.
Schwab JM, Brechtel K, Mueller CA, Failli V, Kaps HP, Tuli SK, Schluesener HJ (2006) Experimental strategies to promote spinal cord regeneration--an integrative perspective. Prog Neurobiol 78:91-116.
Schwab ME, Bartholdi D (1996) Degeneration and regeneration of axons in the lesioned spinal cord. Physiol Rev 76:319-370.
Silver J, Miller JH (2004) Regeneration beyond the glial scar. Nat Rev Neurosci 5:146-156.

Smirkin A, Matsumoto H, Takahashi H, Inoue A, Tagawa M, Ohue S, Watanabe H, Yano H, Kumon Y, Ohnishi T, Tanaka J Iba1(+)/NG2(+) macrophage-like cells expressing a variety of neuroprotective factors ameliorate ischemic damage of the brain. J Cereb Blood Flow Metab 30:603-615.

Stallcup WB, Beasley L (1987) Bipotential glial precursor cells of the optic nerve express the NG2 proteoglycan. J Neurosci 7:2737-2744.

Stirling DP, Khodarahmi K, Liu J, McPhail LT, McBride CB, Steeves JD, Ramer MS, Tetzlaff W (2004) Minocycline treatment reduces delayed oligodendrocyte death, attenuates axonal dieback, and improves functional outcome after spinal cord injury. J Neurosci 24:2182-2190.

Streit WJ, Semple-Rowland SL, Hurley SD, Miller RC, Popovich PG, Stokes BT (1998) Cytokine mRNA profiles in contused spinal cord and axotomized facial nucleus suggest a beneficial role for inflammation and gliosis. Exp Neurol 152:74-87.

Takahashi K (1994) [Development and differentiation of macrophages and their related cells]. Hum Cell 7:109-115.

Tan AM, Zhang W, Levine JM (2005) NG2: a component of the glial scar that inhibits axon growth. J Anat 207:717-725.

Tan AM, Zhao P, Waxman SG, Hains BC (2009) Early microglial inhibition preemptively mitigates chronic pain development after experimental spinal cord injury. J Rehabil Res Dev 46:123-133.

Tan AM, Colletti M, Rorai AT, Skene JH, Levine JM (2006) Antibodies against the NG2 proteoglycan promote the regeneration of sensory axons within the dorsal columns of the spinal cord. J Neurosci 26:4729-4739.

Tang X, Davies JE, Davies SJ (2003) Changes in distribution, cell associations, and protein expression levels of NG2, neurocan, phosphacan, brevican, versican V2, and tenascin-C during acute to chronic maturation of spinal cord scar tissue. Journal of neuroscience research 71:427-444.

Tanga FY, Raghavendra V, DeLeo JA (2004) Quantitative real-time RT-PCR assessment of spinal microglial and astrocytic activation markers in a rat model of neuropathic pain. Neurochem Int 45:397-407.

Taylor DL, Pirianov G, Holland S, McGinnity CJ, Norman AL, Reali C, Diemel LT, Gveric D, Yeung D, Mehmet H Attenuation of proliferation in oligodendrocyte precursor cells by activated microglia. J Neurosci Res 88:1632-1644.

Thanos S, Mey J, Wild M (1993) Treatment of the adult retina with microglia-suppressing factors retards axotomy-induced neuronal degradation and enhances axonal regeneration in vivo and in vitro. J Neurosci 13:455-466.

Tikka T, Fiebich BL, Goldsteins G, Keinanen R, Koistinaho J (2001) Minocycline, a tetracycline derivative, is neuroprotective against excitotoxicity by inhibiting activation and proliferation of microglia. J Neurosci 21:2580-2588.

Ughrin YM, Chen ZJ, Levine JM (2003) Multiple regions of the NG2 proteoglycan inhibit neurite growth and induce growth cone collapse. J Neurosci 23:175-186.

Wagle JR, Ansevin AT, Dessens SE, Nishioka K (1989) Specific translocation of tuftsin (Thr-Lys-Pro-Arg), a natural immunomodulating peptide, into the nuclei of human monocytes. Biochem Biophys Res Commun 159:1147-1153.

Wang J, Tsirka SE (2005) Tuftsin fragment 1-3 is beneficial when delivered after the induction of intracerebral hemorrhage. Stroke 36:613-618.

Waxman SG (2001) Acquired channelopathies in nerve injury and MS. Neurology 56:1621-1627.
Wilms H, Sievers J, Rickert U, Rostami-Yazdi M, Mrowietz U, Lucius R Dimethylfumarate inhibits microglial and astrocytic inflammation by suppressing the synthesis of nitric oxide, IL-1beta, TNF-alpha and IL-6 in an in-vitro model of brain inflammation. J Neuroinflammation 7:30.
Woiciechowsky C, Volk HD (2005) Increased intracranial pressure induces a rapid systemic interleukin-10 release through activation of the sympathetic nervous system. Acta Neurochir Suppl 95:373-376.
Woiciechowsky C, Schoning B, Stoltenburg-Didinger G, Stockhammer F, Volk HD (2004) Brain-IL-1 beta triggers astrogliosis through induction of IL-6: inhibition by propranolol and IL-10. Med Sci Monit 10:BR325-330.
Woiciechowsky C, Asadullah K, Nestler D, Eberhardt B, Platzer C, Schoning B, Glockner F, Lanksch WR, Volk HD, Docke WD (1998) Sympathetic activation triggers systemic interleukin-10 release in immunodepression induced by brain injury. Nat Med 4:808-813.
Wolpe SD, Cerami A (1989) Macrophage inflammatory proteins 1 and 2: members of a novel superfamily of cytokines. FASEB J 3:2565-2573.
Wolpe SD, Davatelis G, Sherry B, Beutler B, Hesse DG, Nguyen HT, Moldawer LL, Nathan CF, Lowry SF, Cerami A (1988) Macrophages secrete a novel heparin-binding protein with inflammatory and neutrophil chemokinetic properties. J Exp Med 167:570-581.
Wrathall JR, Teng YD, Choiniere D (1996) Amelioration of functional deficits from spinal cord trauma with systemically administered NBQX, an antagonist of non-N-methyl-D-aspartate receptors. Exp Neurol 137:119-126.
Wrathall JR, Li W, Hudson LD (1998) Myelin gene expression after experimental contusive spinal cord injury. J Neurosci 18:8780-8793.
Wu J, Yoo S, Wilcock D, Lytle JM, Leung PY, Colton CA, Wrathall JR Interaction of NG2(+) glial progenitors and microglia/macrophages from the injured spinal cord. Glia 58:410-422.
Xu LL, Warren MK, Rose WL, Gong W, Wang JM (1996) Human recombinant monocyte chemotactic protein and other C-C chemokines bind and induce directional migration of dendritic cells in vitro. J Leukoc Biol 60:365-371.
Yamada H, Watanabe K, Shimonaka M, Yamaguchi Y (1994) Molecular cloning of brevican, a novel brain proteoglycan of the aggrecan/versican family. J Biol Chem 269:10119-10126.
Yan P, Li Q, Kim GM, Xu J, Hsu CY, Xu XM (2001) Cellular localization of tumor necrosis factor-alpha following acute spinal cord injury in adult rats. J Neurotrauma 18:563-568.
Yoo S, Wrathall JR (2007) Mixed primary culture and clonal analysis provide evidence that NG2 proteoglycan-expressing cells after spinal cord injury are glial progenitors. Dev Neurobiol 67:860-874.
Yune TY, Lee JY, Jung GY, Kim SJ, Jiang MH, Kim YC, Oh YJ, Markelonis GJ, Oh TH (2007) Minocycline alleviates death of oligodendrocytes by inhibiting pro-nerve growth factor production in microglia after spinal cord injury. J Neurosci 27:7751-7761.

Zhang D, Hu X, Qian L, Wilson B, Lee C, Flood P, Langenbach R, Hong JS (2009) Prostaglandin E2 released from activated microglia enhances astrocyte proliferation in vitro. Toxicol Appl Pharmacol 238:64-70.
Zhou Z, Peng X, Insolera R, Fink DJ, Mata M (2009) IL-10 promotes neuronal survival following spinal cord injury. Exp Neurol 220:183-190.